

**CONTROL OF BACTERIAL WILT IN TOMATO USING  
BIO-ANTAGONISTS ADSORBED ON CHITOSAN-SILICA  
NANOCOMPOSITES**

**DENNIS MAINA GATAHI**

**DOCTOR OF PHILOSOPHY**

**(Horticulture)**

**JOMO KENYATTA UNIVERSITY OF  
AGRICULTURE AND TECHNOLOGY**

**2017**

**Control of Bacterial Wilt in Tomato using Bio-Antagonists Adsorbed  
on Chitosan-Silica Nanocomposites**

**Dennis Maina Gatahi**

**A thesis submitted in fulfillment for the Degree of Doctor of Philosophy  
in Horticulture of the Jomo Kenyatta University of Agriculture and  
Technology**

**2017**

**DECLARATION**

This thesis is my original work and has not been presented for a degree in any other University.

Signature..... Date.....

**Dennis Maina Gatahi**

This thesis has been submitted with our approval as the University Supervisors.

Signature..... Date.....

**Prof. Agnes Wanjiru Kihurani, PhD**  
**Karatina University, Kenya**

Signature..... Date.....

**Dr. Harrison Njuma Wanyika, PhD**  
**JKUAT, Kenya**

Signature..... Date.....

**Prof. Elijah Miinda Ateka, PhD**  
**JKUAT, Kenya**

## **DEDICATION**

To my beloved parents, siblings, my wife Charity, my children Cherry and Karleen for their invaluable support and encouragement.

## **ACKNOWLEDGEMENTS**

I wish to express my gratitude to Jomo Kenyatta University of Agriculture and Technology for funding the research work, supervisors for their guidance during the research work and thesis writing and my family for moral support throughout my studies.

I can't forget the assistance offered by Mr. Patrick Kavagi of Horticulture Department (JKUAT), Mr. Wilson Kung'u of Chemistry Department (JKUAT), Ms. Ann Mwaura of the National Museums of Kenya, Prof. Tshentu Zenixole (University of Rhodes, South Africa) and Mr. Gerald Njiru of Geothermal Development Company, for their assistance during experimentation.

## TABLE OF CONTENTS

<b>DECLARATION</b> .....	<b>ii</b>
<b>DEDICATION</b> .....	<b>iii</b>
<b>ACKNOWLEDGEMENTS</b> .....	<b>iv</b>
<b>TABLE OF CONTENTS</b> .....	<b>v</b>
<b>LIST OF TABLES</b> .....	<b>xv</b>
<b>LIST OF FIGURES</b> .....	<b>xvii</b>
<b>LIST OF PLATES</b> .....	<b>xix</b>
<b>LIST OF APPENDICES</b> .....	<b>xxi</b>
<b>LIST OF ABBREVIATIONS AND ACRONYMS</b> .....	<b>xxii</b>
<b>ABSTRACT</b> .....	<b>xxiv</b>
<b>CHAPTER ONE</b> .....	<b>1</b>
<b>INTRODUCTION</b> .....	<b>1</b>
1.1 Background information .....	1
1.2 Problem Statement .....	4
1.3 Justification.....	6
1.4 Objectives .....	7

1.4.1 Overall Objective .....	7
1.4.2 Specific Objectives.....	7
1.5 Hypotheses.....	7
<b>CHAPTER TWO.....</b>	<b>8</b>
<b>LITERATURE REVIEW .....</b>	<b>8</b>
2.1 Tomato .....	8
2.1.1 Origin, Taxonomy and Botany .....	8
2.1.2 Tomato production .....	9
2.1.3 Importance and utilization of tomato .....	10
2.1.4 Diseases and pests in tomato .....	11
2.2 Bacterial Wilt of Tomato .....	12
2.2.1 Life Cycle, Etiology, Epidemiology and Dissemination of Bacterial Wilt .....	12
2.3 Control of Bacterial Wilt of Tomato.....	13
2.3.1 Cultural Methods.....	13
2.3.2 Chemical Methods.....	14
2.3.3 Biological Methods .....	14
2.4 Nanoparticles, Nanocomposites and Colorimetric Materials.....	16

2.4.1 Chitosan .....	17
2.4.2 Mesoporous Silica Nanoparticles (MSN).....	18
2.4.3 Colorimetric Probes .....	18
<b>CHAPTER THREE .....</b>	<b>22</b>
<b>SYNTHESIS AND EVALUATION OF BIONANOCOMPOSITE MATERIALS FOR THE CONTROL OF BACTERIAL WILT IN TOMATO PRODUCTION..</b>	<b>22</b>
3.1 Introduction.....	23
3.2 Materials and Methods.....	24
3.2.1 Experimental Site and Layout .....	24
3.2.2 Preparation of Chitosan (CHT) and Chitosan Nanoparticles (CHTNP).....	25
3.2.3 Determination of Deacetylation .....	25
3.2.4 Preparation of Chitosan Immobilized Silica Nanocomposite (CISNC) .....	27
3.2.5 Determination of Crystallite Sizes of Chitosan Nanoparticles and Nanocomposites.....	27
3.2.6 Isolation of <i>R. Solanacearum</i> .....	28
3.2.7 Isolation of <i>R. solanacearum</i> Phage.....	28
3.2.8 Isolation of DNA from <i>R. solanacearum</i> and Phage .....	29
3.2.9 Culturing of Biocontrol Antagonists (BCAs).....	30

3.2.10 Adsorption of Biocontrol Agents on Chitosan Immobilized Silica Nanocomposite .....	31
3.2.11 <i>In vitro</i> Tests.....	31
3.2.12 Seed Treatment.....	32
3.2.13 Media Preparation .....	32
3.2.14 Sowing of Seeds and Estimation of Germination Percentage, Chlorophyll Content, Growth Rate and Wilting Incidences .....	33
3.2.15 Illustration of the Process of Development of Bionanocomposite and Efficacy Tests.....	34
3.2.16 Data Analysis.....	35
3.3 Results.....	35
3.3.1 Deacetylation of Chitin.....	35
3.3.2 Characterization of Deacetylated Chitin.....	36
3.3.3 Characterization of Chitosan Nanoparticle and Chitosan Immobilized Silica Nanocomposite (CISNC) .....	38
3.3.4 Detection of Isolated Microbes .....	40
3.3.5 Sorption Properties of Biological Antagonists on Chitosan Immobilized Silica Nanocomposite (CISNC) .....	42

3.3.6 Efficacy of the Biocontrol Agents-Chitosan Immobilized Silica Nanocomposite Complex (BCA-CISNC or Bionanocomposites) on <i>R. Solanacearum</i> , Tomato Wilt and Growth Rate .....	44
3.4 Discussion.....	50
3.4.1 Deacetylation of Chitin.....	50
3.4.2 Characterization of Deacetylated Chitin.....	51
3.4.3 Characterization of Chitosan Nanoparticle and Chitosan Immobilized Silica Nanocomposite (CISNC) .....	52
3.4.4 Detection of Isolated Microbes .....	54
3.4.5 Sorption Properties of Biological Antagonists on Chitosan Immobilized Silica Nanocomposite (CISNC) .....	54
3.4.6 Efficacy of the Bionanocomposite (BCA-CISNC Complex) on <i>R. Solanacearum</i> , Bacterial Wilt and Growth Rate of Tomato .....	56
3.4.7 Effect of Bionanocomposites on Tomato Seed Germination .....	58
3.4.8 Effect of Bionanocomposites on Chlorophyll Content.....	60
3.4.9 Effect of Bionanocomposites on Tomato Plant Growth .....	60
3.4.10 Effect of Bionanocomposites on Wilt in Tomato.....	61

<b>CHAPTER FOUR.....</b>	<b>66</b>
<b>ENHANCEMENT OF BACTERIAL WILT TORELANCE, RHIZOSPHERE HEALTH, YIELD AND POSTHARVEST QUALITY IN TOMATO USING BIONANOCOMPOSITES.....</b>	<b>66</b>
4.1 Introduction.....	67
4.2 Materals and Methods.....	68
4.2.1 Preparation of Bionanocomposites.....	68
4.2.2 Experimental Sites and Design.....	69
4.2.3 Determination of Effective Concentration (EC) for the Chitosan Immobilized Silica Nanocomposite (CISNC) Gel.....	69
4.2.4 Assessment of Mycorrhizal Colonization.....	70
4.2.5 Biochemical Analysis (Glucanase and Chitinase).....	71
4.2.6 Illustration of Elicitation of Resistance in Tomato by Bio-Nanocomposites..	72
4.2.7 Bacterial Wilt Incidence .....	72
4.2.8 Assessment of Yield in Tomato Varieties Treated With Bionanocomposites	73
4.2.9 Determination of Retention of Total Organic Carbon in Soil/Planting Media	73
4.2.10 Determination of pH in the Tomato Rhizosphere .....	74
4.2.11 Determination of the effect of Bionanocomposite on Tomato Flowering, Ripening and Shelf Life of Fruits .....	74

4.3 Results.....	75
4.3.1 Determination of Effective Concentration of Chitosan Immobilized Silica Nanocomposite (CISNC) Gel .....	75
4.3.2 Colonization of Roots by Biocontrol Agents .....	75
4.3.3 Elicitation of Resistance in Tomato by Bionanocomposites .....	79
4.3.4 Bacterial Wilt Assessment.....	82
4.3.6 Total Organic Carbon Accumulation in the Soil.....	85
4.3.7 Effect of Bionanocomposites on Soil pH .....	86
4.3.8 Effect of Bionanocomposites on Flowering, Ripening and Shelf Life of Tomato Fruits.....	87
4.4 Discussion.....	89
4.4.1 Determination of Effective Concentration (EC) of Chitosan Immobilized Silica Nanocomposite (CISNC) Gel.....	89
4.4.2 Colonization of Roots by Biocontrol Agents .....	90
4.4.3 Elicitation of Resistance in Tomato by Bionanocomposites .....	91
4.4.4 Bacterial Wilt Incidence and Severity .....	93
4.4.5 Effect of Bionanocomposites on Tomato Yield .....	93
4.4.6 Total Organic Carbon Accumulation in the Soil.....	94

4.4.7 Effect of Bionanocomposites on Soil pH .....	95
4.4.8 Effect of Bionanocomposites on Flowering, Ripening and Shelf Life of Tomato Fruits.....	96
<b>CHAPTER FIVE.....</b>	<b>98</b>
<b>DEVELOPMENT OF A DIAGNOSTIC KIT FOR THE DETECTION OF <i>Ralstonia solanacearum</i> .....</b>	<b>98</b>
5.1 Introduction.....	99
5.2 Materials and Methods.....	101
5.2.1 Experimental Site and Design .....	101
5.2.2 Preparation of Green Ferrous Oxide Nanoparticles (FeONPs).....	101
5.2.3 Synthesis of Ferrous Oxide Chitosan Immobilized Silica Nanocomposite (FeOCISNC) .....	102
5.2.4 Synthesis of Nylon-FeOCISNC (Nanoprobe).....	102
5.2.5 Characterization of Nylon-FeOCISNC (Nanoprobe) Using XRD.....	103
5.2.6 Isolation and Identification of <i>R. solanacearum</i> and <i>F. oxysporum</i> .....	103
5.2.7 Colorimetric Tests of the Nanoprobe in <i>R. solanacearum</i> Suspension .....	103
5.2.8 Elemental analysis of the Nanocomposites using the X-Ray Fluorescence (XRF) Technique .....	104

5.2.9 Validation of the Colorimetric Nanoprobe using PCR and Conventional Techniques .....	104
5.2.10 Data Analysis.....	105
5.3 Results.....	105
5.3.1 Green Synthesis of Iron Oxide Nanoparticles (FeONPs) .....	105
5.3.2 Characterization of Nylon-ferrous Oxide Chitosan Immobilized Silica Nanoprobe (nylon-FeOCISNC) using Uv-vis and XRD.....	107
5.3.3 Characterization of Nanocomposites using x-ray Florescence (XRF).....	109
5.3.4 Colorimetric Tests of Nylon-ferrous Chitosan Immobilized Silica Nanoprobe .....	110
5.4 Discussion.....	113
5.4.1 Green Iron Oxide Nanoparticles (FeONPs) Synthesis.....	113
5.4.2 Characterization of Nylon-Ferrous Oxide Chitosan Immobilized Silica Nanoprobe (Nylon-Feocisnc) using X-Ray Flourescence, Uv-Vis Spectrophotometer and X-Ray Powder Diffractometer .....	115
5.4.3 Science of Formation of Nylon Ferrous Oxide Chitosan Immobilized Nanoprobe .....	117
5.4.4 Colorimetric Effect of the Nanoprobe .....	118
5.4.5 Validation of the Colorimetric Nanoprobe using Polymerase Chain Reaction (PCR) and Conventional Techniques .....	119

<b>CHAPTER SIX.....</b>	<b>121</b>
<b>GENERAL DISCUSSION, CONCLUSIONS AND RECOMMENDATIONS.....</b>	<b>121</b>
6.1 General Discussion.....	121
6.2 Conclusions.....	122
6.3 Recommendations .....	123
<b>REFERENCES.....</b>	<b>124</b>
<b>APPENDICES.....</b>	<b>151</b>

## LIST OF TABLES

<b>Table 3.1:</b> Content of Carbon and Nitrogen in Acetylated (Chitin) and Deacetylated Chitin (Chitosan).....	35
<b>Table 3.2:</b> Crystallite Sizes of Chitosan Nanoparticles and Nanocomposites.....	40
<b>Table 3.3:</b> <i>In vitro</i> Inhibition of <i>R. Solanacearum</i> Growth on Different Substances .....	44
<b>Table 4.1:</b> Effective Concentrations of CISNC in Tomato Growth, Development and Wilt Resistance.....	75
<b>Table 4.2:</b> Microbial Colonization Frequency in Tomato Root Hairs (AMF Colonization).....	77
<b>Table 4.3:</b> Microbial Colonization Frequency in Tomato Root Hairs (AMF Infection)	77
<b>Table 4.4:</b> Concentration of Chitinase in Tomato Varieties Treated with Bionanocomposites .....	80
<b>Table 4.5:</b> Concentration of Glucanase in Tomato Varieties Treated with Bionanocomposites .....	81
<b>Table 4.6:</b> Pearson Correlations for Chitinase and Bacterial Wilt Incidences Tomato Varieties.....	81
<b>Table 4.7:</b> Wilt Incidences in Tomato Varieties Treated with Bionanocomposites.....	82
<b>Table 4.8:</b> Bacterial Wilt Severity in Tomato Varieties Treated with Bionanocomposites .....	83
<b>Table 4.9:</b> Circumference (cm) of Fruits Treated with Bionanocomposites .....	84

<b>Table 4.10:</b> Weight of Fruits from two Tomato Hybrids (Kgs/Plant).....	84
<b>Table 4.11:</b> Total Organic Carbon (TOC) in Tomato Rhizosphere after Removal of Plant Debris .....	86
<b>Table 4.12:</b> Soil pH in Rhizosphere after Removal of Tomato Plant Debris in Different Planting Media, 6 Months after Application of the Bionanocomposites.....	87
<b>Table 4.13:</b> Days to Flowering and Ripening of Fruits in Tomato Hybrids Treated with Bionanocomposites .....	88
<b>Table 4.14:</b> Shelf Life (Days) of Tomato Fruits Treated with Bionanocomposites.....	89
<b>Table 5.1:</b> Yield (ppm) of FeONPs from Iron Chloride and Green Tea Extracts (Te).	106
<b>Table 5.2:</b> Elemental Analysis of the Nanoprobe.....	109
<b>Table 5.3:</b> Change in Concentrations of Residual <i>R. Solanacearum</i> and <i>F. oxysporum</i> Suspensions after Adsorption on the Nanoprobe .....	110
<b>Table 5.4:</b> Crystallite Sizes of Synthesized Nanocomposites.....	112

## LIST OF FIGURES

<b>Figure 1.1:</b> Structure of chitin and chitosan, Rodrigo <i>et al.</i> , (2006) .....	3
<b>Figure 1.2:</b> Structure and sorption properties of chitosan immobilized silica gel, Kubata <i>et al.</i> , (2005).....	3
<b>Figure 3.1:</b> Linear Fit for Deacetylation of Chitin using Sodium Hydroxide .....	36
<b>Figure 3.2:</b> FTIR Spectra of A-Chitin and B-Chitosan.....	37
<b>Figure 3.3:</b> X-Ray Diffractograms for A-Chitin, B-Chitosan and C-Chitosan Nanoparticle.....	38
<b>Figure 3.4:</b> FTIR Spectra for A-Chitosan Nanoparticle B-CISNC and C-MSN.....	39
<b>Figure 3.5:</b> X-Ray Diffractograms of; I-Chitin, II-Chitosan Nanoparticle and III-CISNC .....	40
<b>Figure 3.6:</b> Adsorption Efficiencies of Microbial Antagonists' .....	42
<b>Figure 3.7:</b> Desorption Efficiencies of Microbial Antagonists' .....	43
<b>Figure 3.8:</b> Germination Rates of Tomato Seeds Treated with Bionanocomposites .....	46
<b>Figure 3.9:</b> Growth Rates of Tomato Seedlings Treated with Bionanocomposites.....	48
<b>Figure 3.10:</b> Bacterial Wilt Incidences in Tomato Varieties Treated with Bionanocomposites. ....	49
<b>Figure 4.1:</b> Colonization and Frequency of Tomato Roots by Beneficial Microbes .....	76

<b>Figure 5.1:</b> Linear Fit of Absorbance of Oxide Iron Nanoparticles versus Concentration .....	105
<b>Figure 5.2:</b> Change in Optical Density of Ferrous Oxide Chitosan Immobilized Silica Nanocomposite (FeOCISNC) due to Adsorption by Nylon Nanofibres ..	107
<b>Figure 5.3:</b> X-ray Diffractograms for CISNC, FeONPs and FeOCISNC.....	108
<b>Figure 5.4:</b> X-ray Diffractograms for i-nylon nanofibre ii-CISNC and iii-.....	112

## LIST OF PLATES

Plate 2.1: Different concentrations of Fe (II), Source: Odingo, 2013.....	19
Plate 2.2: Colorimetric protein sensing, Source: Li et al., 2012.....	20
Plate 2.3: Nylon nanofibres with 200 nm, Source: Odingo et al., 2013.....	21
Plate 3.1: Images of <i>R. Solanacearum</i> and Bacteriophage .....	41
Plate 3.2: Electrophoregrams; A-Amplified DNA of <i>R. Solanacearum</i> and Phage, B- Isolated DNA from <i>R. Solanacearum</i> Bacteria and Phage .....	41
Plate 3.3: Images of Nanocomposites and Bionanocomposites .....	43
Plate 3.4: Zones of inhibition of Cultured <i>R. solanacearum</i> by Bionanocomposites .....	45
Plate 3.5: Images of tomato seedlings treated with bionanocomposites.....	48
3.3.6.5 Effect of Bionanocomposites on Wilt Incidences in Tomato .....	49
3.4.10.1 Biological Control Agents in the Control of Bacterial Wilt in Tomato .....	61
3.4.10.2 Chitosan in the Control of Bacterial Wilt.....	64
3.4.10.3 Silica in the Control of Bacterial Wilt.....	64
4.2.7.1 Bacterial Wilt Severity Assessment.....	73
Plate 4.1: Microbial Root Colonization Images .....	79
Plate 4.2: Gel Image Showing PCR Product of Chitinase and Glucanase .....	80

4.3.5 Effect of Bionanocomposites on Tomato Yield.....	84
Plate 4.3: Images of Tomato Plants Treated with Bio-Nanocomposites .....	85
5.2.2.1 Quantitation and Characterization of Ferrous Oxide Nanoparticles (FeONPs). 102	
Plate 5.1: Compound Microscope Images for Nylon Nanofibres, Nylon-Ferrous Oxide CISNC and FeOCISNC .....	109
Plate 5.2: Images of Nylon-Ferrous Oxide Chitosan Immobilized Silica Nanocomposite Colorimetric Probe .....	111
Plate 5.3: Gel image of a- <i>R. solanacearum</i> and <i>F. oxysporum</i> (PCR), b- <i>R.</i> <i>solanacearum</i> on TZC agar, c- chlamydospores of <i>F. oxysporum</i> (x 400). .....	113
5.4.2.1 Characterization of Nanoprobe using X-Ray Fluorescence (XRF).....	115
5.4.2.2 Characterization of Nanoprobe using Uv-Vis Spectrophotometer .....	115

## LIST OF APPENDICES

<b>Appendix 1:</b> Pearson's Correlation Coefficient- Descriptive Statistics.....	151
<b>Appendix 2:</b> Summary of ANOVA for Iron Nanoparticles Yield .....	152
<b>Appendix 3:</b> Summary of ANOVA for <i>R. Solanacearum</i> Optical Densities (OD) 600 nm .....	153
<b>Appendix 4:</b> Summary of ANOVA for <i>R. solanacearum</i> Inhibition by Bionanocomposites.....	154
<b>Appendix 5:</b> Summary of ANOVA for Bacterial Wilt incidence in Tomato.....	155
<b>Appendix 6:</b> Summary of ANOVA for Hybrid Tomatoes Yield (Size in cm).....	156
<b>Appendix 7:</b> Summary of ANOVA for Tomato Fruits Shelf Life (Days).....	157
<b>Appendix 8:</b> Summary of ANOVA for Days to Flowering in Tomato.....	158
<b>Appendix 9:</b> Summary of ANOVA for Days to Ripening of Tomato Fruits .....	159
<b>Appendix 10:</b> Chitosan Nanoparticles (90% DDA).....	160
<b>Appendix 11:</b> Chitosan Immobilized Silica Nanocomposites (CISNC).....	161
<b>Appendix 12:</b> Iron oxide Nanoparticles.....	162
<b>Appendix 13:</b> Nylon Nanofibres .....	163
<b>Appendix 14:</b> Nylon Iron Oxide Chitosan Immobilized Silica Nanocomposite.....	164
<b>Appendix 15:</b> FeOCISNC- <i>R. solanacearum</i> .....	165

## LIST OF ABBREVIATIONS AND ACRONYMS

<b>AMF-</b>	Arbuscular Mycorrhiza Fungi
<b>ANOVA-</b>	Analysis of Variance
<b>BCAs-</b>	Biological Control Agents
<b>BS-</b>	<i>Bacillus subtilis</i>
<b>CHT-</b>	Chitosan
<b>CHTNP-</b>	Chitosan Nanoparticles
<b>CISNC-</b>	Chitosan Immobilized Silica Nanocomposites
<b>CINC-</b>	Chitosan Immobilized Nanoclay
<b>DNA-</b>	Deoxyribonucleic acid
<b>EM-</b>	Effective Micro-organisms
<b>ELISA-</b>	Enzyme-linked immunosorbent assay
<b>EC-</b>	Effective concentration
<b>FeOCISNC-</b>	Ferrous Oxide Chitosan Immobilized Silica Nanocomposites
<b>FO-</b>	<i>Fusarium oxysporum</i>
<b>MSN-</b>	Mesoporous Silica Nanoparticles

<b>NFeOCISNC-</b>	Nylon Ferrous Oxide Chitosan Immobilized Silica Nanocomposites
<b>PCR-</b>	Polymerase Chain Reactions
<b>PHAGE-</b>	<i>Ralstonia solanacearum</i> bacteriophage
<b>RNA-</b>	Ribonucleic acid
<b>RS-</b>	<i>Ralstonia solanacearum</i>
<b>TV-</b>	<i>Trichoderma viride</i>

## ABSTRACT

*Ralstonia solanacearum* L, the causal agent of bacterial wilt, is a devastating and persistent pathogen in solanaceous crops. In severe infections, up to 100 % crop loss may occur. Chemical control is difficult due to the pathogen's variability and persistence in the soil. Biological control holds promise in managing the disease. However, the efficacy of biological control agents (BCAs) is limited by inability to adapt immediately to the environment and their ineffectiveness after *in situ* application. Hence, the need for suitable carrier materials to enhance their adaptation and efficacy. In addition, for effective management of diseases, precision in disease diagnosis is paramount. The study therefore, entailed synthesis of a suitable nanocarrier material for the delivery of BCAs and development of a diagnostic nanoprobe for *R. solanacearum*. The materials used to synthesize the carriers of the BCAs and diagnostic nanoprobe were selected based on their good sorption, ease of functionality, anti-bacterial properties, colorimetric effect and non-polluting properties. Chitin was deacetylated and functionalized to form chitosan nanoparticles with a crystallite size of 3.2 nm. It was then immobilized on mesoporous silica nanoparticles (4.0nm) to form chitosan immobilized silica nanocomposites (CISNC) gel with a crystallite size of 5.8 nm. Biological antagonists (*Bacillus subtilis*, *Trichoderma viride*, *Glomus mosseae*, effective micro-organisms, and bacteriophage) were adsorbed on CISNC gel and their effect on *R. solanacearum* tested. Green synthesized iron oxide nanoparticles were added to the CISNC gel and the mixture adsorbed on nylon nanofibres to form a *R. solanacearum* diagnostic nanoprobe. Characterization of the CISNC carrier showed physisorption properties, making it ideal for adsorption and desorption of the BCAs. BCAs adsorbed on CISNC carrier were more efficacious than those applied without nanocomposite. Successful adsorption of BCAs on CISNC gel significantly ( $P<0.05$ ) increased the inhibition of the pathogen, enhanced germination rate and growth, increased chlorophyll in treated plants, reduced wilt incidences, increased yield and prolonged shelf life of

tomato fruits. Molecular analysis of treated tomato plants showed increased resistance related biochemicals; chitinase and glucanase. Microscopic observation of the treated root hairs confirmed successful colonization by the BCAs. The enhanced activity of the BCA-CISNC complex (bionanocomposite) was attributed to effective delivery, release and synergy of BCAs and the nanocomposite. The mode of action of the diagnostic nanoprobe for *R. solanacearum* was based on; chitosan molecules rupturing the bacterial cell wall, complexation of iron oxide with the bacteria cell constituents and the resulting colour change. The grey-like nanoprobe turned brown in the presence of the pathogen due to reduction of iron oxide through the process of mineralization. There was also an effect on the nanoprobe crystallinity and peak reduction of the x-ray powder diffractograms for nylon-ferrous oxide chitosan-silicacomposite (nanoprobe). The crystallite size of nanoprobe changed from 20.4 nm to 21.8 nm after complexation with the *R. solanacearum* bacteria. The diffractogram peaks of the nanoprobe shifted from 29, 35 and 38 to 32, 38 and 45 nm after complexation with the pathogenic bacteria. The change indicated a reaction between the nanoprobe and the pathogen. Adsorption of microbial antagonists on CISNC gel enhanced efficacy of the beneficial microbes against *R. solanacearum in vitro* and in the greenhouse. Finally, the developed nanoprobe heralds precision of bacterial wilt diagnosis. Utilization of the developed nanocomposites enhances tomato production by accurate detection of the pathogen, effective wilt management, increased yield and shelf life of the harvested tomato fruits.

## CHAPTER ONE

### INTRODUCTION

#### 1.1 Background information

*Ralstonia solanacearum*, the causal agent of tomato bacterial wilt, is one of the most serious soil borne pathogens in Kenya (Kenya Horticulture Development Project, 2007). It limits production of tomato and other solanaceae crops leading to big losses in yield and income. The pathogen's persistence and variability, makes its control difficult (Champoiseau, Allen & Momol, 2009). Biological control has the potential of controlling the pathogen but there is need to increase the efficacy of the biological control materials (Jeong, Kim, Kang, Lee & Hwang, 2007).

A number of soil bacteria and plant growth promoting rhizobacteria are currently being investigated for their role in the control of *R. solanacearum*. Various biological antagonists such as *Bacillus subtilis*, *Bacillus thuringiensis*, *Pseudomonas fluorescense*, *Trichoderma viride* and *Glomus mosseae* are able to produce volatile compounds and different lytic enzymes that suppress the pathogen (Nguyen & Ranamukhaarachchi, 2010), but their commercial utilization has not been realized (Obradovic, Jones, Olson, Jackson & Balogh, 2005; Iriarte *et al.*, 2012).

Bacteriophages are other biological antagonists of *R. solanacearum*. These phages are viruses that specifically target and reproduce within bacterial cells using the host DNA for replication, translation and transcription, leading to eventual death of the infected cells. The host specificity nature of phages, offers a suitable technology for viral therapy in the control of bacterial pathogens in livestock, plants, fish and humans (Balogh, Jones, Iriarte & Momol, 2010). The advantage of viral therapy over other disease control methods is the ability to target particular hosts, evolve with the host and does not elicit

pathogen resistance (Jones, 2007; Fujiwara, Fujisawa, Hamasaki, Kawasaki, Fujie & Yamada, 2011).

The application of microbial antagonists and viral therapy for bacterial disease control is an attractive and likely prospect and the benefits could be considerable. However, their commercial success will depend on developing improved delivery systems for consistent and positive results. The field efficacy of the antagonists is constrained by their short shelf life, inability to adapt and lack of virulence to the pathogen when applied in a harsh environment, hence the need for an appropriate carrier material for delivery of the biological control agents (BCAs) through soil and plant system (Roberts, Lohre, Meyer, Buyer & Lewis, 2005; Iriarte *et al.*, 2012). This necessitated exploration of various nanoparticles as carrier materials for the BCAs. The choice of the materials for adsorbing the microbes was based on safety of the material, sorption properties, antibacterial properties and ability to form complex nanocomposites. These properties informed the choice of chitosan and mesoporous silica nanoparticles as carrier materials for the BCAs. Chitin and its derivatives have antagonistic effects on soil pathogens and possess potential to deliver biological control antagonists due to ease of functionalization (Mandal, Kar, Mukherjee & Acharya, 2013).

The effect of chitin as an antimicrobial agent is however, hampered by its low solubility in most non-toxic solvents and being less active (Zouhour, Salah, Saloua & Amor, 2010). This limitation has been overcome by activation of chitin to chitosan through deacetylation using concentrated alkalis (Figure 1.1). Deacetylation of chitin makes it soluble in acidic conditions due to the free protonable amino groups present in the D-glucosamine units. The deacetylated chitin can further be functionalized by surface modification of the polymer to form chitosan nanoparticles with a larger surface area for adsorption (Nasriet *al.*, 2009). In order to prevent rapid degradation after administration, increase lifespan and efficacy, the biocompatible polymer coating was immobilized on silica nanoparticles through physisorption (Figure 1.2) (Freier, Koh, Kazazian &

Shoichet, 2005; Kubata, Matsui, Chiku, Kasashima, Shimojoh & Sakaguchi, 2005). Nano-silica is preferred due to its inherent antimicrobial characteristic, enhancement of host plant resistance, large surface area due to large gallery spaces that appear like “honey comb” structures when observed under transmission electron microscope (Balakhina & Borkowska, 2013).

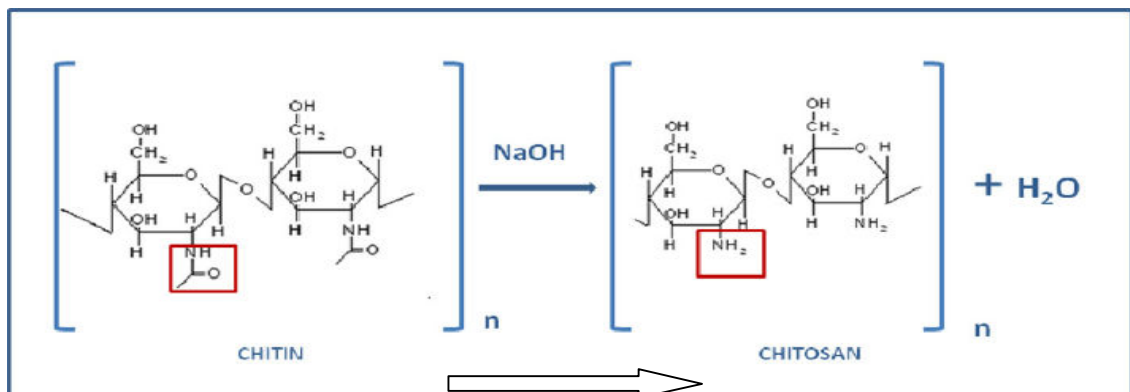


**Figure 1.1:** Structure of chitin and chitosan, Rodrigo *et al.*, (2006)

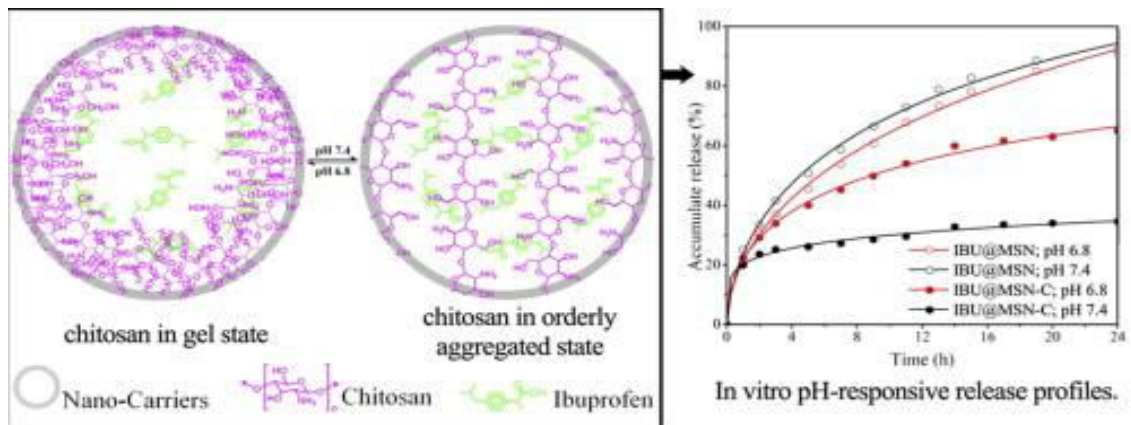


**Figure 1.2:** Structure and sorption properties of chitosan immobilized silica gel, Kubata *et al.*, (2005)

Control of *R. solanacearum* in tomato plants is also hampered by accuracy during diagnosis. Most farmers rely on wilt symptoms to determine the causal agent. This is subjective and at times there is no adequate inoculum to cause the milk ooze for confirmation (Jahanshir & Dzhililov, 2010). This therefore calls for a simple, inexpensive and rapid test to confirm whether the wilt in tomato occurs due to *R. solanacearum* or *Fusariumspp* (Agasti, Rana, & Park, 2010). Recently there has been development of diagnostic probes using PCR, nanotechnology and fluorescence technologies (Michailides, Morgan, Ma, Luo, Felts, Doster & Reyes, 2005). These techniques have been used to objectively confirm pathogens without ambiguity prior to disease control. Use of PCR diagnostics may require a particular level of training while the fluorescence diagnostics require special equipment thus inaccessible to most farmers in Kenya. Use of nanotechnology in development of sensitive and rapid diagnosis of pathogens has been done and recommended due to the ease of use, cost effectiveness and rapid results (Chaumpluk, Chaiprasart & Vilaivan, 2012).

## **1.2 Problem Statement**

The solution with wilt management in tomato lies in accurate diagnosis of the causal agent (bacterial or fungal), detection of the exact stage for prevention and ineffectiveness of the management strategy (Kailash, Dilip & Vinod, 2012). Variability of *R. solanacearum* makes application of chemicals an ineffective control strategy. Apart from losing their efficacy due to pathogen variability, applied pesticides lead to residue toxicity and environmental pollution. In addition, application of pesticides after appearance of wilt symptoms results in losses since the pathogen is highly fastidious, thus hard to control after infection. Moreover, most of the chemicals used for soil fumigation have been banned by the World Health Organisation (WHO). Such chemicals include; methyl bromide, chloropicrin and metham sodium (Renwick, 2008; Christos, Damalas & Eleftherohorinos, 2011). The export markets have also introduced

stringent conditions on minimum and maximum residue levels (Karungi, Kyamanywa, Adipala & Erbaugh, 2011).

Biological control agents (BCAs) have the potential of managing the disease to below economic injury levels but their efficacy is hampered by the harsh environmental conditions, short shelf life and inability to reach the target sites with potency. The efficacy of these BCAs is affected by soil pH, soil moisture, soil electrical conductivity, environmental temperature and other biotic factors which hinder penetration and efficacy in the plant system (Paulitz & Belanger, 2001).

Another important precursor for an effective disease control method is precise and accurate disease diagnosis which should be pathogen-based. For instance, wilting in tomato is associated with both fungal and bacterial pathogens that is, *Fusarium oxysporum* and *R. solanacearum*, respectively. Unlike the fungal wilts that can be controlled by chemical application, bacterial wilt is very difficult to control and often results in huge yield losses (Jahanshir & Dzhililov, 2010). The most common method of determining whether the causal agent for the wilt is either fungal or bacterial is the bacterial oozing test (Kim, Olson, Schaad & Moorman, 2003). The problem with the test is that it only happens when the bacterial load is very high and may have spread widely. Also, most accurate methods like PCR and enzyme based tests require specialized skills and equipment which may not be available to most farmers in Sub-Sahara Africa (SSA) (Christian, Kammer & Baalousha, 2008).

Additionally, application of most control measures only occurs after a significant damage has been done on the crop. The problem is also compounded by lack of effective biological pre-infection packages for the disease prevention (Paulitz & Belanger, 2001).

### 1.3 Justification

Use of resistant varieties is the simplest and most effective method in plant disease control (Muriungi, Mutitu, Muthomi & Muriungi, 2014). But resistance is overcome by development of new pathotypes as well as the genotype by environment interactions (Abdalla, 1998). Therefore stabilizing host plant resistance in the framework of an integrated disease management is the most suitable approach in disease control. Thus need for development of a pre-infection package to be applied before infection of tomato plants by the pathogen. Additionally, a mechanism for accurate diagnosis of the *R. solanacearum* pathogen at the below injury level threshold is paramount in the wilt disease management.

In spite of being environmentally friendly, increasing plant productivity and improving soil structure, use of microbial antagonists is hampered by harsh environmental conditions, reduced potency during storage and inability to reach the target sites after application. Biocontrol agents, thus require to be combined with other materials for increased vitality and effective delivery within the plant system to enhance efficacy. Nanocomposites have the potential for delivery of biocontrol agents due to their ease of functionalization, large surface area for adsorption and ability to penetrate epithelial layers. Chitosan and silica nanoparticles are preferred because they are non-toxic, have potential of enhancing host plant resistance, are easily assimilated by the root hairs thus delivery of the adsorbed materials and are abundant naturally. The chitosan-silica nanocomposites also induce other effects in plants such as increased yield and elicitation of resistance (Helander, Nurmiäho-Lassila, Ahvenainen, Rhoades & Roller, 2001).

Nanoparticles and nanocomposites can also be tuned to develop disease diagnostic probes due to their compatibility, reactivity, large surface area, colorimetric properties, structural changes and other observable variations under different conditions. Development of a colorimetric nanoprobe for detection of *R. solanacearum* was

desirable in management of the disease (Chi, Liu & Guan, 2010). The nanoprobe is preferred for use by farmers mainly in SSA due to its simplicity, rapidity and accuracy. Thus, use of an environmentally sound and effective remedial measure with effect on crop productivity and performance is a panacea for optimal greenhouse tomato production to many farmers and consumers in Kenya (Jones, 2012). Hybrid tomato varieties of Anna and Chonto were used in this study due to their high yield, adaptability to greenhouse conditions and susceptibility to *R. solanacearum* wilt (Monsatto, 2013).

## **1.4 Objectives**

### **1.4.1 Overall Objective**

To control bacterial wilt in tomato using antagonistic microbes adsorbed on chitosan immobilized silica nanocomposites

### **1.4.2 Specific Objectives**

1. To develop bionanocomposite materials for the control of bacterial wilt in tomato
2. To determine the efficacy of bionanocomposites in the control of bacterial wilt in tomato
3. To develop a nanocomposite diagnostic tool for *R. solanacearum*

## **1.5 Hypotheses**

H<sub>0</sub>: Biocontrol agents are not compatible with nanocomposite materials to form a synergistic complex

H<sub>0</sub>: Bionanocomposites have no effect on bacterial wilt in tomato plants

H<sub>0</sub>: Nanocomposites are not potential disease diagnostic tools

## CHAPTER TWO

### LITERATURE REVIEW

#### 2.1 Tomato

##### 2.1.1 Origin, Taxonomy and Botany

Tomato (*Lycopersicon esculentum mill*, Linneus, 1753) belongs to the order solanales and family solanaceae. The family consists about 1,500–2,000 species making it one of the most diverse family of flowering plants (Sato *et al.*, 2012). The two main food crops with global distribution are potato and tomato. Other members are the nightshades, eggplants, tamarillo, horse nettles and other numerous ornamental flowers and fruit plants cultivated for their nutritional benefit. Tomato is thought to have originated in the South American Andes but its use as a food originated in Mexico and spread throughout the world following the Spanish colonization of the Americas (Jacobsen, Daniel, Bergervoet-van, Huigen & Ramanna, 1994).

Tomato is a model species for classical genetic and genomic studies. It has a chromosome number of  $2n=2x=24$ , though incidences of  $2n=2x=26$  have been reported. The cultivated tomato has about 12 wild relatives. These wild tomatoes have a large genetic diversity, which has contributed greatly to the breeding of modern tomato cultivars. This has resulted in tomato varieties with a polyploidy state and hybrids desired by the market. Thus many varieties are now widely grown, sometimes inside greenhouses in the cooler climates (Sato *et al.*, 2012).

The plant typically grows to 1–3 meters in height and has a weak stem that often sprawls over the ground and vines over other plants. It is perennial in its native habitat, although often grown outdoors in temperate climates as an annual. An average common tomato weighs approximately 100 grams. While tomatoes are botanically and scientifically the

berry-type fruits of the tomato plant, they can also be considered a culinary vegetable, causing some confusion (Peralta, 2005).

There exist two main types of tomato cultivars, that is, the determinate and indeterminate. Determinate varieties of tomatoes, also called "bush" tomatoes, are varieties that are bred to grow to a compact height of about 1.2 m. They stop growing when fruit sets on the terminal or top bud, ripen their entire crop at or near the same time, usually about a month and then die. They may require a limited amount of caging and/or staking for support, should not be pruned or "desuckered" as it severely reduces the crop. Examples are: Cal. J (Kamongo), Marglobe, Assila F1, Eden and Onyx (Musyoki, Omari & Mwangi, 2005; Peralta, 2005).

The indeterminate varieties of tomatoes are also called "vining" tomatoes. They grow and produce fruit over a long period of time at times over 1 year and can reach heights of up to 3-6 m. The varieties bloom, set new fruit and ripen fruit all at the same time throughout the growing season. They require substantial caging and/or staking for support and pruning and the removal of suckers. Examples are: Anna F1, Chonto F1, Joy F1, Monicah F1, Tylka F1, Kenom, Marglobe, Monset, Nemonneta among others. These varieties are mainly grown inside greenhouses due to the ideal growing conditions such as temperature, humidity, water utilization efficiency and pest management (Monsatto, 2013; Odame, 2009).

### **2.1.2 Tomato production**

Kenya is among the Africa's leading producer of tomato and is ranked 6<sup>th</sup> in Africa (Food and Agriculture Organization, 2012). The crop is one of the most important vegetable crop ranking 2<sup>nd</sup> to Brassicas (cabbages and kales) in quantities produced and value (Masinde, Anastacia, Kwambai, Thomas & Wambani, 2001). It accounts for 14% of the total vegetable produce and 6.72% of the total horticultural crops (Government of

Kenya, 2012). Tomato is an attractive cash and food crop for small scale farmers and provides a potential source of employment to many rural and urban Kenyans. In 2013, it is estimated that the country produced 539,151 tons of tomato valued at over 10 billion Kenya shillings (FAO, 2013). Tomato is grown almost in all arable areas in Kenya including the arid and semi arid lands (ASALs) using irrigation, this therefore makes the crop an attractive source of food and income in a wide ecological area. Production of greenhouse tomato has also gained currency in the country due to the near ideal conditions, shortened maturity rate and prolonged production phase. Greenhouse tomato production in Kenya accounts for over 5 % of the total tomato yield though there is an exponential rate of adoption by farmers (Seminis, 2007; Kenya Horticulture Competitiveness Project, 2012).

The greenhouse tomato production has however been adversely affected by bacterial wilt caused by *R. solanacearum*. The pathogen has a wide host range including potato, tobacco, banana and ornamental plants (Cerkauskas, 2004). Secondary hosts include pepper, sweet potato and weeds. Soil is a potential source of primary inoculum where the disease has been noted even in the 1<sup>st</sup> planting season of newly cleared land (Kim, Olson, Schaad & Moorman, 2003). The bacterium can survive in soil for prolonged period without a host plant. This makes cultural and chemical control practices ineffective (Cerkauskas, 2004).

### **2.1.3 Importance and utilization of tomato**

Tomato is a major vegetable crop that has achieved tremendous popularity over the last century. It is grown in practically every country of the world in outdoor fields, greenhouses and nethouses. The plant is versatile and the crop can be divided into two categories; fresh market tomatoes and processing tomatoes. Tomato fruits, aside from being tasty, are healthy as a good source of vitamins A and C. Vitamin A is important for bone growth, cell division and differentiation, for helping in the regulation of

immune system and maintaining surface linings of eyes, respiratory, urinary and intestinal tracts. Vitamin C is important in forming collagen, a protein that gives structures to bones, cartilage, muscle and blood vessels. It also helps maintain capillaries, bones and teeth and aids in the absorption of iron (Maria, Rafael, Clara & Diego, 2014).

Another important nutritional benefit is the lycopene which is a powerful antioxidant that can help prevent development of many forms of cancer. Cooked tomatoes and tomato products are the best source of lycopene since lycopene is released from tomato when cooked. A raw tomato has about 20% of the lycopene content found in cooked tomatoes. However, raw or cooked tomatoes are considered the best source for this antioxidant (United State Department of Agriculture, release 28).

#### **2.1.4 Diseases and pests in tomato**

Tomato varieties vary in their resistance to pests and diseases. Modern hybrids focus on improving disease resistance over the heirloom plants. Common tomato diseases include; mosaic virus, mildew and blight are also common tomato afflictions. Other dreaded diseases are wilts caused by bacteria and fungi and anthracnose. Some common tomato pests are stink, cutworms, tomato hornworms, aphids, whiteflies, fleabeetles, red spider mites, slugs, nematodes and moths including *Tuta absoluta* (Karungi *et al.*, 2011). Tomato plants produce peptide hormone systemin after an insect attack. Systemin activates defensive mechanisms, such as the production of protease inhibitors to slow the growth of insects. Other proteins and compounds have also been produced in tomato plants infected by pathogens such as glucanases, chitinases, catalyses, hydrogen peroxide (Barea, Azcon & Azcon-Anguilar, 2002).

## **2.2 Bacterial Wilt of Tomato**

### **2.2.1 Life Cycle, Etiology, Epidemiology and Dissemination of Bacterial Wilt**

Bacterial wilt of tomato is caused by *R. solanacearum* which is a gram-negative bacterium. The bacterium is reported to be primarily a soil and water borne pathogen (Adebayo & Ekpo, 2005). It has a biphasic life cycle characterized by life in open systems and life in association with plants. The pathogen infects host plants mainly through the roots, entering through wounds formed by lateral root emergence or by damage caused by soil borne organisms like the nematodes (Adebayo & Ekpo, 2006). Once inside the roots or stems, the bacterium colonises the plant through the xylem in the vascular bundles and blocks water uptake resulting in wilting and eventual death. The bacteria also secretes cell degrading enzymes such as endoglucanase, exoglucanase, endopolygalacturonase, exopolygalacturonases, pectin methylesterase which are all associated with the virulent strains (Deeny, 2006). Additionally, after colonization of the vascular system, the virulent strains produce copious amounts of extracellular polysaccharides which are long polymer N-acetylated monosaccharides which are implicated to cause wilting in the affected crops (Newman, Dow & Daniels, 2001). An important virulence factor is the swimming motility mediated by chemotaxis. Application of fumigants in the soil was observed to inactivate the flagellin structural gene affecting the bacterial motility hence reduced virulence of the mutants (Yao & Allen, 2006). In addition, compounds that result in synthesis of enzymes antagonizing the aforementioned ones has an effect on disease establishment in plants (Prevost, Couture, Shipley, Brzezinski & Beaulieu, 2006).

There exists five races and five biovars of *R. solanacearum* based on host range and differential ability to produce acid from a panel of carbohydrates (Deeny, 2006). The pathovars have different host ranges and geographical distribution. Different races infect different crops like the race 3 mainly affects potatoes while race 1 infects tomatoes. The

race 1 biovar 2, 3 and 5 infect tomatoes with biovar 2 being the most prevalent and devastating pathovar of the tomato crop. The tomato race of *R. solanacearum* has a wide host range, is highly variable in genotype and aggressive; they are therefore able to cause severe wilting, even to tomato varieties classified as resistant (Deeny, 2006; Messiha, 2006).

Bacterial wilt disease is most severe in greenhouses due to high temperature (25-35°C), humidity (80-95%) and low edaphic pH (<6) which are the ideal greenhouse conditions. These conditions make the pathogen more aggressive thus devastating the crop. The pathogen is mainly spread from infested to healthy fields by farm equipment, irrigation water and plant-to-plant through the rhizosphere. The pathogen is highly persistent and only antagonistic micro-organisms and environmental factors that can affect its survival (Champoiseau, Allen & Momol, 2009).

## **2.3 Control of Bacterial Wilt of Tomato**

### **2.3.1 Cultural Methods**

Attempts have been made to use different growing methods in order to overcome the bacterial wilt disease. These methods include; selection of fairly resistant varieties and planting sites that are not endemic with the pathogen, reduced density of planting to reduce spread, use of drip irrigation and manipulating the microclimate with greenhouses to minimize the environmental agents of dispersal. Other methods such as rotational cropping where a solanaceae crop is alternated with a crop from a different family, field solarization and roguing infected plants have been employed with minimum success (Muriungi *et al.*, 2014).

### 2.3.2 Chemical Methods

Use chemicals such as methyl bromide, metham sodium, basamid, furadan and copper derivatives have been tried unsuccessfully because of the variability of the pathogen. The chemicals have also been associated with adverse environmental pollution. Recently, the use of methyl bromide has been banned due to effect on environment and biodiversity (Kyoto Protocol, 2005; Christos *et al.*, 2011; GoK UNEP, 2008). There has also been increased consumer awareness and strictness on phytosanitary issues. Chemical use also features highly in the eleven hurdles to pass when exporting produce to the European markets. There have been deliberate efforts to introduce certifications for compliance, maximum residue levels and global good agricultural practices. These attempts endeavour to reduce or eliminate use of synthetic chemicals in production of food (Nguyen & Ranamukhaarachchi, 2010).

### 2.3.3 Biological Methods

Plant growth regulating rhizobacteria and fungi (PGPR/F) have been observed to play a role in the biocontrol of BWT. There is a negative correlation between biocontrol agents and the *R. solanacearum* caused disease, in that, when the bioagents are in high concentration in the rhizosphere, the pathogen is highly suppressed. Biological control agents work very well in managing the disease in rhizospheres rich in organic matter as they act as good reservoir for these biocontrol agents enhancing their efficacy (Ahemad & Khan, 2010; Guo, Tang, Ju, Ding & Liao, 2011).

In related studies, Elphinstone and Aley (1992) found a decline of *R. solanacearum* in the maize rhizosphere due to an increased population of *Pseudomonas fluorescens* which was antagonistic *in vitro* to *R. solanacearum*. Additionally, colonization of the rhizosphere by Arbuscularmycorrhiza fungi (AMF) has been shown to reduce the damage caused by soil-borne pathogens (Rini, 2001; Harrier & Watson, 2004).

According to Rini and Solachana (2006), *T. viride* has been found to have antagonistic effect on most bacterial and fungal pathogens. *P. fluorescens* was found to be effective in reducing bacterial wilt (BW) incidence in both glass house and field conditions. This follows earlier work by Weller (1988) leading to the suggestion that, it can be evaluated as a possible bio-control agent for the BW pathogen.

Bacteriophages also offer an alternative to conventional management strategies for controlling bacterial plant diseases. Although many studies provided positive results using phage, phage therapy has not been considered a good strategy for controlling plant pathogenic bacteria because of its unreliability and the narrow spectrum of activity intrinsic to phages. Additionally, the plant environments in which phages are required to operate are less than ideal. Within the phyllosphere, ultra violet (UV) exposure, intense visible light and desiccation are all factors that reduce phage viability and disease control ability. In studies examining persistence in the phyllosphere, phages applied to tomato leaves during the early morning were unrecoverable 24 h after application. Compared with the phyllosphere, the rhizosphere environment is less harsh, but the phages have significant obstacles including a relatively low diffusion rate through heterogeneous soil matrices that changes as a function of available free water, biofilms that can trap phages, soil particles that can reversibly adsorb phages, and low soil pH that can inactivate phages. In natural environments, as a result of low rates of phage diffusion and high rates of phage inactivation, low numbers of viable phages are available to lyse target bacteria. One additional factor needed for a high degree of success is that high populations of both phage and bacterium must exist in order to initiate a chain reaction of bacterial lysis (Yamada, 2007; Yamada, 2010).

Although some success has been achieved with use of biocontrol agents in controlling plant diseases, deployment of these agents in agricultural systems is challenging given the need to maintain high populations in soil and/or plant surfaces and the inability to adapt easily in a harsh environments (Balogh *et al.*, 2010). In addition to reduction of

the pathogen virulence, Nowak (1997) found out that treatment of plants with biological control agents had a higher biomass (fresh and dry weight) compared to untreated plants. Reduction of BWT by the biocontrol agents is attributed to the competition of space, nutrients and ecological niches or production of anti-microbial substances and indirectly, through induction of systemic resistance (ISR).

To ameliorate microbial agents' inability to adapt to the environment, various materials have been used for encapsulation, coating, adsorption and attachment to enhance their efficacy. Some of these materials include clay, silica, organic polymers such as cellulose and chitin. Other materials are inorganic polymers like the polyethylene. These materials provide the microbes with a substrate for attachment and reversibly release the microbial agents on reaching the target sites. Recently with technological advancement, nanomaterials have been found to be suitable microbial delivery materials. The materials are preferred due to their ability to penetrate cellular walls of plants and affinity for pathogenic microbes thus precision in delivering the microbial agents to the pathogen infected areas within a plant. In addition, some materials such as chitin and silica possess antimicrobial effect on pathogens and may act synergistically with the beneficial microbes in the control of the pathogens. The materials also play nutritional roles in plants as they provide plant nutrients such as nitrogen, silicates, carbon and other micro nutrients enhancing plant productivity (Kubata *et al.*, 2005).

#### **2.4 Nanoparticles, Nanocomposites and Colorimetric Materials**

A nanoparticle is a submicron moiety with particle size ranging from 1-500 nm. Some nanoparticles are quite small with the particle size ranging from 0.1-20 nm and are known as quantum dots. Due to their minute sizes, the particles are easily tuned depending on their intended use. The materials are also easy to interact in multiphase systems forming nanocomposites. This confers the resultant composites the aspects of the constituent materials and reduces aggregation of homologous materials, ensuring

activity takes place under certain conditions only which increases their efficacy. Nanoparticles and nanocomposites are easily synthesized by use of physical, chemical and biological methods. Chemical methods and their combinations have been used successfully in commercial scale while biological synthesis has not reached commercial scale. The main chemical methods used involve use of reagents for solubilizing, reducing and stabilizing while physical methods entail centrifuging and electrospinning. A combination of the two methods is more common where materials are mixed with reagents and centrifuged or electrospun (Tim *et al.*, 2008, Agasti *et al.*, 2010).

#### **2.4.1 Chitosan**

Chitosan is a cationic linear polysaccharide composed of D-glucosamine (deacetylated unit) and N-acetyl-D-glucosamine (acetylated unit) in varying ratios. The polymer is processed through deacetylation of chitin using an alkali. Chitin occurs naturally in shells of crustaceans, cell walls of fungi and exoskeletons of insects (Krajewska, 2004). It can also be processed biologically by use of enzymes, but this method is limited due to the insoluble nature of chitin in water. The amount of chitosan formed from chitin is expressed as a percentage known as the degree of deacetylation (% DDA) often determined using spectral and quantitative methods. Chemically, chitosan has good chelating ability associated with the hydroxyl and amino groups which serves as ligands for most ions to form complexes (Dutta, Rayikumar & Dutta, 2002). The polymer has been used in agriculture for seed treatment, fruit coating and as a soil amendment (Prevost *et al.*, 2006). It has also been used in medicine in delivery of enzymes, genes and drugs. Chitosan can be synthesized into chitosan nanoparticles by centrifuging or electrospinning using polyphosphates solvents. The formed nanoparticles have a larger surface thus, increased utilization (Li, Deng, Liu & Xin, 2010).

### **2.4.2 Mesoporous Silica Nanoparticles (MSN)**

Silica is easily synthesized into silica nanoparticles enhancing its utilization. The nanoparticle has a higher enzyme loading and retention ability and facilitate transport of materials as a substrate due to its; exceptionally high immobilization efficiency, large gallery spaces internally and functionable surface. The material is also compatible with other materials such as cellulose, chitin and transition metals. Additionally, the mode of action of silica in disease control as well as of bacterial antagonists against *R. solanacearum* has not been clarified to date (Currie & Perry, 2007). Apart from helping in suppressing pathogens, mesoporous silica nanoparticles are good carriers of biological agents as the material is non-toxic and has a good functional surface. The surface can allow adsorption of bioagents and desorption when a suitable host is available. This helps in precision and sustained delivery of fragile bioagents enhancing their efficacy upon reaching the target site (Kim *et al.*, 2005).

### **2.4.3 Colorimetric Probes**

Some materials such as iron, gold, copper have the ability of binding analytes resulting in a colour change. Other materials also change their colour when analytes remove or add ion (s) to them (Qian, Goodell & Felix, 2002). The materials can be harnessed in development of colorimetric detection products for determination the presence of such analytes (Chi, Liu & Guan, 2010). The technology is preferred due to its simplicity as it utilizes visual aspects for sensing unlike use of other methods that require special skills like spectrometry (Chi *et al.*, 2010). The method has been used in determination of industrial water pollution, presence of water borne pathogens and presence of particular enzymes in biotic systems (Helander, Nurmiäho-Lassila, Ahvenainen, Rhoades & Roller, 2001).

### 2.4.3.1 Iron Nanoparticles

Iron is the fourth most abundant material in the earth's crust (5.6%) by mass. Being a transition metal, it possesses desirable characteristics such as ease of synthesis into supermagnetic, nanoparticles and colorimetric forms due to redox activities (Plate 2.1). Synthesis of the nanoparticles is easily done by use of physiochemical methods like reduction using sodium hydride and centrifuging or electrospinning (Sun, Zhang, Lu & Gao, 2008). Green synthesis of the nanoparticles is also possible by use of organic polyphenols as reducing agents followed by centrifuging or electrospinning (Hutchison, 2008).



**Plate 2.1: Different concentrations of Fe (II),** Source: Odingo, 2013.

Iron nanoparticles are also characterized by colour change when complexed with different compounds such as other metals and biological agents such as enzymes or proteins. For instance, iron oxide nanoparticles have been used to recognize elements and detect proteins through interactions between cationic monolayers on the iron oxide nanoparticles and analyte proteins (Plate 2.2). The resulting complexation is colorimetric and can be applied in the detection identification of proteins (Liet *al.*, 2012).

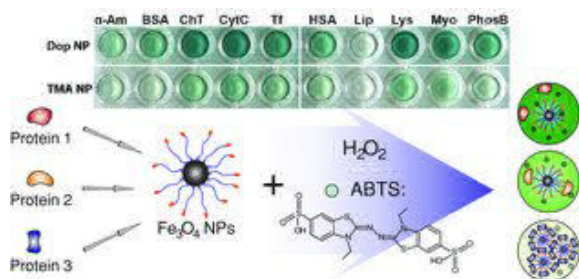


**Plate 2.2: Colorimetric protein sensing**, Source: Li et al., 2012.

### 2.4.3.2 Nylon Nanofibres

The use of nylon-6 electrospun nanofiber mats as reinforcement with synergistic effect in tensile strength and toughness is important in development of materials of a particular shape, size and form. Nylon nanofibres are easily synthesized by passing a solution of MF resin in a high voltage electrospinning machine (Dutta, Mahapatra & Datta, 2011). This results with dense a mass of nylon nanofibres with a range of applications (Plate 2.3). The nylon fibers are preferred due to their ability to adsorb other nanoparticles, particularly the polar ones resulting in formation of complex composites. In such cases, nylon nanofibres host the nanoparticles preventing disintegration and/or selective aggregation of similar nanoparticles which can potentially destroy or affect their intended activity (Rosi & Mirkin, 2005).

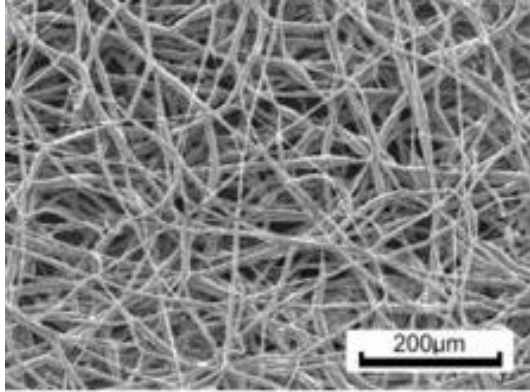


**Plate 2.3: Nylon nanofibres with 200 nm,** Source: Ondingo et al., 2013.

## CHAPTER THREE

### SYNTHESIS AND EVALUATION OF BIONANOCOMPOSITE MATERIALS FOR THE CONTROL OF BACTERIAL WILT IN TOMATO PRODUCTION

#### ABSTRACT

Biological control agents (BCAs) have potential for disease management but their efficacy is limited by reduced vitality during storage, harsh environment and inability to reach the target site for effective disease control. Use of carrier materials has been adopted in delivery of botanical extracts, biological agents and enzymes. Such active ingredients require sustained release, adsorption material to increase shelf life and precise delivery to the target sites. Various materials such as polymers, fibers and nanomaterials have been used as carriers for genes, enzymes and biological agents. Use of nanomaterials has become popular recently due to their ease of functionalization, ability to carry numerous materials on their large surfaces and that the quantum dots are able to penetrate epithelial and epidermal layers easily ensuring precise delivery of the adsorbed materials. In this study, chitosan immobilized silica nanocomposite (CISNC) was synthesized. The nanocomposite was then used to deliver BCAs for controlling *R. solanacearum*. The process entailed deacetylation of chitin into chitosan, functionalization of chitosan into chitosan nanoparticles and immobilization of chitosan on sparingly dissolved mesoporous silica nanoparticles (MSN). The formed nanocomposite was used to adsorb BCAs by vortexing and shaking on rotary shake and then characterized using Fourier transform infra red (FTIR) and x-ray powder diffraction (XRD) techniques. Bioassays on effect of the BCA-nanocomposite complex were also conducted to determine efficacy. There was successful formation of nanomaterials such as chitosan nanoparticle, CISNC and nanoclay with crystallite sizes of 2.5, 3.8 and 23 nm respectively. Characterization of the nanocomposites showed physisorption properties indicating good sorption properties desirable for a carrier material. Adsorption

of BCAs on the nanocomposite carriers enhanced their efficacy significantly ( $P \leq 0.05$ ) by increasing antimicrobial effect, enhancing germination and growth vigour of tomato plants. Effective microorganisms adsorbed on CISNC had the highest pathogen inhibition and germination/growth vigour both *in vitro* and in greenhouse tests. Deacetylation and subsequent immobilization of chitin on MSN increased its efficacy in controlling the pathogen and increasing tomato wilt resistance. For sustainability in production of the nanocarrier material, montmorillonite clay was functionalized into nanoclay to substitute MSN in developing chitosan immobilized nanoclay composites (CINC).

### **3.1 Introduction**

Bacterial wilt of tomato is a serious disease of tomato in Kenya (Kenya Horticulture competitiveness project, 2012). The disease pathogen thrives under high temperature and humidity in greenhouse and under field conditions (Champoiseau *et al.*, 2009). Use of chemicals to control the disease has resulted in accumulation of chemicals in the food chain, environmental pollution and ineffectiveness due to pathogen mutations. Thus need for a sustainable and safe method of disease management (Jeonget *al.*, 2007). Biological control has the potential of controlling the pathogen and several plant growth promoting rhizobacteria and fungi have been tested. The microbes are able to produce volatile compounds and different lytic enzymes that are known to suppress the pathogen (Nguyen & Ranamukhaarachchi, 2007). However, commercial utilization of the BCAs has not been realized (Pal & Mc Spadden, 2006).

Application of microbial antagonists and viral therapy for bacterial disease control is an attractive and a likely antidote for the pathogen. However, field efficacy of the antagonists is constrained by their short shelf life, inability to adapt and reduced virulence to the pathogen when applied in a harsh environment, hence need for an appropriate carrier material in delivery of the biological antagonist through soil and

plant system (Spadaro & Gullun, 2005). In order to increase the efficacy of the BCAs, compatible carrier materials such as clay, silica and polymers have been tested (Kubata *et al.*, 2005). Hybrid tomato varieties of Anna and Chonto were used in this study due to their high yield, adaptability to greenhouse conditions and susceptibility to *R. solanacearum* wilt (Monsatto, 2013).

## **3.2 Materials and Methods**

### **3.2.1 Experimental Site and Layout**

The experiments were carried out at Jomo Kenyatta University of Agriculture and Technology (1.0891° S, 37.0105° E and altitude 1400 metres above sea level (m ASL)) at the Departments of Chemistry and Horticulture in GoK and phytotechnology laboratories and greenhouse for synthesis, *in vitro* and field tests respectively.

All reagents were at least analytical grade. Sodium hydroxide (NaOH) pellets, acetic acid, glutaraldehyde (25%), L-cysteine, hydrogen peroxide (H<sub>2</sub>O<sub>2</sub>), phosphate buffered saline (PBS), tri-poly phosphate (TPP), potassium dichromate (K<sub>2</sub>Cr<sub>2</sub>O<sub>7</sub>), sulphuric acid, hydrochloric acid, orthophosphoric acid, diphenyl amine indicator, ammonium ferrous sulphate, copper sulphate, mesoporous silica nanoparticles (MSN), chlorox, tetrazolium chloride (TZC) were obtained from Sigma Aldrich, UK. PCR kit, primers forward–GAA CGC CAA CGG TGC GAA CT-, and reverse –GGC GGC CTT CAG GGA GGT C- for *R. solanacearum*, forward–GTG CCT GCC TCC AAA ACG ACT- and reverse–GAC GCC ACC CGA TCC CGC ATC CCT C- for *R. solanacearum* phage, agarose gel, ethidium bromide, Casamino acid-Peptide-Glucose (CPG) medium, nutrient broth and potato dextrose agar (PDA), were obtained from Bioneer Corporation, hybrid tomato seeds (Anna and Chonto) were purchased from De ruiters, chitin (99 %) was acquired from Laborex, *Bacillus subtilis* and *Trichoderma viride* from Real IPM, *Glomus mosseae* (*mycorrhiza*) was obtained from Juanco SPS Ltd Kenya and effective micro-

organisms were obtained from EM Technologies ltd, Embu, Kenya. Cocopeat and planting trays were obtained from Amiran (K) Ltd.

### **3.2.2 Preparation of Chitosan (CHT) and Chitosan Nanoparticles (CHTNP)**

Chitin was ground using a milling machine to obtain fine powder which was filtered on a 0.1 mm mesh to obtain very fine powder. It was then autoclaved at 121 °C for 15 min after the autoclave attained a constant temperature of 121 °C. It was then divided into 6 equal portions of 100 g each. The samples were treated separately with 20, 40, 60, 80 and 100 % (w/v) NaOH solutions. The samples were then placed in an oven at 100 °C for 4 hr for deacetylation (removal of acetyl groups from the polymer) to take place. Modified centrifuge-ionic gelation method was used for synthesizing chitosan nanoparticles by solubilizing chitosan in 1 M acetic acid to obtain a concentration of 1g/10 ml, 1 ml hydrogen peroxide and 10 ml TPP (10% w/v) were added followed by centrifuging at 6000 rpm for 10 min to form chitosan nanoparticles. The sample was then characterized using SHIMADZU Fourier transform infra red (FTIR) spectrometer (Domszy and Roberts, 1985) and Rigaku X-ray powder diffractometer (XRD) (Ogawa &Yui, 1993; Wazed, Joshi &Rajendran, 2011).

### **3.2.3 Determination of Deacetylation**

The degree of deacetylation was determined by estimation of carbon and nitrogen contents in chitin and chitosan. The elemental ratio of carbon and nitrogen were used to determine deacetylation. Equations i, ii and iii were used as shown below.

#### **3.2.3.1 Percent of Carbon**

This was done by determination of percent (%) carbon in the chitin and chitosan based on the Walkey-Black chromic acid wet oxidation method. The amount of carbon was estimated as percentage using the following equation;

$$C = \frac{(B-T \times 0.3 \times V \times 0.75)}{WB} \dots\dots\dots i$$

Where; C=carbon percentage, B=amount of titrant consumed by blank, T= amount of titrant consumed by sample, W=weight of the sample, V=volume of K<sub>2</sub>Cr<sub>2</sub>O<sub>7</sub>, 0.3=constant, 0.75=assumption that the sample had 75% carbon (Jaber, Mehanna & Sultan, 2009).

### 3.2.3.2 Percent of Nitrogen

Percentage nitrogen in chitin and chitosan were determined using the Kjeldahl method.

$$\frac{N(\%) = (V_{HCl} \times NHCl) - (V_{BK} \times NNaOH) - (V_{NaOH} \times NNaOH)}{1.4007W/100} \dots\dots\dots ii$$

Where;

**V<sub>HCl</sub>** – Volume (mL) of standard **HCl** pipetted into titrating flask for sample

**NHCl** - Normality of **HCl**

**V<sub>BK</sub>** – Volume (mL) of standard **NaOH** needed to titrate 1 mL standard **HCl** minus B

B – Volume (mL) of standard **NaOH** needed to titrate reagent blank carried through the method and distilled into 1 mL standard **HCl**

**NNaOH** - Normality of **NaOH**

**V<sub>NaOH</sub>** – Volume (mL) of standard **NaOH** needed to titrate the sample

1.4007- milliequivalent weight of nitrogen \*100

W - Weight of the sample in grams. (Jaber *et al.*, 2009).

### 3.2.3.3 Calculation of Degree of Deacetylation (DDA)

The % C and N in chitosan were used to determine the DDA in chitin using the Kasaii

$$\text{equation; DDA \%} = \frac{(6.857) - \left(\frac{C}{N}\right)}{1.7148} \dots\dots\dots\text{iii}$$

Where; DDA-degree of deacetylation, 6.857-Constant, C-Percentage Carbon, N-Percentage Nitrogen, 1.7148-Constant (Cullity & Stock, 2001).

### 3.2.4 Preparation of Chitosan Immobilized Silica Nanocomposite (CISNC)

A 500 mg sample of mesoporous silica nanoparticles (MSN) was dispersed in 100 ml phosphate buffered saline (PBS) to form a partial solution. Solubilized chitosan nanoparticles (50 ml) were added to 100 ml of MSN suspension. The mixture was vortexed for 2 min and placed in a vibratory shaker for 2 hr then stirred with a magnetic stirrer for 2 hr. The excess suspension of MSN that was not adsorbed in the chitosan gel matrix was poured carefully and disposed leaving behind a gelly substance of chitosan-silica nanocomposites. A drop of 25% glutaraldehyde was added to the chitosan nanoparticles-MSN mixture using a syringe. The mixture was vortexed and placed on a magnetic stirrer for 1 hr (Kubata *et al.*, 2005) and (Zhang, Chen & Chen, 2002). This resulted in the formation of chitosan immobilized silica nanocomposite gel denoted CISNC.

### 3.2.5 Determination of Crystallite Sizes of Chitosan Nanoparticles and Nanocomposites

The CISNC was dried at 50 °C for 48 hr to obtain a plaque that was used for XRD characterization. The crystallite sizes were determined using Scherrer equation;

$$D = \frac{K\lambda}{\beta \cos\theta} \dots\dots\dots\text{iv}$$

Where,  $D$  is the crystallite size  $\lambda$  is wavelength of X-ray,  $\beta$  is full width and half maxima value,  $\theta$  is Bragg's angle (Cullity & Stock, 2001).

### **3.2.6 Isolation of *R. Solanacearum***

Diseased hybrid tomato plant materials were obtained from a greenhouse in Thika, Kiambu County. The area is an endemic zone of *R. solanacearum* pathogen with reported wilt incidences of over 70% (KHCP, 2012). The plants were thoroughly washed to remove dirt. They were then dipped in 1% chlorox for sterilization. The lower stem was cut into small pieces of 5cm cross-sectionally and cut longitudinally then placed in a 1 L beaker containing distilled water to allow flow of bacterial exudates. The obtained bacteria were cultured in a sterilized growth chamber for 48 hr at 32 °C on TZC medium contained in petri-dishes. The colonies observed using a hand lens and light microscope. Virulence of the pathogen was associated with the appearance of whitish and irregular round colonies with pink margins in cultured pathogen under light microscope (Denny & Hayward, 2001; Jeonget *al.*, 2007).

### **3.2.7 Isolation of *R. solanacearum* Phage**

A viral suspension was prepared from soil samples collected from the *R. solanacearum* infested greenhouses. The soil was sieved through a 1 mm sieve to obtain fine particles. 50 g of the soil, adjusted to 40 % moisture holding capacity with sterile distilled water was placed in 500 ml conical flasks. Each flask was seeded for 48 hr with cultures of the host bacteria (2.000 optical density *R. solanacearum* inoculum). The enriched soil samples were suspended in phosphate buffered saline (PBS). The mixture was centrifuged in 50 ml plastic tubes at 2000 revolutions per minute (rpm) for 10 min. The supernatant was aseptically transferred to a sterile 15 ml tube without disturbing the pellet. A viral suspension was prepared by aseptically filtering the supernatant through a 0.8  $\mu$ m pore sized cellulose filter to remove particulates, followed by

filtration through a 0.45 µm pore sized filter to remove bacterial cells and cellular debris. Three drops of 2.000 optical density *R. solanacearum* inoculum were added to 1 ml of the isolated phage and cultured on nutrient broth for 48 hr at 32 °C. The phage was cultured in a sterilised growth chamber for 48 hr at 32 °C on 20 ml nutrient-TZC agar. The plaques on the cultured pathogen confirmed positive isolation of the phage (Yamada, 2007).

### **3.2.8 Isolation of DNA from *R. solanacearum* and Phage**

Suspensions of isolated and cultured *R. solacearum* and *R. solanacearum*-phage cells were prepared using distilled water. The suspensions were standardized to an optical density (O.D) of 2.000 observed at 600 nm on the SHIMADZU Ultra violet visible (Uv-vis) spectrophotometer. The suspensions were used for DNA extraction using the CTAB extraction method. CTAB extraction buffer (500µl) comprising of (100Mm Tris Hcl (pH 8), 2% (wt/vol) CTAB, 50Mm EDTA, 0.7 M NaCl, 0.17% (vol/vol) β-mecarptoethanol and 1% (w/v) PVP), pre-warmed to 65 °C, two glass beads added and the mixture placed in miller at a frequency of 30/sec for 5 minutes. Samples were incubated at 65 °C for 30 min in a water bath. Chloroform (500 µl) -isoamylchloroform) (24:1 v/v) was added and the two phases were mixed several times by vortexing. The tubes were centrifuged at 14,000 rpm for 10 min at room temperature in a microfuge. The supernatant was removed and transferred into new 1.5 Eppendorf tube. 10 µl of RNase A was added and mixed by vortexing. The samples were then incubated in a water bath at 37 °C for 30 min. Centrifuging and addition of RNase A were repeated to ensure that all RNA was removed from the DNA. An equal volume of cold isopropanol (pre-chilled in a -20 °C freezer) was added, mixed and incubated at -20 °C in a freezer for 30 min. The samples were then centrifuged at 14000 rpm for 10 min at room temperature in a microfuge and supernatant removed. 500 µl of 70% ethanol (at room temperature) was added to the tube containing DNA, centrifuged at 14000 rpm for 5 min and the supernatant carefully poured off. The 70% ethanol wash was repeated once, the supernatant carefully poured

off and the DNA pellet dried for 60 min by leaving the tube open. Low salt TE buffer (100 µl) was added to the dried pellet. The pellet was dissolved by incubating at 37 °C in a water bath for 30 min. A 1.0 µl of DNA was used for electrophoresis on agarose gel to determine presence of the DNA. The DNA was then stored at -20 °C (Korbie & Mattick, 2008).

### **3.2.8.1 Amplification of DNAs for detection**

The polymerase chain reaction (PCR) was done using touchdown procedures as described by Korbie and Mattick, 2008. The primers used were a 20 mer forward primer –GAA CGC CAA CGG TGC GAA CT-, and reverse –GGC GGC CTT CAG GGA GGT C- for *R. solanacearum* and 21 mer forward primer–GTG CCT GCC TCC AAA ACG ACT- and reverse –GAC GCC ACC CGA TCC CGC ATC CCT C- for *R. solanacearum* phage. The amplification reactions were performed in 25 µl volumes in thin-walled PCR tubes after optimization in a thermocycler (PTC-100), programmed for an initial 5 cycles of 30 sec at 94 °C, 3 min at 48 °C, annealing at 58 °C for 1 min, extension for 1 min at 72 °C, followed by 10 and 15 cycles at the same timing and conditions. The samples were cooled up to 4 °C, subjected to electrophoresis on a 1.5% agarose gel in 1X TAE buffer (40 mM Tris acetate and 1.0 mM EDTA). The obtained amplicons were interpreted using the stain ladders in the detection of the microbes (Wydra & Semrau, 2006; Fujiwara *et al.*, 2008).

### **3.2.9 Culturing of Biocontrol Antagonists (BCAs)**

The microbial products (*B. subtilis*, *T. viride*, *G. mosseae*) and effective microorganisms were centrifuged at 2000 rpm for 10 min to obtain a supernatant containing the cellular suspension. Five (5) drops of the supernatant were cultured on the respective media contained in petridishes to confirm viability. Nutrient agar (NA) was used to culture bacterial microbes while potato dextrose agar (PDA) was used to culture fungal

microbes. The cultured microbes in petridishes were tightly sealed to prevent cross-infection then placed in a growth chamber for 48 hr and 96 hr at 32 °C and 28 °C for the bacterial and fungal microbes respectively. After multiplication of the microbes, each bacterial microbes were carefully collected using a wire loop and the fungal microbes were collected using a needle, then placed in 10 ml distilled water and mixed for 5 min on a vortex mixer (Spadaro & Gullun, 2005).

### **3.2.10 Adsorption of Biocontrol Agents on Chitosan Immobilized Silica Nanocomposite**

Aliquot volumes of 50 ml for *B. subtilis*, effective micro-organisms and *R. Solanacearum* phage were adjusted to 2.000 optical density (O.D) at 600 nm using a Uv-vis spectrophotometer. A fungal stock solution with a concentration of  $10^{12}$  spores of *G. mosseae* and *T. viride* was prepared using a haemocytometer. The microbes were then added separately to each sample of 100 ml CISNC, placed on a rotary mixer (130 rpm) for 2 hr and on a magnetic stirrer for 2 hr to allow for adsorption. The concentration of microbes in the supernatant after adsorption was determined using Uv-vis spectrophotometer and haemocytometer for the bacterial and fungal microbes' respectively in determination of the adsorption efficiency. The desorption efficiency was determined after addition of 1 g/100 ml L-cysteine to the BCA-nanocomposite gel and centrifuging at 6000 rpm for 10 min (Kubata *et al.*, 2005). Adsorbed BCAs on CISNC gel were observed under the Nixon compound microscope.

### **3.2.11 In vitro Tests**

Freshly isolated *R. solanacearum* bacteria were used in the all experiments. *R. solanacearum* suspension was standardized to 2.000 O.D using UV-vis spectrophotometer then cultured on nutrient agar contained in a petridish. The experiment was laid out in a completely randomized design (CRD) with 18 treatments

and 4 replications inside a growth chamber at 32 °C for 96 hr. the treatments included; mesoporous silica nanoparticles (MSN), *Trichoderma viride* (TV), *Glomus mosseae* (AMF), *Bacillus subtilis* (BS), chitin, chitosan, chitosan nanoparticles, chitosan immobilized silica nanocomposites (CISNC), phage, effective micro-organisms (EM), CISNC-TV, CISNC-AMF, CISNC-BS, CISNC-Phage, CISNC-EM, glutaraldehyde and controls (acetic acid, distilled water).

Filter papers adsorbed with bionanocomposite were placed on particular pathogen colonies to determine inhibition of *R. solanacearum* using;

$$\text{Inhibition} = \frac{\text{Colony size after inhibition (mm)}}{\text{Colony size before inhibition (mm)}} \times 100 \dots\dots\dots V$$

(Algam, Xie, Li, Yu, Su & Larsen, 2010).

### 3.2.12 Seed Treatment

Tomato seeds (50) per treatment were soaked in 50 ml of 10% (bionanocomposite: distilled water) solution for 4 hr followed by drying for 1 hr in a growth chamber at 25 °C. They were then challenge inoculated with a 2.000 O.D *R. solanacearum* suspension for 30 min and left to dry overnight in a sterile lamina flow chamber. Seeds treated with acetic acid and distilled water served as controls (Champoiseau *et al.*, 2009).

### 3.2.13 Media Preparation

Cocopeat block (5 kg) was soaked in tap water to fragment and form a friable planting material. It was then washed with running water until a pH of 6.5 was obtained and autoclaved before placing in planting trays. Compound fertilizer NPK 17.17.17 (50 g), trace elements (5 g poly feed) and 100 ml of nutrient broth mixed thoroughly with prepared cocopeat to provide tomato seeds and micro-organisms with necessary starter nutrients respectively. Cocopeat was then placed on 60 hole- plastic trays.

### 3.2.14 Sowing of Seeds and Estimation of Germination Percentage, Chlorophyll Content, Growth Rate and Wilting Incidences

Treated hybrid tomato seeds from two varieties (Anna and Chonto) were sown in plastic trays. The seeds were closely monitored to determine germination, growth vigour and wilt incidences. The chlorophyll content in leaves was also determined 8 weeks after planting. Germination rate was estimated as a percentage of the seeds emerging against the number of seeds sown per treatment. The relative chlorophyll content in leaves was measured using the Chlorophyll Meter SPAD 505 (Minolta, Japan). The meter measured leaf transmittance at 600 nm. Measurement entailed sampling any three top leaves from one plant per treatment. The measurements were taken at different points and averages used to determine the chlorophyll content. Plant vigour or growth rate was taken by measuring the shoot growth using a tape measure after every 10 days. The change in shoot length was taken to represent growth rate. Wilting incidence was based on symptoms of wilting leaves which was monitored daily for 90 days after planting.

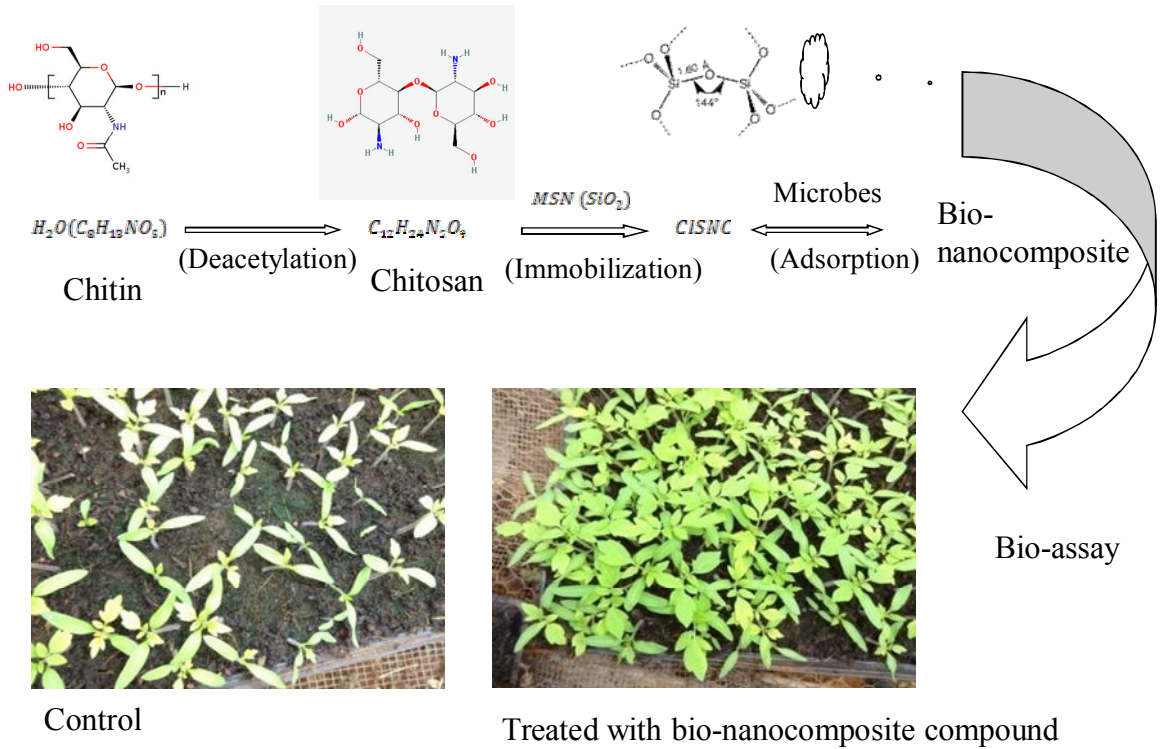
Disease severity was assessed using modified Champoiseau *et al.*, (2009) wilting scale of 1–5. Where 1-healthy; 2-mild wilting of one or two leaves during day time; 3-wilting of all but the top two leaves during the day time; 4-wilting of all leaves during the day; or 5-wilting of all leaves during daytime and no recovery when cool early in the morning or late in the evening.

Wilting incidence was calculated using the formula:  $\frac{(5A+4B+3C+2D+E)}{1.75 N}$ .....vi

Where, A=number of plants on scale 5; B=number of plants on scale 4; C=number of plants on scale 3; D=number of plants on scale 2; E=number of plants on scale 1; N=total number of plants. From the scale, the lower incidence level the better the control measure (Ramesh & Phadke 2012).

Each experiment consisted of 20 plants per treatment. The plants were arranged in a growth chamber in a completely randomized design (CRD). The plants were grown in the growth chamber for 21 days then transplanted in plastic pots containing cocopeat in the greenhouse. Another set of tomato plants treatments were sown directly on well prepared ground inside the greenhouse. During transplanting, the seedlings were inoculated with the respective bionanocomposite by soaking in a 10% solution for 15 min and inoculated with the *R. solanacearum* pathogen for 5 min. The transplanted plants were arranged in a CRD with three replicates (Wydra & Semrau, 2006).

**3.2.15 Illustration of the Process of Development of Bionanocomposite and Efficacy Tests**



### 3.2.16 Data Analysis

The data on pathogen colony inhibition, germination rates, growth rates and wilt incidences were log transformed before being subjected to analysis of variance (ANOVA), then back log transformed and means separated by protected Fischer's Least Significant Difference (LSD  $_{0.05}$ ). Origin-pro statistical package and genstat version 7.0 were used for data analysis (Hinkelmann & Kempthorne, 2008).

## 3.3 Results

### 3.3.1 Deacetylation of Chitin

Deacetylation affects the quantity of carbon and nitrogen in chitin resulting in a reduction of the elements. Thus carbon and nitrogen contents in chitin and chitosan were used to estimate the degree of deacetylation (Table 3.1).

**Table 3.1: Content of Carbon and Nitrogen in Acetylated (Chitin) and Deacetylated Chitin (Chitosan)**

Substance	Content	
	Carbon %	Nitrogen %
Chitin*	41.5	5.9
Chitin**	38.7	5.3
Chitin***	35.1	4.9
Chitin****	33.8	4.3
Chitin*****	32.1	3.9
Chitin*****	30.3	3.6

\*-As purchased, \*\*-20% NaOH treated, \*\*\*-40% NaOH treated, \*\*\*\*-60% NaOH treated, \*\*\*\*\*-80% NaOH treated, \*\*\*\*\*-100% NaOH treated

The degree of deacetylation (DDA) of chitosan was affected by concentration of sodium hydroxide. High concentration of sodium hydroxide resulted in high deacetylation of chitin (Figure 3.1).

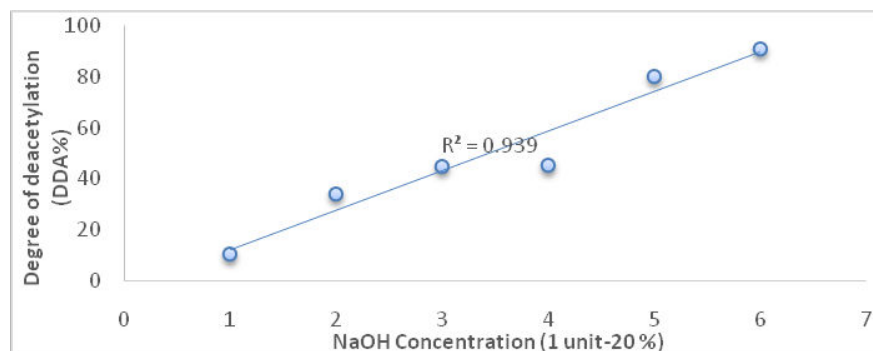


**Figure 3.1: Linear Fit for Deacetylation of Chitin using Sodium Hydroxide**

### **3.3.2 Characterization of Deacetylated Chitin**

#### **3.3.2.1 Fourier Transform Infra-Red Spectrometer (FTIR) Characterization**

The FTIR displayed spectral changes after deacetylation of chitin in the formation of chitosan. The spectral changes represented the changing functional bonds of hydroxyl (OH), amine (NH) and carbonyl (CO) these bonds are unique to different compounds and used as fingerprints in identification of substances (Figure 3.2).

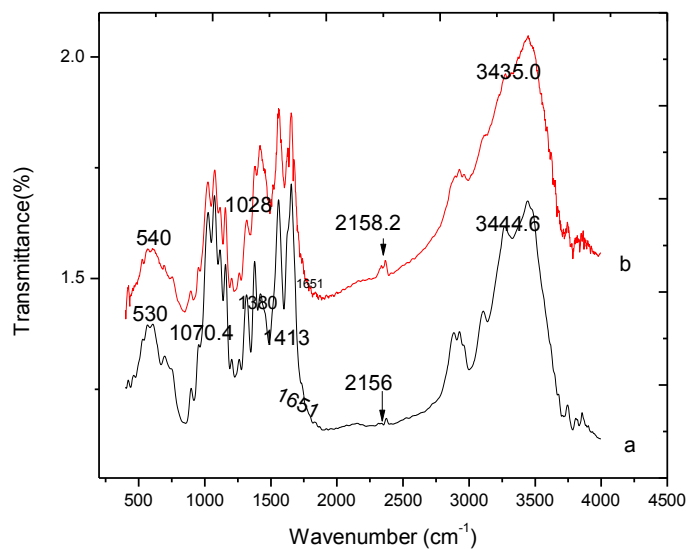


**Figure 3.2: FTIR Spectra of A-Chitin and B-Chitosan**

### 3.3.2.2 X-Ray Powder Diffractometer (XRD Characterization)

Diffractogram images of chitin changed after deacetylation. The fingerprints were compared to images from secondary sources of chitin and chitosan in terms of d-spacing, full width half maxima (FWHM), crystallinity, braggs angle and miller indices (Figure 3.3).

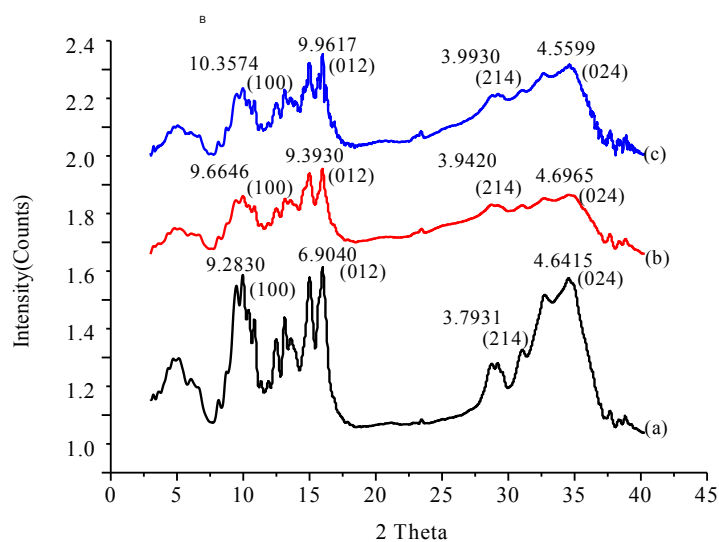


**Figure 3.3: X-Ray Diffractograms for A-Chitin, B-Chitosan and C-Chitosan Nanoparticle**

### **3.3.3 Characterization of Chitosan Nanoparticle and Chitosan Immobilized Silica Nanocomposite (CISNC)**

#### **3.3.3.1 Fourier Transform Infra-Red Spectrometer (FTIR) Characterization**

Formation of chitosan nanoparticles and CISNC were also characterized by the changes in spectral outputs of the compounds. These compounds were observed to have wave numbers shifting to the right or left due to stretching or vibrational forces on the functional bonds. In addition, new bonds are also formed in composites due to integration of different substances in a composite matrix (Figure 3.4).

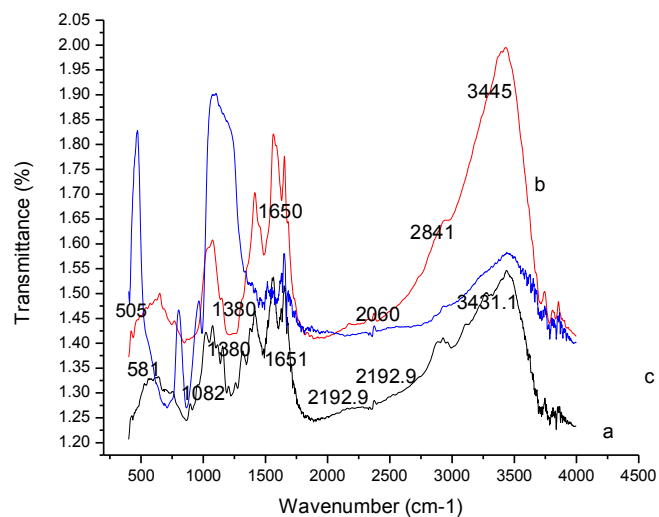


**Figure 3.4: FTIR Spectra for A-Chitosan Nanoparticle B-CISNC and C-MSN**

### 3.3.3.2 X-Ray Powder Diffractometer (XRD Characterization)

There was change in the crystallite sizes of chitosan nanoparticle when CISNC was formed. Chitosan nanoparticle had a smaller crystallite size than the nanocomposite (Table 3.2). The XRD diffractograms indicated notable differences of; d-spacing, 2-theta and full width half maxima (FWHM) values between chitin, chitosan, chitosan nanoparticles and CISNC (Figure 3.5). The crystallite sizes were derived from the X-ray diffractograms using the Scherrer equation (iv).

**Table 3.2: Crystallite Sizes of Chitosan Nanoparticles and Nanocomposites**

Substance	FWHM	2 $\Theta$ (deg)	$\lambda$ (nm)	Crystallite size (nm)
Chitosan nanoparticle1	0.41	56.64	1.5418	3.84
Chitosan nanoparticle 2	0.36	56.58	1.5418	4.37
Chitosan nanoparticle 3	0.24	56.53	1.5418	6.56
CISNC1	0.31	45.47	1.5418	4.80
CISNC2	0.33	45.37	1.5418	4.80
CISNC3	0.29	45.20	1.5418	5.18

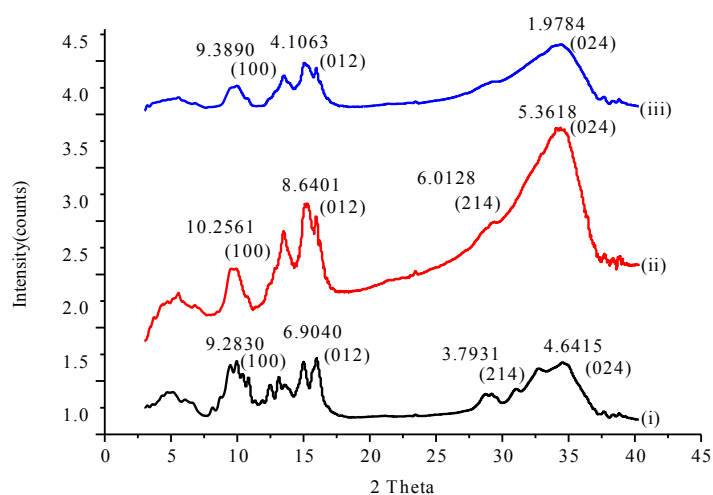


**Figure 3.5: X-Ray Diffractograms of; I-Chitin, II-Chitosan Nanoparticle and III-CISNC**

### 3.3.4 Detection of Isolated Microbes

The isolated *R. solanacearum* pathogen and phage were confirmed after culturing by morphological characterization on compound microscope (Plate 3.1).

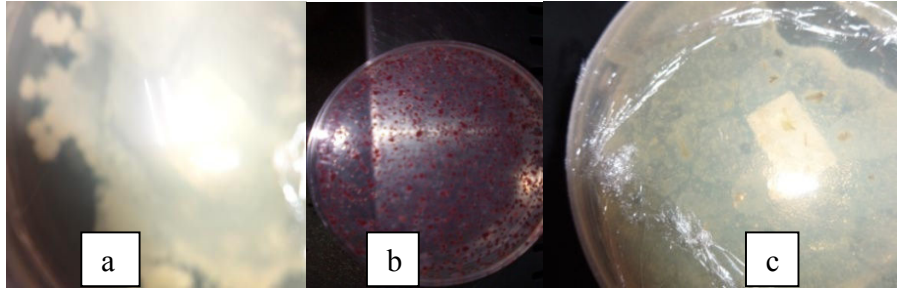


**Plate 3.1: Images of *R. Solanacearum* and Bacteriophage**

a) *R. solanacearum* cultured on nutrient agar b) *R. solanacearum* cultured on nutrient-TZC c) Plaques formed in cultured *R. solanacearum* cells due to lysis by the phage.

In addition to microscopic observations, PCR detection was employed as the ultimate confirmation test (Plate 3.2).

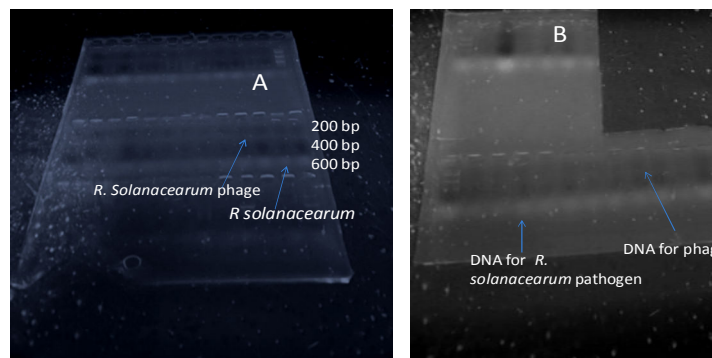


**Plate 3.2: Electrophoregrams; A-Amplified DNA of *R. Solanacearum* and Phage, B-Isolated DNA from *R. Solanacearum* Bacteria and Phage**

### 3.3.5 Sorption Properties of Biological Antagonists on Chitosan Immobilized Silica Nanocomposite (CISNC)

#### 3.3.5.1 Adsorption Efficiencies

Deacetylation of chitin to chitosan increased the adsorption effect on microbes. Immobilization of chitosan nanoparticles on mesoporous silica nanoparticles increased the adsorption effect of the formed composite thus; CISNC gel had the highest adsorption activity on biocontrol agents (Figure 3.6). The nanocomposites and bionanocomposite images were observed under a Nikon compound microscope (Plate 3.3).

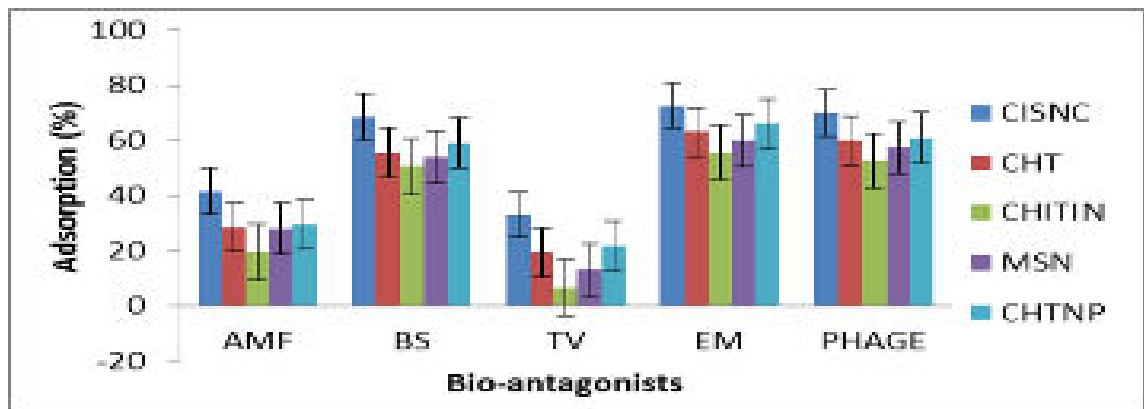


**Figure 3.6: Adsorption Efficiencies of Microbial Antagonists'**

Means significant at L.S.D  $_{0.05}$  (F-test)  $\pm$  standard error bar

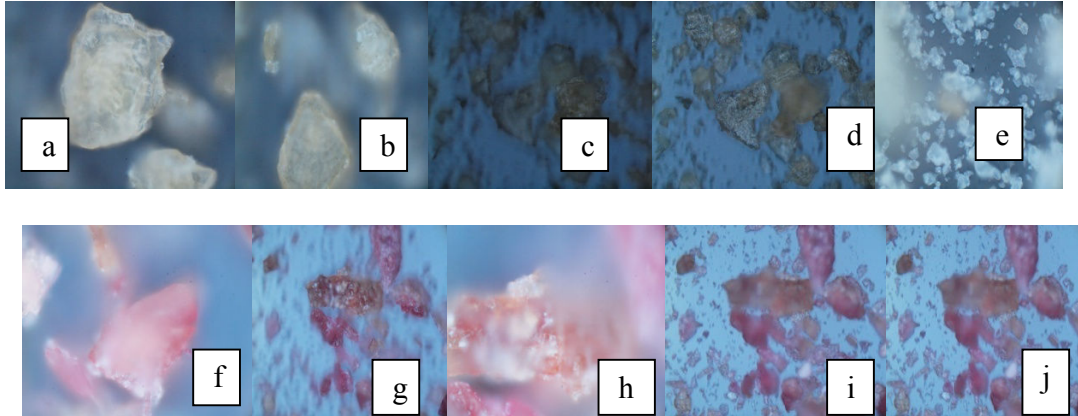


**Plate 3.3: Images of Nanocomposites and Bionanocomposites**

- a- chitin, b-chitosan, c-chitosan nanoparticle, d-chitosan immobilized silica nanocomposite, e-mesoporous silica nanoparticles, f-CISNC-BS, g- CISNC-AMF, h- CISNC-TV, i- CISNC-PHAGE, j- CISNC-EM

### 3.3.5.2 Desorption Efficiencies

Despite having the highest adsorption efficiency, CISNC gel had the highest desorption efficiency of microbial antagonists when L-cysteine was added prior to centrifugation.

In contrast, chitin had the least desorption efficiency (Figure 3.7).

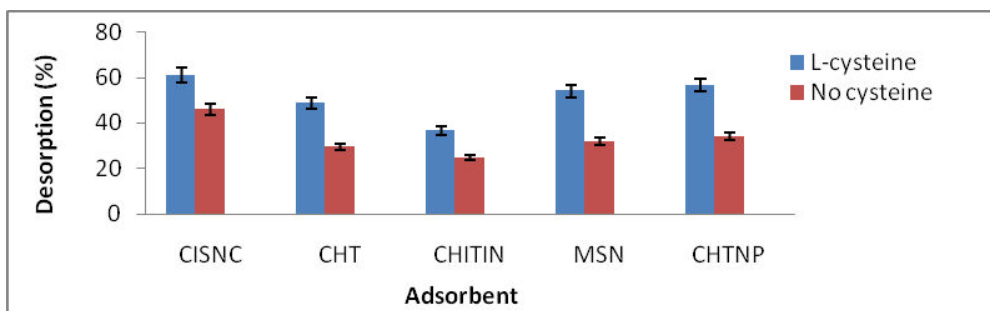


**Figure 3.7: Desorption Efficiencies of Microbial Antagonists'**

Means significant at L.S.D<sub>0.05</sub> (F-test) <sup>1</sup>-standard error bar

### 3.3.6 Efficacy of the Biocontrol Agents-Chitosan Immobilized Silica Nanocomposite Complex (BCA-CISNC or Bionanocomposites) on *R. Solanacearum*, Tomato Wilt and Growth Rate

#### 3.3.6.1 In vitro Inhibition of *R. solanacearum*

Deacetylation of chitin to chitosan increased the inhibition effect on the pathogen. Immobilization of chitosan nanoparticles on mesoporous silica nanoparticles also increased the composite's bacterial inhibitory effect. Finally, adsorption of biocontrol agents (BCAs) on CISNC gel had the highest significant ( $P \leq 0.05$ ) pathogen inhibition effect (Table 3.3 and Plate 3.4).

**Table 3.3: *In vitro* Inhibition of *R. Solanacearum* Growth on Different Substances**

Treatments	Inhibition
Control (Distilled water)	12.0 a
Control (Acetic acid)	15.0 a
L-cysteine	16.0 a
Mesoporous silica nanoparticles	28.0 b
Trichoderma viride (TV)	40.0 bc
Glomus mosseae (AMF)	50.0 c
Bacillus subtilis (BS)	51.0 c
Chitin	53.0 c
Phage	57.0 c
Effective micro-organisms (EM)	58.0 c
Chitosan	65.0 d
Chitosan nanoparticles	67.0 d
Chitosan immobilized silica nanocomposite (CISNC)	71.0 e
CISNC-TV	70.0 e
CISNC-AMF	71.0 e
CISNC-BS	74.0 e
CISNC-Phage	77.0 e
CISNC-EM	79.0e
Glutaraldehyde	85.0 ef

Means followed by the same letter are not significantly different at L.S.D  $_{0.05}$  Protected

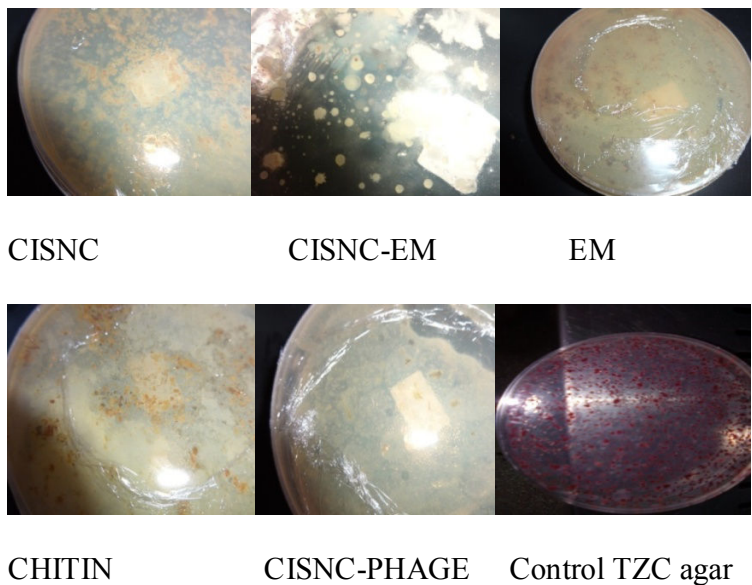


**Plate 3.4: Zones of inhibition of Cultured *R. solanacearum* by Bionanocomposites**

**Key:** CISNC-Chitosan immobilized silica nanocomposite, CISNC-EM-Chitosan immobilized silica nanocomposite adsorbed with effective micro-organisms, CISNC-PHAGE- Chitosan immobilized silica nanocomposite adsorbed with bacteriophage, EM-Effective micro-organisms

### 3.3.6.2 Effect of Bionanocomposites on Tomato Seed Germination

Deacetylation of chitin to chitosan increased the potential of chitin for enhancing tomato seed germination. Formation of the CISNC gel also increased the effect of the composites on tomato seed germination. The highest effect on tomato seed germination was observed when bionanocomposites (BCA-CISNC complex) were used. Glutaraldehyde inhibited germination of tomato seeds. Chonto F1 variety had a significantly ( $P \leq 0.05$ ) higher germination % than Anna F1 (Figure 3.8).

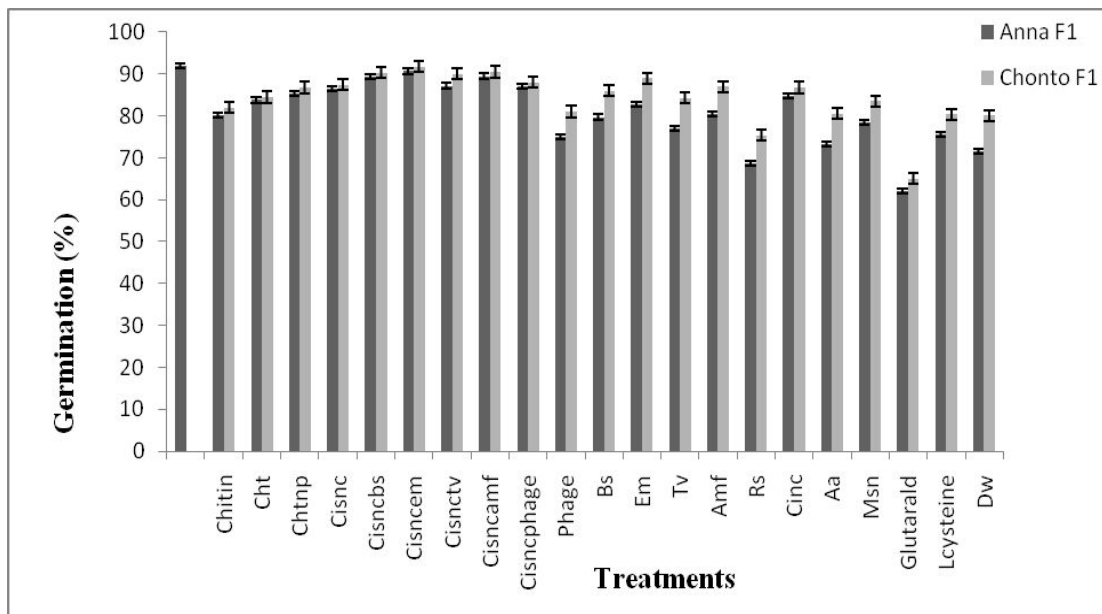


**Figure 3.8: Germination rates of tomato seeds treated with bionanocomposites**

Means significant at L.S.D  $_{0.05}$  (F-test)  $\pm$ LSD bar

### 3.3.6.3 Effect of Bionanocomposites on Chlorophyll Content

Treatment of tomato seedlings with chitin, chitosan, chitosan immobilized silica nanocomposite and bionanocomposites increased the chlorophyll content significantly ( $P \leq 0.05$ ) (Table 3.4).

**Table 3.4: Chlorophyll Content in Tomato Seedlings Treated with Bionanocomposites**

Treatment	Chlorophyll
Chitin	30.7a
Chitosan	38.6a
Chitosan nanoparticles	41.4a
Chitosan immobilized silica nanocomposite (CISNC)	35.6a
CISNC-Phage	32.2a
CISNC-AMF	37.6a
CISNC-BS	34.0a
CISNC-EM	35.3a
CISNC-TV	33.0a
L-cysteine	26.5b
Trichoderma viride (TV)	28.8b
Effective micro-organisms (EM)	29.6b
Bacillus subtilis (BS)	29.3b
Glomus mossae (AMF)	29.7b
Control (Distilled water)	20.8b
Control (Acetic acid)	22.0b
Phage	27.9b
Mesoporous silica nanoparticles	30.8a

Means followed by the same letter along a column are not significantly different. LSD<sub>0.05</sub>

Protected

### 3.3.6.4 Effect of Bionanocomposites on Tomato Plants Growth

Biocontrol agents, chitin, chitosan, chitosan immobilized silica nanocomposite and bionanocomposites stimulated growth rates in tomato seedlings. The highest significant ( $P \leq 0.05$ ) growth rates were observed when bionanocomposites were used. The Chonto F1 variety however, had a significantly ( $P \leq 0.05$ ) higher growth rate than Anna F1 (Figure 3.9 and Plate 3.5).

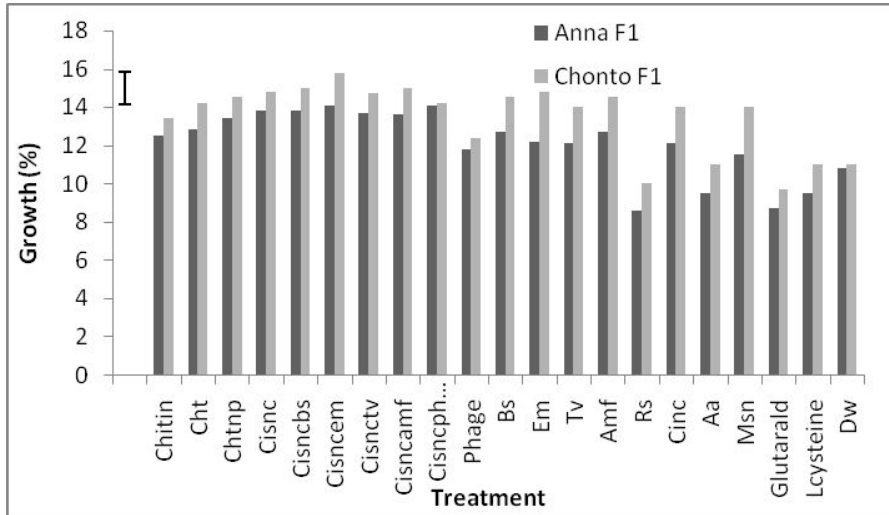


**Figure 3.9: Growth Rates of Tomato Seedlings Treated with Bionanocomposites**

Means significant at L.S.D  $_{0.05}$  (F-test) 'LSD bar

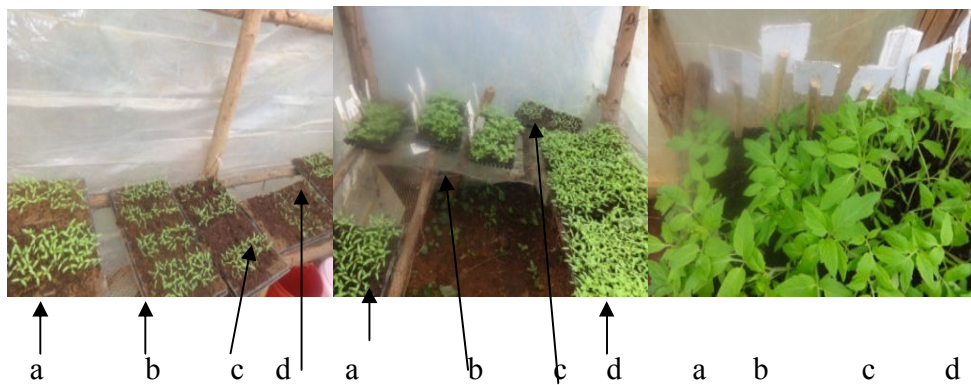


**Plate 3.5: Images of tomato seedlings treated with bionanocomposites**

**Key:** a-Chitosan immobilized silica nanocomposite (CISNC), b-biocontrol agents (BCAs), c-control and d-bionanocomposites (BCAs adsorbed on CISNC)

### 3.3.6.5 Effect of Bionanocomposites on Wilt Incidences in Tomato

Deacetylation of chitin to chitosan enhanced its effect on wilt incidences in tomato. Chitosan immobilized on silica nanoparticles had a higher effect on wilt incidences while the highest significant ( $P \leq 0.05$ ) effect of wilt incidence suppression was on tomato seedlings treated with bionanocomposites (BCA-CISNC complex) particularly the effective micro-organisms and phage. The Anna F1 had significantly ( $P \leq 0.05$ ) higher wilt incidences than Chonto F1. It was evident that the effect of bionanocomposites on wilt incidences between the two tomato varieties was not significantly different (Figure 3.10).

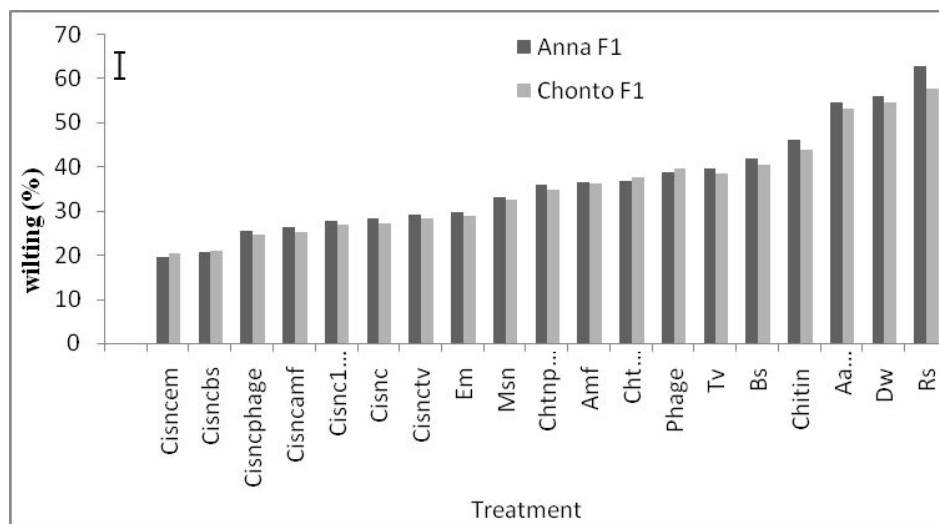


**Figure 3.10: Bacterial Wilt Incidences in Tomato Varieties Treated with Bionanocomposites.**

Means significant at L.S.D<sub>0.05</sub> (F-test) <sup>1</sup>LSD bar, F value (58.73) > F prob (3.17)

### 3.4 Discussion

#### 3.4.1 Deacetylation of Chitin

Reduction of C and N contents in chitin after deacetylation (Table 3.1) was attributed to the loss of acetyl groups resulting in a polar and soluble chitosan (Chatelet, Damour & Domard, 2001). The positive charge in chitosan is due to the amino group formed after deacetylation. Solubility of chitosan in dilute acids is always associated with D-glucosamine units. This compound results after deacetylation of chitin. Hence, pure chitosan is composed entirely of D-glucosamine units and is highly soluble in dilute acids. On the contrary, pure chitin is composed of N-acetyl-D-glucosamine units (Domszy & Roberts, 1985). In most cases, only impure chitin and chitosan are obtained. The compounds are therefore, comprised of N-acetyl, D-glucosamine and D-glucosamine units at varying degrees respectively. Chitin used in this study comprised of 10.2 % D-glucosamine units while the purest form of chitosan obtained was 90.9 %.

The linear fit obtained between the degree of deacetylation (DDA %) and NaOH concentration indicated that concentration of NaOH affects deacetylation. This was confirmed by the fact that, the highest deacetylation of 90.9 % was obtained when a concentration of 100% w/v of NaOH was used. It was in agreement with the Tsaih and Chen, 2003 observation that, as the concentration of alkaline increased, deacetylation increased proportionally. The resultant linear fit of deacetylation had a strong coefficient of determination ( $R^2$ ) value of 0.939 (Figure 3.1) confirming that deacetylation of chitin is directly proportion to the concentration of alkaline media used. In addition to the linear graph, FTIR spectra for the deacetylated chitin showed reduced peak intensities attributed to loss of acetyl groups. The most pronounced peak reduction was on chitin with a DDA of 90.9 % (Figure 3.2). Diffractogram variances were noted on the XRD output for chitin and its derivatives (Figure 3.3) an indication of successful deacetylation (Harish, Kittur, & Tharanathan, 2002). It was also found out that, deacetylation of chitin

at low sodium hydroxide concentration below 60%, yielded less than 50 % chitosan. This observation had been postulated by Cao, Jing, Li, Gong, Zhao & Zhang (2005) that, effective deacetylation of chitin occurs at high concentration of alkali since the temperature, time and pH remained constant (Knaul, Kasaai, Bui & Creber, 1998).

### **3.4.2 Characterization of Deacetylated Chitin**

The Fourier Transform infra-red (FTIR) spectrum of chitin was slightly different from that of chitosan with DDA above 60 %. The differences in spectra were observed in form of wave number shifts. This was attributed to stretching and vibrations of the functional bonds in this case occasioned by loss of acetyl groups during formation of chitosan (Figure 3.2). However, since a 100 % deacetylation was not attained (Table 3.1), there were notable similarities in the spectra of chitin and chitosan. Occurrence of glucosamine units were attributed to spectral similarities between chitin and chitosan involved in this study (Choong & Wolfgang, 2003). The two, had absorption peaks around 3444.6 and 3435.0  $\text{cm}^{-1}$  for chitin and chitosan respectively. These peaks indicated the presence of -OH stretching and amine N-H symmetric vibrations. The slight shift to the left marked reduced intensity of -OH stretching and N-H vibrations between chitin and chitosan. The bands at 1070.4  $\text{cm}^{-1}$  and 1028  $\text{cm}^{-1}$  for the chitin and chitosan respectively are due to the -C-O groups stretching vibrations. The C-O groups in chitosan were depressed due to deacetylation. The absorption band at 1413  $\text{cm}^{-1}$  characterized stretching vibration of amino group in chitosan. Also, peaks between 1070.4-1028  $\text{cm}^{-1}$  and 530-540  $\text{cm}^{-1}$  indicated the presence of saccharide structure of chitin and chitosan respectively due to the varying C-O groups (Jolanta *et al.*, 2010). This confirmed the polysaccharide nature of chitin and its derivatives used in the study.

The X-ray powder diffractogram of chitin was observed to be partly crystalline while chitosan had a clearer crystalline structure. The difference in crystallinity between the two compounds was attributed to deacetylation (Figure 3.3). Higher concentration of

sodium hydroxide resulted in pronounced peaks. The chitin spectra showed characteristic peaks at 2-theta 9.25 and 19.05 but were shifted to 9.45, 20.5 and 31.89 nm suggesting formation of inter and intra-molecular hydrogen bonds in the presence of free amino groups. The shifts were attributed to formation of amine groups and cleavage of intra-molecular hydrogen bond of chitosan (Ogawa & Yui, 1993). There was systematic reduction in d spacing from chitin to chitosan confirming that chemical change had occurred between the compounds. The process of deacetylation was necessary in synthesizing a soluble and reactive compound since pure chitin is neutral in charge and almost inert. Solubility of chitosan is attributed to the presence of protonable amino group developed after deacetylation (Nasri *et al.*, 2009).

### **3.4.3 Characterization of Chitosan Nanoparticle and Chitosan Immobilized Silica Nanocomposite (CISNC)**

Fourier transform infrared (FTIR) spectrometry indicated a peak at  $1413\text{ cm}^{-1}$  assigned to stretching vibrations of amino groups in chitosan that shifted to  $1415.7\text{ cm}^{-1}$  in the nanoparticle and then changed to  $1380\text{ cm}^{-1}$  in the CISNC after adsorption/impregnation of silica nanoparticles on chitosan nanoparticles. The broad peak at  $1028\text{ cm}^{-1}$  in chitosan became less intense in chitosan nanoparticle by shifting to  $1076.2\text{ cm}^{-1}$  showing that C-O stretching vibrations reduced in the chitosan nanoparticle spectrum. The vibration band at  $3431.1\text{ cm}^{-1}$  denoted increased intensity of chitosan nanoparticle confirming that vibrations of N-H increases as the particle sizes decrease (Figure 3.4). The absorption band at  $3431.1\text{ cm}^{-1}$  shifted to  $3445\text{ cm}^{-1}$ , the shift indicated possible overlapping and stretching of hydrogen bounded -OH and -NH<sub>2</sub>. The characteristic band at  $2841\text{ cm}^{-1}$  was attributed to presence of glutaraldehyde in the compound. This is because of the typical -CH bond around  $2900\text{ cm}^{-1}$  in glutaraldehyde. Thus the new band at  $2841\text{ cm}^{-1}$  in the nanocomposite confirmed cross-linking. There were distinct spectral shifts in chitosan nanoparticle from  $1415.7$ ,  $1076.2$  and  $565.1\text{ cm}^{-1}$  to  $1383$ ,  $1082$  and

505  $\text{cm}^{-1}$  associated with formation of new hydrogen bonds between molecules in the nanocomposite (Wang & Helliwell, 2005; Zouhour *et al.*, 2010).

Moreover, there was a slight increase in the size of the chitosan nanoparticles from 2.8 nm to 4.4 nm in the synthesized CISNC (Table 3.2). The change in crystallite size was attributed to immobilization of mesoporous silica nanocomposite into the chitosan nanoparticles matrix. Addition of glutaraldehyde which is a good cross-linking agent enhanced adsorption of MSN on the chitosan nanoparticles gel. The nanocomposite acquired the sorption properties of the two nanoparticles making the nanocomposite superior (Li *et al.*, 2010).

Chitosan diffractogram showed characteristic peaks at 2-theta 9.45 and 19.05 but were shifted to 9.46, 20.5 and 31.89 nm and 9.46, 20.5, 31.89 and 45.69 nm for chitosan nanoparticle and nanocomposite respectively. This illustrated formation of physical molecular bonds in nanoparticles and nanocomposites. The physical bonds in the nanocomposite were the basis of using it as a carrier material due to ease of disintegration when pH and moisture contents are varied. In addition, the d-spacing of chitosan nanoparticles and nanocomposites of chitosan and silica varied with notable reduction in interlayer distances. The peaks sensitive to crystallinity decreased and/or disappeared in the spectrum of chitosan and chitosan nanoparticles due to reduced crystallinity (Figure 3.5). Formation of chitosan nanoparticle resulted in a fairly new product with a slightly small d-spacing than chitosan. Immobilization of chitosan nanoparticles on silica nanoparticles was a physical process thus the small difference in the d-spacing. The d value however, reduced after formation of chitosan nanoparticles showing that the nanoparticle layers have a smaller d-spacing than chitosan. Immobilization of MSN and glutaraldehyde were responsible for the marked differences between chitosan nanoparticle and its nanocomposite product, it also resulted in amplified peaks, exemplifying successful capping and formation of a composite (Figure 3.3 and 3.5) (Kim *et al.*, 2005; Ogawa & Yui, 1993).

#### **3.4.4 Detection of Isolated Microbes**

The bacterial ooze obtained from infected and wilting tomato plants was cultured on nutrient-TZC media. This ensured that a virulent *R. solanacearum* pathogen was obtained and used for inoculation (Wydra & Semrau, 2006). Isolated phage was visible from the *R. solanacearum* plaques. The plaques indicated lysis which results after colonization of the pathogen by bacteriophage (Kalpage & Costa, 2014). In addition to microscopic observations, PCR detection was employed as the ultimate confirmation test (Plate 3.2). The *R. solanacearum* phage and *R. solanacearum* bacteria were detected at 300 base pairs (bp) and 600 bp respectively (Plate 3.1) (Fujiwara *et al.*, 2011). The method clearly confirmed the presence of the two bioagents. Touchdown PCR method was preferred because other PCR procedures had limitations in the determination of the optimal annealing temperature resulting in unclear bands of genomic DNA after amplification (Korbie & Mattick, 2008).

#### **3.4.5 Sorption Properties of Biological Antagonists on Chitosan Immobilized Silica Nanocomposite (CISNC)**

The increased sorption efficiency after deacetylation, immobilization of chitosan on silica nanoparticles and adsorption of biocontrol agents on the CISNC was attributed to changed functionable surfaces, large surface area to volume ratio and increased functional bonds. For instance, deacetylation of chitin to chitosan, enhanced adsorption of biocontrol agents because chitosan has free amino groups creating a charged environment that attracts the charged microbial membranes (Jolanta, Malgorzata, Zbigniew, Anna, Krysztof, Jorg & Piotr, 2010; Kolodynska, 2012). Immobilization of chitosan nanoparticles on mesoporous silica nanoparticles increased the gallery spaces in the gel matrix, these spaces provided adsorption surfaces in the composites which were in turn occupied by the biocontrol agents and the released biochemicals (Figure 3.6). Immobilization of MSN on the chitosan nanoparticles also resulted in formation of Si-

OH bonds with polar characteristics enhancing further adsorption (Fleming & Wingender, 2010). The enhanced sorption properties in chitosan-silica hybrid had also been made by Pab *et al.* (2004); Spirk, Findenig, Doliska, Reichel, Swanson & Kargl (2013). This is because chitosan polysaccharides are polyhydroxyl compounds and the hydroxyl groups get into the condensation reaction with silanol groups produced during the hydrolysis of silica catalysed by presence of amino groups in the chitosan molecule. The increased sorption properties were attributed to the increased functional groups in the hybrid composite.

Desorption of microbial antagonists was enhanced when L-cysteine was added to the bionanocomposite gel (Figure 3.7). The suitability of a carrier material is in its ability to desorb the substrate (s) on reaching the target site. Desorption efficiencies were carried to ensure that biocontrol agents were not permanently bound to the CISNC carrier. This is because after successful delivery to the target site either root hairs or in the plant membranes, the biocontrol agents should be discharged and synergistically with the dissociated nanoparticles destroy the pathogen. The change of conditions in plants which can cause desorption include; pH, pressure and moisture level. Addition of glutaraldehyde ensured successful adsorption of the biocontrol agents on to CISNC gel by increasing stability of the nanocomposite through cross-linking activity which reduces leakages during delivery (Iriarte *et al.*, 2012). Conversely, addition of L-cysteine after synthesis of the bionanocomposite enhanced desorption of the biocontrol agents. Thus a dilute solution of L-cysteine should be added to the bionanocomposite complex prior to application in the field to enhance desorption. L-cysteine enhances desorption by overcoming cross-linking effect associated with the glutaraldehyde and electrostatic membranes attraction between the microbes, silica and chitosan charges (Spadaro & Gullun, 2005).

### **3.4.6 Efficacy of the Bionanocomposite (BCA-CISNC Complex) on *R. Solanacearum*, Bacterial Wilt and Growth Rate of Tomato**

Deacetylation of chitin to chitosan, functionalization of chitosan to chitosan nanoparticles and immobilization of chitosan nanoparticle on MSN, to form CISNC gel, significantly ( $P \leq 0.05$ ) increased *R. solanacearum* pathogen growth *in vitro*. For instance, application of chitin on cultured *R. solanacearum* caused a colony inhibition of 53.9 %. The bacterial inhibition was attributed to the fact that, the near neutral charged chitin possessed antibacterial effect due to the presence of glucosamine units. Further, chitosan with a deacetylation degree of 90.9 % depicted a 65.3 % inhibition. This enhanced inhibition was attributed to positive charges of amino groups that disrupted cellular functions of the charged bacterial membrane that destroyed the bacterial cells (Table 3.3 and Plate 3.1). Interactions between positively charged chitosan molecules and negatively charged residues of bacterial cell surface also played an important role in the inhibitory effect of gram negative bacterial pathogen. The inhibition was also attributed to direct toxicity, chelation of nutrients and minerals from the pathogen (Rodrigo, Vieira & Beppu, 2006). Additionally, chitosan stimulate microbial degradation of *R. solanacearum* in a manner resembling the application of a hyper-parasite. Chitosan has also been found to inhibit other plant pathogens like *Pseudomonas syringe* resulting in reduced crop losses (Fleming & Wingender, 2010). Also, a gram negative bacterium lacks teichoic acids and has a thin peptidoglycan layer compared to the gram positive bacteria which enables chitosan to engulf the bacterial cell thus causing death by suffocation. This makes the gram negative bacteria highly susceptible to polar materials which interferes with the bacterial membrane stability thus loss of cellular integrity (Gupta, 2011).

Formation of chitosan with a high degree of deacetylation (DDA) was paramount in this study. This is because DDA has an effect on the positive charge density which impacts on polycationic effect. This has been observed by Christian, Kammer and Baalousha

(2008); Taraskiewicz, Fila, Grinholc and Nakonieczna (2013), where chitosan with higher DDA conferred stronger antibacterial activity than moderate DDA against *Staphylococcus aureus* (*S. aureus*) at acidic pH. Development of low molecular weight chitosan nanoparticles enhanced the *R. solanacearum* pathogen inhibition significantly ( $P \leq 0.05$ ). The nanochitosan had an inhibition of 67.2 %, attributed to ease of penetration of the nanoparticles through the pathogen membranes, causing rapid cell destruction and death. The observation was in agreement with Liu *et al.* (2004) findings, where bactericidal activity of chitosan correlated strongly with the molecular weight of chitosan. An increase in molecular weight of chitosan reduced effect on *E. coli*. The current study was in agreement with the previously reported work by Jaworska, Sakurai, Gaudon & Guibal (2003), where formation of chitosan nanoparticles corresponded with a lower molecular weight. Low molecular weight increases ease of penetration of molecules through cell membranes. The inhibitory effect on *R. solanacearum* by chitosan nanoparticles was associated with the ability of the low molecular weight and water-soluble glucosamine units penetrating the bacterial cell wall and combining with DNA inhibiting synthesis of mRNA and transcription of DNA (Freier *et al.*, 2005). According to Taraskiewicz *et al.* (2013), higher molecular weight and soluble chitosan interacts with cell surface altering the cell permeability. The interaction cause cellular leakage or formation of an impermeable layer around the cell which blocks transportation of essential solutes into the cell. Also according to Wazed, Rajendran & Joshi (2010), chitosan nanoparticles had higher antibacterial effect due to the large surface area of molecular interface between the microorganisms and the nanoparticles. The effect of immobilizing cross-linked chitosan with nanosilica enhanced the efficacy of the nanocomposite by increasing inhibition of *R. solanacearum* colonies from 67.2 % to 70.4 % for the chitosan nanoparticles and nanocomposite respectively. The increased efficacy was attributed to the synergy of the nanocomposite.

Adsorption of biocontrol agents on CISNC gel increased inhibition of the pathogen significantly ( $P \leq 0.05$ ) due synergistic effect of the composites (Table 3.3). Adsorption

of biocontrol agents was made possible by the fact that, most microbes have a net charge on their membranes, which allow their adsorption to polar materials. This formed the basis for adsorption of bacteria, fungi and viruses achieved in the study. The negatively charged *R. solanacearum* strongly adhered to the inhibiting bionanocomposite hence destroying the pathogen (Kubata *et al.*, 2005).

Use of glutaraldehyde increased entrapment efficiency ensuring effective delivery of biocontrol agents (Cao *et al.*, 2005). Choong and Wolfgang (2003) reported that, glutaraldehyde increases entrapment efficiency by up to 73%. On the other hand, L-cysteine aided desorption of biocontrol agents from CISNC gel and provided surface for adsorption of the gram negative *R. solanacearum* due to higher affinity of the for the positive charge in the nanocomposite for the gram negative bacteria. This resulted in destruction of the weakened and immobilized pathogen by both the biocontrol agents and CISNC gel (Chatelet *et al.*, 2001).

#### **3.4.7 Effect of Bionanocomposites on Tomato Seed Germination**

Seeds treated with chitin, chitosan, chitosan immobilized silica nanocomposite and bionanocomposites showed a significant ( $P \leq 0.05$ ) effect on tomato seed germination rate compared to the controls (Figure 3.8). The variation in germination was attributed to the ability of the chitin derivatives to form a semi-permeable film on the seed surface which maintained seed moisture in the growing media promoting seed germination (Guan, Wang & Shao, 2009). Chitosan contained in the CISNC gel increased seed germination in tomato seeds as it caused a decline in malonydialdehyde content, a compound that inhibits germination. Chitosan also altered the relative permeability of the plasmalemma, increased concentration of soluble sugars and enzymes such as proline, peroxidase, polyphenol oxidase and catalase. In addition, it acts as a permeation enhancer by opening epithelial tight junctions allowing free entry of water, nutrients and air. The mechanism underlying this effect is based on the interaction of positively

charged chitosan and the cell membrane resulting in a re-organisation of the tight junction-associated proteins. Algam *et al.* (2010) indicated that, chitosan has an amino group (-NH<sub>2</sub>) that makes it hygroscopic. When it gets in contact with water, the amino group is protonated turning it into ammonia (-NH<sub>3</sub>) which confers more hygroscopicity to the chitosan molecule making the seed or plant trap more moisture. Furthermore, Chitosan increases the water utilization efficiency of plants, increase mineral uptake and stimulate growth rate (Figure 3.9).

The enhanced germination in CISNC gel treatments can also be attributed to the role of silica nanoparticles. The material has a large surface area and surface reactivity. It has the ability of penetrating cell walls acting as a media for transport intracellularly. The increased permeability enhances water and air uptake hence accelerated germination (Kubata *et al.*, 2005). Treatment of tomato seeds with silica increases germination and growth vigour of most plants. This is because silica results in high availability of phosphorous through formation of anions by silicates which competes with phosphates for the same sorption sites (Currie & Perry, 2007). Phosphorus is one of the macro nutrient elements that promote growth and development in plants. In related studies, Moussa (2006) observed that, silica increased seed germination in wheat and maize. It also corrects acidity in the growing media thus enhanced growth in acidic media. Furthermore, it increases seed weight and heavier seeds have better developed embryo due to higher amount of food reserves with better germination ability.

Adsorption of biocontrol agents (BCAs) on CISNC gel increased tomato seeds germination significantly ( $P \leq 0.05$ ). For instance, effective micro-organisms adsorbed on CISNC gel had the highest germination rate of 90.7 % from 82.7 %. All biocontrol agents had a significant ( $P \leq 0.05$ ) effect on germination. According to Roberts *et al.* (2005), BCAs' synthesize plant hormones such as auxins and cytokinins which solubilize soil phosphorus and enhance soil porosity. The synthesized phytohormones triggers faster germination, reduce the mean germination index and result in more

vigorous plants. Other studies have shown that application of *Paernibacillus polymyxa* increased tomato seed germination by 44 %. This qualifies BCAs as germination stimulants. There was an important observation in this study where, although glutaraldehyde had the highest antibacterial effect on *R. solanacearum*, it reduced germination capacity to 61%. This was attributed to its oily characteristic that inhibited imbibition rendering the testa slightly impervious. However, its effect as a germination inhibitor was alleviated when used in cross-linking of CISNC using minute quantities (0.1 %).

#### **3.4.8 Effect of Bionanocomposites on Chlorophyll Content**

The application of chitosan derivatives and/or mesoporous silica nanoparticles (MSN) resulted in tomato seedlings plants with significantly ( $P \leq 0.05$ ) higher chlorophyll content (Table 3.4). The increased chlorophyll is caused by accelerated biochemical activities in the tomato plants triggered by the glucosamine units in chitosan and silicates in MSN. Confirming the above observation, Dzung *et al.*, 2013 reported that spraying of coffee seedlings with chitosan solution increased the content of chlorophyll and carotenoids in leaves by 15 % for plants grown in the field and by 46–73 % for plants grown in the greenhouses. Inclusion of silica in the chitosan gel matrix was also attributed to the increased chlorophyll activity. These results are consistent with the finding of Cao *et al.* (2005) where, leaf senescence of sugarcane (*Saccharum officinarum* L.) could be delayed with silica application. Effects of silica deposited in leaves improved chlorophyll efficiency in rice, barely, wheat and sugarcane (Zeng, Liang & Tan, 2007).

#### **3.4.9 Effect of Bionanocomposites on Tomato Plant Growth**

Tomato Seedlings treated with chitin, its derivatives and biocontrol agents showed significant ( $P \leq 0.05$ ) plant vigour inferred from the shoot growth and germination rates.

Seedlings treated with CISNC gel adsorbed with effective micro-organisms had the highest plant vigour (14.2 %). The enhanced growth rate was attributed to the role of biocontrol agents as biostimulants and provision of nutrients in the rhizosphere. Chitosan played a role in stimulating growth of beneficial microbes due to high carbon content in the polymer. The activated microbes accelerated decomposition of organic matter into inorganic forms. The biocontrol agents in addition, enhanced root system development enabling the plants to absorb more nutrients from the soil. Chitosan also acted as a fertilizer due to the high nitrogen and carbon contents. Cao *et al.* (2005) found out that, chitosan contains oligosaccharides that act on plants as phytohormones which regulates morphogenesis and development. It also promotes plant growth by increasing availability and uptake of water and essential nutrients by adjusting osmotic pressure. Chitosan treatment increased chlorophyll content in tomato plants (Table 3.4), hence, increased photosynthetic efficiency (Li *et al.*, 2010; Dzung, Minh & Van Nguyen, 2013). Guan *et al.* (2009) found out that, chitosan enhanced germination index, reduced mean germination time, increased shoot height, root length, shoot and dry weights. It also promoted the growth of microbial species with antagonistic action against pathogens. High molecular weight chitosan stimulated faster growth than low molecular weight chitosan nanoparticles (Figure 3.9 and Plate 3.5) (Iriti, Pichi, Maffi & Faoro, 2009). Mesoporous silica nanoparticles increased the plant vigour significantly ( $P \leq 0.05$ ). This was attributed to stress reduction, physiological roles and increased chlorophyll in plants. Hence, inclusion of MSN in the nanocomposite fortified effect of CISNC gel (Li & Ma, 2002).

#### **3.4.10 Effect of Bionanocomposites on Wilt in Tomato**

##### **3.4.10.1 Biological Control Agents in the Control of Bacterial Wilt in Tomato**

Biocontrol agents (BCAs) significantly ( $P \leq 0.05$ ) reduced wilting in tomato seedlings. Effective micro-organisms for instance, had the highest effect of reducing the tomato

seedlings wilt incidence (0.205) (Figure 3.10). The high efficacy of effective micro-organisms was attributed to innate synergy between the microbial composites which are; photosynthetic bacteria, lactobacillus and the actinomycetes fungi (Obradovic *et al.*, 2005; Nguyen & Ranamukhaarachchi, 2010; Pal & Mc Spadden 2006; Ramesh & Phadke, 2012).

The *R. solanacerum*-phage had a significant ( $P \leq 0.05$ ) effect on wilt suppression in tomato seedlings. Viral therapy is an effective control strategy due to specificity of the virus to the pathogen. The control is also sustainable due to the fact that, it can easily be isolated from the soil. Phages are persistent and are easily translocated in tomato plants infected by the pathogen, particularly the xylem vessels. The problem with phage as a reliable therapy mechanism is in timing when to apply the phage (Balogh *et al.*, 2010). Thus the need to apply phages before pathogen infestation. Moreover, efficacy of the phage was greatly reduced when applied without use of carriers. The current study had consistent results with Iriarte *et al.* (2012), where bacteriophage completely controlled the *R. solanacearum* pathogen *in vitro*.

*Bacillus subtilis* reduced wilt incidences significantly ( $P \leq 0.05$ ). The ability of *B. subtilis* to produce volatile compounds and different lytic enzymes such as protease and cell wall degrading enzymes; chitinase and glucanase which are known to destroy most pathogens. *B. subtilis* are also known to be a rich source of lysine enzyme which is associated with resistance in most plants (Agrios, 2005).

Additionally, *T. viride* reduced wilting in tomato seedlings. The reduction was attributed to the fact that, *Trichoderma spp.* especially *T. viride* and *T. harzianum* are able to stimulate production of secondary metabolites in plants (Nguyen & Ranamukhaarachchi, 2010). The metabolites play a major role in suppressing pathogens directly or indirectly by promoting plant growth and enhancing plant disease resistance as well as the lytic enzymes. Moreover, *T. viride* inhibits growth of pathogens by

competition for nutrients and for space as it grows more rapidly. Trichoderma species are also known to be pathogenic to most plant pathogens. Trichoderma species have also been implicated of depressing plant growth in some crops by acting as plant pathogens. This depressing effect of trichoderma was not observed in this study (Obradovic *et al.*, 2005; Pal & Mc Spadden, 2006).

Finally, *G. mossesae* significantly ( $P \leq 0.05$ ) reduced wilt incidence. The fungi reduce wilting in plants is by colonizing the root hairs, denying soil borne pathogens entry in to the plant system (Jeon, Lee, Kim, Ahn & Song, 2003). It also reduces *R. solanacearum* populations in the rhizosphere of plants by denying the pathogen access to nutrients and space for replication. The fungus also stimulates production of phenolic compounds in plants. Phenols are known to have antimicrobial effect on most pathogens. Therefore, biocontrol agents are able to reduce wilt incidences by antagonizing pathogens and eliciting systemic protection in plants (Nguyen & Ranamukhaarachchi, 2010).

Complementarily, adsorption of the biocontrol agents on the synthesized CISNC gel reduced bacterial wilt significantly ( $P \leq 0.05$ ). The efficacy of the bionanocomposites (BCA-CISNC complex) was several folds higher than the non-adsorbed microbes. The reduced wilt incidence was attributed to positive synergy of all constituent substances. The nanocomposite played a major role in ensuring the vitality of the microbial antagonists during storage and after application (Se & Niranjana, 2005). It was construed that the nanocomposite delivered the biocontrol agents precisely to the target site and protected them from harsh environmental conditions enhancing their efficacy. In addition, the CISNC gel ensured sustained release of the microbes and antagonistic biochemicals trapped in its matrix (Xu & Du, 2003; Spadaro & Gullun, 2005; Algam *et al.*, 2010).

#### **3.4.10.2 Chitosan in the Control of Bacterial Wilt**

Chitosan and its derivatives reduced wilting in tomato plants significantly ( $P \leq 0.05$ ). Directly, chitosan stimulates microbial degradation of pathogens in a way resembling the application of a hyper-parasite. Additionally, due to high polysaccharides, it stimulates the activity of beneficial micro-organisms upsetting pathogenic microbial equilibrium in the rhizosphere (El-Hadrami, Adam, El-Hadrami & Daayf, 2010).

Costa, Silva., Tavaría & Pintado (2013) reported that, chitosan is easily degraded producing pathogen repellents like ammonia which pre-dispose pathogens to the emboldened biological antagonists making the adsorbed micro-organisms more efficacious in controlling the pathogen. The wilt reduction was also attributed to induction and accumulation phytoalexins in tomato plants by chitosan. Chitosan contains oligosaccharides which induce proteinase inhibitors in tomato leaves that cause an increase in host plant resistance. Chitosan also increases lignification, increased lignin accumulation makes pathogen penetration in plants difficult by fortifying the cell wall (Ambrorabe, Bonmort, Fleurat-Lessard & Roblin, 2008). Finally, chitosan also acts as a resistance elicitor through induction of hydrolytic enzymes such as chitinase, chitokanase and  $\beta$ -glucanase (Mandal *et al.*, 2013).

#### **3.4.10.3 Silica in the Control of Bacterial Wilt**

Mesoporous silica nanoparticles (MSN) reduced wilt incidence significantly ( $P \leq 0.05$ ) (Figure 12). The reduction of wilt caused by *R. solanacearum* was attributed to the fact that silica augments resistance in tomato seedlings. This is because assimilated silica in plants inhibits fungal and bacterial diseases by physically inhibiting penetration of the epidermis through lignification of the membranes (Balakhina & Borkowska, 2013). Silica is a precursor in the synthesis of lignin. Hence, improves seed coat resistance, decreases seed susceptibility to mechanical damage and metabolite leaching. In contrast

to the above observation, Datnoff, Deren and Snyder (1997) found out that, silica did not significantly ( $P \leq 0.05$ ) improve a susceptible cultivar resistance. However, Jian (2004) proved that application of silica led to activation of pathogenesis-related proteins such as catalase, peroxidase, polyphenol oxidase, glucanase, chitinase in a pathogen infected plant. The proteins are associated with in increased plant resistance to pathogens. This was in agreement with the current study where tomato seeds and seedlings treated with MSN and its derivatives had higher wilt resistance due to *R. solanacearum*. Formation of a chitosan-MSN, a complex hitherto not reported to have been used in controlling bacterial wilt increased the role of the composite manifold. The composite significantly ( $P \leq 0.05$ ) reduced wilt incidences in tomato after treatment. The nanocomposite also had better sorption properties than MSN. This was attributed to the increased active sites for reaction due to the gel forming properties of the composite. According to Mandal *et al.* (2013), induced lignification and antimicrobial biochemicals, could have played an important role in host plant resistance of tomato plants in this study.

## CHAPTER FOUR

### ENHANCEMENT OF BACTERIAL WILT TOLERANCE, RHIZOSPHERE HEALTH, YIELD AND POSTHARVEST QUALITY IN TOMATO USING BIONANOCOMPOSITES

#### ABSTRACT

Biological control agents are useful in enhancing plant disease resistance and productivity. The agents also improve soil properties. Effect of biological control agents (BCAs) as a disease control measure in plants is hampered by their vulnerability to environmental and edaphic conditions. This study entailed the use of chitosan-silica nanocomposites for delivery of BCAs. Effect of BCAs-nanocomposite complexes on resistance of tomato plants to bacterial wilt, mycorrhizal root colonization, yield and shelf life of the harvested tomato fruits was investigated. Substitution of mesoporous silica nanoparticles (MSN) in the nanocomposite with nano synthesized clay was also assessed on disease resistance, yield and shelf life. The tomato bacterial wilt pathogen (*R. solanacearum*) was isolated from diseased greenhouse tomato and inoculated on tomato seeds and seedlings pre-treated with the bionanocomposites. There was significant ( $P \leq 0.05$ ) increase in level of the pathogenesis related biochemicals such as chitinases and glucanases in bionanocomposites treated plants. In addition, there was a significant ( $P \leq 0.05$ ) beneficial microbial colonization of tomato plant roots, yield and shelf-life of tomato fruits treated with BCAs adsorbed on nanocomposites. Wilting disease incidence was reduced by over 50%, tomato productivity increased by 50% and shelf-life increased by 30% when bionanocomposites were used compared to the control. Interestingly, there was no significant effect ( $P \leq 0.05$ ) on induced host plant resistance, yield and shelf life of tomato fruits when MSN were substituted with nanoclay particles. Substitution of MSN with nanoclay in synthesis of the BCAs-nanocomposite complex can be recommended due to cost benefits and ease of

availability with no significant ( $P \leq 0.05$ ) difference in efficacy between the nanoparticles. Use of nanoclay *in lieu* of MSN makes the process of synthesizing the nanocomposite carriers more sustainable.

#### **4.1 Introduction**

Variability of *R. solanacearum* pathogen makes applied chemicals an infective control method (Agrios, 2005). Apart from losing efficacy due to pathogen variability, synthetic pesticides results in chemical residue, especially when applied on harvested produce to prolong shelf life (Christoset *et al.*, 2011). The chemicals also cause environmental pollution (Noor, 1999). In addition, application of pesticides after appearance of wilt symptoms leads to losses since the pathogen is highly fastidious, thus hard to control after infection. Moreover, most of the chemicals used for soil fumigation have been banned by the World Health Organisation for instance, the Kyoto protocol of 2005 (Christos *et al.*, 2011). The export markets have also introduced stringent conditions on minimum and maximum residue levels (KHDP, 2007).

There is therefore, need for development of an environmentally sound and effective remedy for the pathogen. This may entail preparation of a pre-infection package which should be applied before infection of tomato plants by the pathogen (Jach *et al.*, 1995). In addition to reduced produce loss during production, biocontrol disease mechanisms enhance shelf life of agricultural produce which accounts to over 30 % loss of harvested produce (KHCP, 2012). BCAs have the potential of managing the bacterial wilt disease to below economic injury level, but their efficacy is hampered by harsh environmental conditions, short shelf life and inability to reach the target sites with potency. The efficacy of these BCAs is affected by the soil pH, moisture, temperature, electrical conductivity and other biotic factors which hinder penetration in the plant system and virulence to the pathogens (Nguyen & Ranamukhaarachchi, 2010).

Apart from environmental factors, efficacy of biological control agents is also hampered by reduced potency during storage and inability to reach the target sites after application (Algam *et al.*, 2010). Thus require to be combined with other materials for increased vitality, efficacy and effective delivery within the plant system. Nanocomposites have potential to deliver biocontrol agents due to their ease of functionalization, large surface area for adsorption and ability to penetrate epithelial layers. Chitosan and silica nanoparticles are preferred because of their non-toxicity, elicitation of host plant resistance, ease of assimilation by the root hairs and natural abundance (Soad, Algam, Ahmed, Mahdi & Guan, 2013). The chitosan-silica nanocomposites also induce other effects in plants like increased yield and resistance. This has been attributed to the antimicrobial effect of the useful microbes, chitosan and silica materials. Previous work in this study, showed compatibility and synergy when the microbes were incorporated and applied together with chitosan-silica nanocomposites (Dennis, Harrison, Agnes & Erastus, 2016).

## **4.2 Materials and Methods**

### **4.2.1 Preparation of Bionanocomposites**

Chitosan immobilized silica nanocomposite were synthesized through physisorption (Dennis *et al.*, 2016). The nanocomposites were used for adsorbing biocontrol agents including: *Bacillus subtilis*, *Glomus mosseae*, *Trichoderma viride*, *R. solanacearum* phage and effective micro-organisms (EM). The microbes were cultured on the respective growth media namely nutrient and potato dextrose agar for bacteria and fungi respectively. A cellular suspension was prepared and standardized to 2.000 optical density (O.D) using Shimadzu Ultra violet visible (Uv-vis) spectrophotometer. The suspension was then adsorbed on 10% chitosan immobilized silica nanocomposite (CISNC) and chitosan immobilized nanoclay (CINC). The nanocomposites and bionanocomposites were characterized on Rigaku X-ray powder diffractometer

(Christian *et al.*, 2008). A suspension of 10% was prepared (1:10 for bionanocomposite to distilled water) for inoculation.

#### **4.2.2 Experimental Sites and Design**

The microbial and bionanocomposite complexes were applied on tomato seeds prior to seeding by priming. A similar treatment was done on the planting media (cocopeat) and the primed seeds sown on a matching treatment in a tray. The seedlings were also treated with a similar complex prior to transplanting. Transplanting was done in greenhouses at 2 sites that is; Gatundu-Theta Tea Factory (0.9621 ° S, 36.7683 ° E and altitude 2050 m ASL) and Juja-JKUAT (1.0891° S, 37.0105° E and altitude 1400 ASL) on plastic pots with well prepared soil in the ratio of 3:0.5:1 for soil, sand and manure respectively. Another treatment was sown on cocopeat media with nutrients applied through fertigation. The experiments involved 18 treatments and 3 replications laid on a completely randomized design. Respective data was collected during the growth of plants.

#### **4.2.3 Determination of Effective Concentration (EC) for the Chitosan Immobilized Silica Nanocomposite (CISNC) Gel**

The EC of the CISNC was determined by a so-called “up and down” or the “staircase method” using two hybrid tomato varieties (Choi, 1990). Twelve concentrations of CISNC and bionanocomposites were applied *In vitro* and *In vivo* for the determination of EC of the *R. solanacearum* and wilt reduction respectively. The *In vitro* tests were observed for 5 days after treatment while *In vivo* tests lasted for a period of 6 months. The tests entailed *R. solanacearum* inhibition for *in vitro* while germination, growth rate and wilting incidences were done for the greenhouse experiments.

#### **4.2.4 Assessment of Mycorrhizal Colonization**

Root portions were sampled from all treatments. A sample from each replicate was taken. The roots were carefully rinsed to avoid loss of fine roots and preserved in 70% ethanol. The preserved roots were then assessed for mycorrhizal colonization according to the procedures of Koske & Gemma, 1989. Estimation of percentage root mycorrhizal fungi colonization frequency and intensity was done using the subjective visual technique by Kormanik and McGraw, 1982, commonly referred to as the slide method. The roots were cleared with 2.5% KOH (25g KOH in 1000 ml water) by heating in an oven at 70 °C for one hour and then rinsed with tap water. To remove phenolic substances, alkaline hydrogen peroxide (60 ml of 28-30% NH<sub>4</sub>OH, 90 ml of 30% H<sub>2</sub>O<sub>2</sub> and 840 ml distilled water) was added. The roots were then placed in an oven at 70 °C for 20 min. The process was repeated for all samples. Oven dried roots were rinsed with tap water and acidified with 1% hydrochloric acid (HCl) for 30 min. The HCl was decanted and without rinsing the roots, 0.05% Trypan blue in acid glycerol (500 ml glycerol, 450 ml water, 50 ml of 1% HCl and 0.5g Trypan blue) staining reagent added. The stained roots were placed in an oven at 70 °C for 1 hr. The stain was decanted and a destaining solution comprising of acid glycerol (500 ml glycerol, 450 ml distilled water, 50 ml of 1% HCl) added. Fine root segments were cut into 1 cm-long pieces and 30 pieces randomly picked, mounted on slides and observed under the Nikon compound microscope to assess the frequency and intensity mycorrhizal colonization. Presence of arbuscules, vesicles, internal and external hyphae was examined. The frequency of mycorrhizal colonization was recorded as the number of root fragments infected with mycorrhizal fungi and expressed as a percentage of total number of root fragments observed. The intensity of mycorrhizal fungi colonization was also recorded as percentage cover of mycorrhizal fungi infective propagules in each 1cm root fragment.

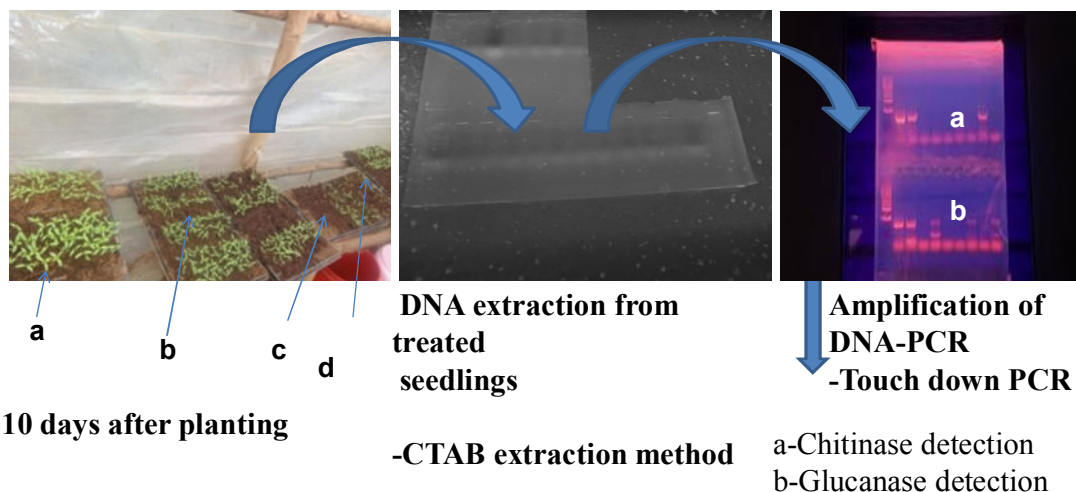
#### 4.2.5 Biochemical Analysis (Glucanase and Chitinase)

The efficacy of resistance elicitation was carried out by determining the levels of chitinase and glucanase biochemicals. A confirmatory test of the presence of the chitinase and glucanase enzymes was done after amplification of DNA by use of polymerase chain reactions (PCR).

Foliage from treated tomato plants was ground to obtain a suspension for DNA isolation. DNA was extracted following the CTAB extraction method and then stored at -20 °C (Kumlachew, 2014). The polymerase chain reaction (PCR) was carried out using touchdown procedures as described by Khalil *et al.* 2003. The primers were a 21 mer forward primer –CGA ACC TAA TGG TGG TAG TGC-, and reverse –TCG CAA CTA AAT CAG GGT TG- for chitinases. A 22 mer forward primer –CGC CAT TGC TCG TGT TGA CAT G- and reverse -AAT TTC TCG CTC GGC GGT GGT G for glucanases. The samples were cooled at 4 °C and subjected to electrophoresis on a 1.5% agarose gel in 1X TAE buffer (40 mM Tris acetate and 1.0 mM EDTA) and photographs taken under ultra-violet (Uv) light. The obtained ladders were interpreted using base pair amplicons of the enzymes (Chilvers, 2012 method). Amplified DNA (100 µL) was mixed with a binding buffer in a ratio of 1:1 mixed thoroughly by vortexing. Sodium acetate (10 µL of 3 M) was added and vortexed until a yellow colour appeared. A solution (800 µL) was transferred to the GeneJET purification column, Centrifuged for 30-60 sec and the flow-through discarded. Wash buffer (700 µL) was added to the GeneJET purification column, centrifuged for 30-60 sec, flow-through discarded and the purification column placed back into the collection tube. The empty GeneJET purification column was centrifuged for 1 min. The GeneJET purification column was transferred to a clean 1.5 mL microcentrifuge tube and centrifuged for another 1 min. the GeneJET purification column was discarded and the purified enzyme stored at -20 °C. Enzyme concentration was determined using Bioneer, nanodrop machine at 680/620 nm on purified samples of chitinase and glucanase enzymes (Korbie & Mattick, 2008).

#### 4.2.6 Illustration of Elicitation of Resistance in Tomato by Bio-Nanocomposites

##### Determination of induced resistance in tomato plants by nanocomposites



##### Key

- a-CISNC –Chitosan immobilized silica nanocomposites treated tomato seedlings
- b-BCAs-Biocontrol agents treated tomato seedlings
- c-Control
- d-CISNC-BCAs (Bionanocomposites)

#### 4.2.7 Bacterial Wilt Incidence

Incidences of bacterial wilt disease symptoms were observed and recorded as number of wilting plants per treatment. Wilting incidence was calculated using the formula;

$$\frac{(5A+4B+3C+2D+E)}{1.75 N} \dots\dots\dots i$$

Where, A=number of plants on scale 5; B=number of plants on scale 4; C=number of plants on scale 3; D=number of plants on scale 2; E=number of plants on scale 1;

N=total number of plants. From the scale, the lower incidence level the better the control measure (Tim, Pingsheng, Ken, Robert & Steve, 2008).

#### **4.2.7.1 Bacterial Wilt Severity Assessment**

The bacterial stem browning and streaming scoring scale was used in estimation of bacterial wilt disease severity. A scoring scale of 0-3 was adopted where, 0- no browning, 1-light brown colour at the base, 2- light brown colour above the basal part and 3-dark brown colour spread throught the vascular sytem. In addition, the streaming test was conducted by suspending cut stems in distilled water in a beaker and the ooze rate score of 0-3 used to determine severity, where, 0- no ooze, 1- thin strands of bacteria oozing, 2- continuous thin flow and 3- heavy ooze turning the water turbid (Elphinstone, Stanford & Stead, 1998). The bacterial stem browning and streaming were done by selecting and evaluating 3 plants per treatment collected 120 days after planting.

#### **4.2.8 Assessment of Yield in Tomato Varieties Treated With Bionanocomposites**

Data on cumulative yield per treatment were recorded as weight (kg) of tomato fruits harvested per tomato plant within a treatment throughout the harvesting period. The weight measurements were done using a 2 kg digital weighing scale. The fruit size diameter was measured using a string and actual dimension taken from a 30 cm ruler.

#### **4.2.9 Determination of Retention of Total Organic Carbon in Soil/Planting Media**

This was done by determination of percent (%) carbon in the soil based on the Walkley-Black chromic acid wet oxidation method. The amount of carbon was estimated as percentage using the following equation;

$$C = \frac{(B-T*0.3*V*0.75)}{WB} \dots\dots\dots ii$$

Where; C=Carbon percentage, B=amount of titrant consumed by blank, T= amount of titrant consumed by sample, W=weight of the sample, V=volume of  $K_2Cr_2O_7$ , 0.3=constant, 0.75=assumption that the sample had 75% carbon (Mylavarapu, 2009).

#### **4.2.10 Determination of pH in the Tomato Rhizosphere**

Soil pH was determined using a digital pH meter on all the treatments. The soil was dried at room temperature (25 °C) for 7 days then separated on the 6.3 mm sieve to obtain the fine soil for testing. A sample of  $30 \pm 0.1$  g was weighed and placed in a glass beaker. Equivalent volume of distilled water was added to the soil sample and stirred thoroughly to obtain soil slurry and then cover with watch glass. The sample was allowed to stand for 1 hr with continued stirring every 10 to 15 min to allow the pH of the soil slurry to stabilize. The readings were taken after stabilization using electrodes of pH meter standardized with 7.0 buffer solution.

#### **4.2.11 Determination of the effect of Bionanocomposite on Tomato Flowering, Ripening and Shelf Life of Fruits**

Data on days to 50% flowering, ripening and post harvest shelf life of tomato varieties treated with bionanocomposites was taken to indicate the effect bio-nanocomposites on growth and development of tomato plants and fruits. Harvested fruits were placed on a shelf rack under normal room temperature (25 °C). The data on shelf life enhancement was recorded in form of days before fruit rot blemishes were observed. Observations of the tomato fruit condition was done daily for 1 month.

### 4.3 Results

#### 4.3.1 Determination of Effective Concentration of Chitosan Immobilized Silica Nanocomposite (CISNC) Gel

The concentration of the nanocomposite significantly ( $P \leq 0.05$ ) affected inhibition of *R. solanacearum*, germination of tomato seeds, induction of chitinases, wilt incidence and tomato fruits shelf life. However, the effect of concentration on most of the parameters assessed was not significant between 10-40% (Table 4.1).

**Table 4.1: Effective Concentrations of CISNC in Tomato Growth, Development and Wilt Resistance**

Treat/ conc.	Inhibition	Germination	Wilt incidence	Chitinase	Shelf life (days)
0	15.33 a	72.11 a	30.00 a	1.543 a	12.01 a
0.5	18.67 a	77.89 b	31.11 a	2.029 ab	20.11 b
5	45.00 b	82.56 bc	33.78 bc	2.081 b	21.67 bc
10	75.33 c	82.89 cd	34.00 bc	2.096 b	21.67 bc
20	77.33 cd				
30	81.00 de	85.11 cde	36.11 c	2.157 bc	21.78 bc
40	84.33 ef				
50	87.67 fg	85.22 de	36.67 c	2.279 bc	22.22 bc
60	88.67 fgh				
70	90.00 gh	86.11 ef	36.78 c	2.800 c	23.00 c
80	91.67 gh				
90	92.33 h	88.22 f	55.00 d	2.966 cd	23.56 c
100	92.33 h				

Means followed by the same letter along a column are not significantly different. LSD 0.05

#### 4.3.2 Colonization of Roots by Biocontrol Agents

Adsorption of *Glomus mosseae*, a type of arbuscular mycorrhizal fungi (AMF) onto chitosan immobilized silica nanocomposite, induced the highest and most significant

( $P \leq 0.05$ ) root microbial colonization frequency (76.7%) and infection (81.7%). Interestingly, all microbes (BCAs), bionanocomposites, chitosan immobilized silica nanocomposite (CISNC) and chitosan immobilized nanoclay composites (CINC) treatments showed over 50% mycorrhizal infection rates compared to the controls acetic acid (AA) and distilled water (DW). There was significant ( $P \leq 0.05$ ) difference in colonization when different soils and media were used. The clay soil (JKUAT) had the highest microbial colonization and infection, followed by the acidic nitrisol (Theta tea factory). The inert media had the least (Figure 4.1, Tables 4.2, 4.3 and Plate 4.1).

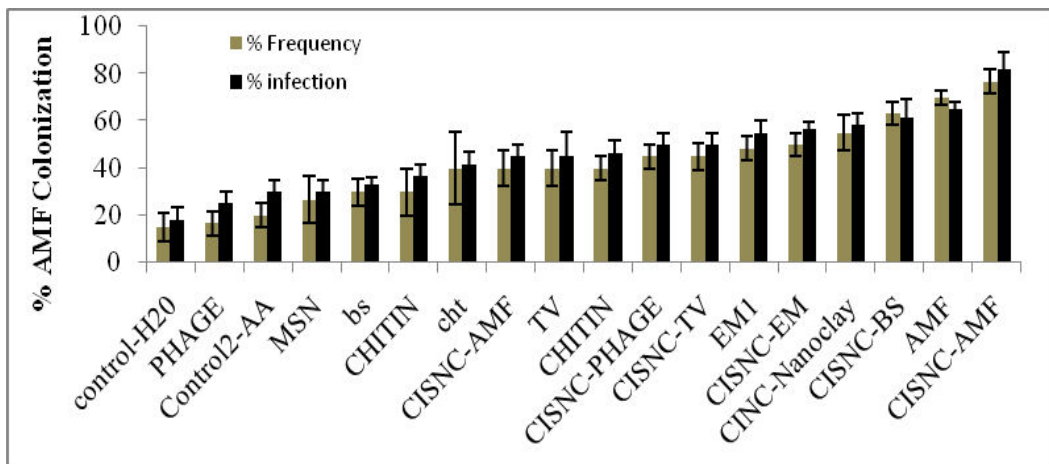


**Figure 4.1: Colonization and Frequency of Tomato Roots by Beneficial Microbes**

Means significant at L.S.D  $_{0.05}$  (F-test) <sup>1</sup>-LSD bar

**Table 4.2: Microbial Colonization Frequency in Tomato Root Hairs (AMF Colonization)**

Treat	Nitrisol	Clay	Cocopeat
Control (Distilled water)	15 a	19 a	0 a
Phage	17 ab	24 ab	5 a
Control (Acetic acid)	20 bc	27 b	0 a
Mesoporous silica nanoparticles (MSN)	27 c	30 bc	0 a
Bacillus subtilis (BS)	30 c	34 c	4 a
Chitin	30 c	35 c	0 a
Chitosan	40 d	40 cd	0 a
Chitosan immobilized silica nanocomposite (CISNC)	40 d	44 d	0 a
Trichoderma viride (TV)	40 d	44 d	4 a
Chitosan nanoparticles	40 d	45 d	0 a
CISNC-Phage	42 de	48 e	0 a
CISNC-TV	45 de	50 e	6 ab
Effective micro-organisms (EM)	45 de	52 e	8 ab
CISNC-EM	48 de	54 e	10 b
Chitosan immobilized nanoclay (CINC)	50 e	54 e	10 b
CISNC-BS	63 f	66 f	10 b
Glomus mosseae (AMF)	70 g	72 g	10 b
CISNC-AMF	77 g	74 g	20 c

Means followed by the same letter along a column are not significantly different. LSD

0.05 Protected

**Table 4.3: Microbial Colonization Frequency in Tomato Root Hairs (AMF Infection)**

Treat	Nitrisol	Clay	Cocopeat
Phage	18 a	23 a	0 a
Control (Distilled water)	25 ab	28 ab	0 a
Control (Acetic acid)	30 bc	34 bc	0 a
Mesoporous silica nanoparticles (MSN)	33 bc	37 bc	0 a
Chitin	37 cd	40 c	0 a
Bacillus subtilis (BS)	45 de	44 c	5 a
Chitosan	45 de	44 c	0 a
Trichoderma viride (TV)	47 def	45 c	5 a
Effective micro-organisms (EM)	50 efg	49 cd	8 b
CISNC-Phage	50 efg	49 cd	4 a
Chitosan nanoparticles	50 efg	49 e	0 a
Chitosan immobilized silica nanocomposite (CISNC)	55 fg	54 e	0 a
Chitosan immobilized nanoclay (CINC)	55 fg	59 ef	4 a
CISNC-EM	57 gh	62 f	15 c
CISNC-TV	58 gh	62 f	15 c
Glomus mosseae (AMF)	62 h	68 g	40 d
CISNC-BS	65 h	69 gh	10 ab
CISNC-AMF	82 i	85 i	50 e

Means followed by the same letter along a column are not significantly different. LSD

<sub>0.05</sub> Protected

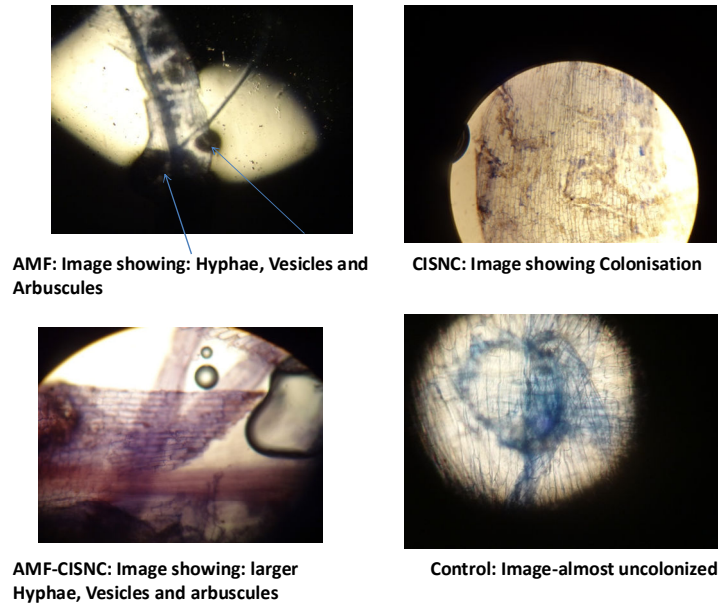


**Plate 4.1: Microbial Root Colonization Images**

### **4.3.3 Elicitation of Resistance in Tomato by Bionanocomposites**

Effect of treating tomato plants with bionanocomposites (BCA-CISNC complexes) was expressed by induced pathogenesis related biochemicals in the tomato plant in form of chitinase and glucanase. Biocontrol agents, chitosan-silica nanocomposites and their complexes increased concentration of chitinase and glucanase significantly ( $P \leq 0.05$ ). There was no significant difference ( $P \leq 0.05$ ) in chitinase and glucanase elicitation when bionanocomposites were applied on Anna and Chonto F1 tomato varieties. Expression of the enzymes was confirmed by amplification of the DNA. Data on concentration of the two enzymes and their expression in tomato plants is shown in tables 4.4, 4.5 and Plate 4.2 respectively. Correlation relationship of chitinase and wilt incidences in tomato plants is shown in table 4.6.



**Plate 4.2: Gel Image Showing PCR Product of Chitinase and Glucanase**

**Table 4.4: Concentration of Chitinase in Tomato Varieties Treated with Bionanocomposites**

Treatment	Anna F1	Chonto F1
Control (Acetic acid)	1.16 a	1.18 ab
Mesoporous silica nanoparticles (MSN)	1.23 b	1.26 b
Trichoderma viride (TV)	1.26 b	1.29 b
Nanoclay	1.31 c	1.42 c
Control (Ralstonia solanacearum)	1.33 cd	1.40 c
Phage	1.41 d	1.48 cd
Glomus mosseae (AMF)	1.42 de	1.54 e
Bacillus subtilis (BS)	1.42 de	1.54 e
Effective micro-organisms (EM)	1.56 e	1.55 e
Chitosan	1.60 e	1.59 ef
Chitosan nanoparticles	1.69 f	1.60 f
Chitosan immobilized nanoclay (CINC)	1.70 f	1.61 f
Chitosan immobilized silica nanocomposite (CISNC)	1.76 g	1.61 f
CISNC-Phage	1.93 h	1.98 g
CISNC-TV	2.00 i	2.20 h
CISNC-AMF	2.03 i	2.37 i
CISNC-BS	2.24 j	2.45 j
CISNC-EM	2.61 k	2.74 k

Means followed by the same letter along a column are not significantly different. LSD<sub>0.05</sub> Protected

**Table 4.5: Concentration of Glucanase in Tomato Varieties Treated with Bionanocomposites**

Treatment	Anna F1	Chonto F1
Control (Acetic acid)	0.13 a	0.15 a
Mesoporous Silica Nanoparticles (MSN)	0.14a b	0.16 a
Trichodermaviride(TV)	0.15 ab	0.18 ab
Nanoclay	0.17 b	0.20 b
Control (Ralstonia solanacearum)	0.23 c	0.22 b
Phage	0.24 c	0.25 bc
Glomus mosseae (AMF)	0.25 cd	0.25 bc
Bacillus subtilis(BS)	0.26 cd	0.25 bc
Effective micro-organisms (EM)	0.26 cd	0.25 bc
Chitosan	0.26 cd	0.26 c
Chitosan nanoparticles	0.26 cd	0.26 c
Chitosan Immobilized Nanocomposites (CINC)	0.26 cd	0.26 c
Chitosan immobilized silica nanocomposite (CISNC)	0.27 d	0.27 cd
CISNC-Phage	0.27 d	0.28 d
CISNC-TV	0.27 d	0.28 d
CISNC-AMF	0.27 d	0.28 d
CISNC-BS	0.27 d	0.28 d
CISNC-EM	0.27 d	0.28 d

Means followed by the same letter along a column are not significantly different. LSD<sub>0.05</sub> Protected

**Table 4.6: Pearson Correlations for Chitinase and Bacterial Wilt Incidences in Tomato Varieties**

N	Correlation for chitinase and wilt incidence in Anna F1	Correlation for chitinase and wilt incidence in Chonto F1
18	Chitinase	
18	Wilt incidence	0.8459***
		0.7367***

P<0.001

### 4.3.4 Bacterial Wilt Assessment

#### 4.3.4.1 Bacterial Wilt Incidence Assessment

Tomato seedlings treated with bionanocomposites (BCA-CISNC complex) particularly the effective micro-organisms and phages had the least wilt incidences. Incidences of wilting least occurred in bionanocomposites, CISNC and CINC composite treatments compared to plants treated with biocontrol agents or on nanocomposites only. Control experiments; acetic acid and distilled water had significantly ( $p \leq 0.05$ ) higher wilt incidences compared to all other treatments. The wilt incidences were also not significantly different ( $P \leq 0.05$ ) between the tomato varieties used when bionanocomposites were used and the seedling inoculated with the pathogen. However, in the control experiments, Anna F1 had a significantly ( $P \leq 0.05$ ) higher wilt incidence than Chonto F1 (Table 4.7).

**Table 4.7: Wilt Incidences in Tomato Varieties Treated with Bionanocomposites**

Treatments	Anna F1	Chonto F1
CISNC-EM	17.6 a	19.3 a
CISNC-BS	20.5 ab	22.9 ab
CISNC-Phage	26.4 bc	24.5 b
CISNC-AMF	26.3 bc	24.7 b
Chitosan immobilized nanoclay (CINC)	28.6 c	26.1 c
Chitosan immobilized silica nanocomposite (CISNC)	28.1 c	26.8 c
CISNC-TV	28.0 c	29.2 cd
Effective micro-organisms (EM)	30.7 d	28.8 c
Mesoporous silica nanoparticles (MSN)	34.1 e	32.5 d
Chitosan nanoparticles	35.8 e	34.2 de
Glomus mossea (AMF)	37.5 ef	35.4 e
Chitosan	37.8 ef	38.5 ef
Phage	39.7 f	38.4 ef
Trichoderma viride (TV)	41.5 fg	39.3 f
Bacillus subtilis (BS)	40.7 fg	39.8 f
Chitin	46.0 h	43.7 h
Control (Acetic acid)	54.5 i	52.0 i
Control (Distilled water)	55.8 ij	54.4 ij

Means followed by the same letter along a column are not significantly different. LSD<sub>0.05</sub>

#### 4.3.4.2 Bacterial Wilt Severity

There was significant ( $P \leq 0.05$ ) difference in bacterial browning and streaming effect scores when different bionanocomposites were used to control bacterial wilt in the two tomato varieties. Comparatively, Chonto F1 had lower bacterial browning and streaming than Anna F1 variety (Table 4.8).

**Table 4.8: Bacterial Wilt Severity in Tomato Varieties Treated with Bionanocomposites**

Treatment	Anna F1	Chonto F1	Anna F1	Chonto F1
	Bacterial browning effect		Bacterial streaming effect	
CISNC-EM	0.4 a	0.4 a	0.1 a	0.1 a
CISNC-BS	0.6 ab	0.5 a	0.4 b	0.3 b
CISNC-Phage	0.9 b	0.8 b	0.4 b	0.3 b
CISNC-AMF	0.5 a	0.4 a	0.1 a	0.1 a
Chitosan immobilized nanoclay	1.2 c	0.9 b	0.8 c	0.7 c
Chitosan immobilized silica nanocomposite (CISNC)	0.8 b	0.7 ab	0.6 bc	0.6 c
CISNC-TV	0.7 ab	0.8 b	0.6 bc	0.6 c
Effective micro-organisms (EM)	1.4 c	1.1 c	0.7 c	0.6 c
Mesoporous silica nanoparticles	1.8 d	1.5 cd	1.0 d	1.0 d
Chitosan nanoparticles	1.3 c	1.2 c	0.8 c	0.9 d
G. mossea (AMF)	0.8 b	0.7 ab	0.8 c	0.6 c
Chitosan	0.8 b	0.8 ab	0.8 c	0.7 c
Phage	1.4 c	1.2 c	1.0 d	0.9 d
T. viride	2.2 e	1.6 cd	1.3 de	1.2 e
B. subtilis	1.6 cd	1.4 c	1.0 d	1.0 d
Chitin	1.0 b	0.9 b	1.0 d	1.0 d
Acetic acid	2.2 e	2.0 e	1.8 f	1.6 f
Distilled water	2.4 e	2.2 e	2.1 g	2.0 g

Means followed by the same letter along a column are not significantly different LSD<sub>0.05</sub> Protected, Score 0- no browning, 1- light browning at the basal stem 2 cm, 2- light brown colour spread in the vascular system and 3- dark brown colour widespread browning. Ooze rate score 0- no ooze, 1- thin strands of bacteria oozing, 2- continuous thin flow and 3- heavy ooze turning the water turbid (Elphinstone *et al.*, 1998).

#### 4.3.5 Effect of Bionanocomposites on Tomato Yield

There was a significantly ( $p \leq 0.05$ ) higher yield of harvested tomato fruits from plants treated with biocontrol agents, chitosan-silica nanocomposites and their bionanocomposites. The difference in tomato yield was not significantly ( $p \leq 0.05$ ) different when the various bionanocomposites were applied. However, Chonto F1 had a significantly ( $P \leq 0.05$ ) higher yield than Anna in all treatments (Tables 4.9, 4.10 and Plate 4.3).

**Table 4.9: Circumference (cm) of Fruits Treated with Bionanocomposites**

Treatments	Anna F1	Chonto F1
Control (Distilled water)	15.0 a	14.4 a
Control (Acetic acid)	15.5 a	14.9 a
Phage	15.7 a	15.1 b
Trichodermaviride (TV)	16.0 b	15.3 b
Bacillus subtilis (BS)	16.6 b	15.3 b
Chitosan	17.1 c	15.7 b
CISNC-TV	17.3 c	16.6 c
CISNC-Phage	17.3 c	17.0 d
Chitosan nanoparticles	17.2 e	17.4 d
Chitosan immobilized silica nanoparticles (CISNC)	17.3 c	17.6 d
Mesoporous silica nanoparticles (MSN)	17.7 c	17.8 d
Nanoclay	17.8 c	18.0 e
Chitosan immobilised nanoclay (CINC)	18.1 d	18.4 e
CISNC-BS	18.8 d	18.6 e
Effective micro-organisms (EM)	18.8 e	18.9 e
CISNC-EM	19.0 d	19.4 f
Glomus mosseae (AMF)	19.0 e	19.5 f
CISNC-AMF	20.0 f	21.0 g

Means followed by the same letter along a column are not significantly different. LSD

0.05

**Table 4.10: Weight of Fruits from two Tomato Hybrids (Kgs/Plant)**

Treatment	Anna F1	Chonto F1
Control (Distilled Water)	5.7 a	6.1 a
Control (Acetic acid)	6.2 ab	7.4 ab
Phage	7.4 bc	7.8 b
<i>Trichoderma viride</i> (TV)	7.7 cd	8.6 c
Mesoporous silica nanoparticles (MSN)	8.2 cde	8.9 c
Nanoclay	8.0 cde	9.2 cd
Bacillus subtilis (BS)	8.5 cdef	9.6 d
Effective microorganisms (EM)	8.8 defg	9.8 d
Chitosan	8.9 defg	10.1 de
CISNC-Phage	8.9 defg	10.3 def
Chitosan nanoparticles	9.4 defgh	10.7 efg
Glomus mossesae (AMF)	9.6 efghi	10.9 efg
CISNC-TV	9.7 fghi	11.1 fgh
CISNC-BS	9.9 ghi	11.4 ghi
Chitosan immobilized silica nanocomposite (CISNC)	10.2 hi	11.8 hi
Chitosan immobilized nanoclay (CINC)	10.3 hi	12.3 i
CISNC-EM	10.5 i	12.6 i
CISNC-AMF	12.7 j	13.1 j

Means followed by the same letter along a column are not significantly different LSD<sub>0.05</sub>



**Plate 4.3: Images of Tomato Plants Treated with Bio-Nanocomposites**

#### 4.3.6 Total Organic Carbon Accumulation in the Soil

Addition of biocontrol agents, chitosan-silica composites and bionanocomposites in the rhizosphere, increased the carbon content significantly ( $P \leq 0.05$ ) compared to the

controls. Application of bacteriophage did not increase the total organic carbon significantly ( $P \leq 0.05$ ). The level of total organic carbon (TOC) was significantly ( $P \leq 0.05$ ) higher in Juja clay soils than Gatundu's nitrisol, while cocopeat had the least carbon build up (Table 4.11).

**Table 4.11: Total Organic Carbon (TOC) in Tomato Rhizosphere after Removal of Plant Debris**

Treatment	Nitrisol	Clay	Cocopeat
Control (Distilled Water)	2.4 a	3.8 a	30.6 a
Phage	2.7 a	3.9 a	31.4 ab
Control (Acetic acid)	2.8 a	4.3 b	30.8 a
Bacillus subtilis (BS)	3.2 b	4.8 bc	33.7 b
Trichoderma viride(TV)	3.3 bc	5.0 bc	34.3 b
Effective microorganisms (EM)	3.5 bc	5.3 c	35.8 c
Glomus mosseae (AMF)	3.6 c	5.3 c	36.2 d
Mesoporous silica nanoparticles (MSN)	3.6 c	4.4 b	30.7 a
CISNC-Phage	4.1 d	5.7 d	37.9 de
Chitosan nanoparticles	4.3 de	5.8 de	38.3 ef
CISNC-BS	4.3 de	5.9 e	38.6 ef
Chitosan	4.3 de	5.8 de	39.1 f
Chitosan immobilized silica nanocomposite (CISNC)	4.4 e	5.8 de	37.9 de
Chitosan immobilized nanoclay (CINC)	4.4 de	5.9 d	38.3 e
CISNC-AMF	4.5 de	5.7 d	38.6 e
CISNC-EM	4.5 de	5.8 de	39.6 fg
CISNC-TV	4.6 e	5.8 de	39.7 fg
Chitin	5.6 f	6.1 f	40.3 g

Means followed by the same letter along a column are not significantly different. LSD

0.05

#### 4.3.7 Effect of Bionanocomposites on Soil pH

Chitosan immobilized silica or chitosan immobilized on nanoclay had significant ( $P \leq 0.05$ ) effect on soil pH around the rhizosphere compared to the controls. Adsorption of BCAs on the nanocomposites increased their effect on soil pH significantly ( $P \leq 0.05$ ).

There was also significant ( $P \leq 0.05$ ) change in pH levels in all the planting media used i.e. clay, nitrisol and cocopeat (Table 4.12).

**Table 4.12: Soil pH in Rhizosphere after Removal of Tomato Plant Debris in Different Planting Media, 6 Months after Application of the Bionanocomposites**

Treatment	Nitrisol	Clay	Cocopeat
Control (Distilled Water)	5.2 ab	6.7 c	6.5 a
Control (Acetic acid)	5.0 a	6.6 b	6.2 a
Effective microorganisms (EM)	5.1 a	6.5 a	6.6 ab
Mesoporous silica nanoparticles (MSN)	5.1 a	6.5 a	6.6 ab
Phage	5.1 a	6.5 a	6.6 ab
Bacillus subtilis (BS)	5.2 ab	6.6 a	6.7 b
Glomus mossease (AMF)	5.4 b	6.7 c	6.8 bc
Trichoderma viride(TV)	5.3 ab	6.8 d	6.7 b
Chitin	5.6 c	6.8 d	6.9 c
Chitosan nanoparticle	5.7 cd	6.8 d	7.0 cd
CISNC-EM	5.8 d	6.8 d	7.1 d
Chitosan immobilized nanoclay (CINC)	5.7 cd	6.8 d	6.9 c
Chitosan	5.7 cd	6.8 d	7.0 cd
CISNC-AMF	5.8 d	6.8 d	7.1 d
CISNC-Phage	5.7 cd	6.8 d	7.0 cd
Chitosan-silica nanocomposite (CISNC)	5.7cd	6.8 d	7.1 d
CISNC-BS	5.7 cd	6.8 d	7.2 de
CISNC-TV	5.8 e	6.9 e	7.3 e

Means followed by the same letter along a column are not significantly different. LSD

0.05

#### **4.3.8 Effect of Bionanocomposites on Flowering, Ripening and Shelf Life of Tomato Fruits**

Tomato plants treated with chitosan-silica nanocomposites and bionanocomposites (BCA-CISNC) had a significant ( $P \leq 0.05$ ) effect on days to 50% flowering and ripening. There was accelerated flowering and ripening on hybrid tomato plants of Anna and Chonto varieties treated with the bionanocomposites. In addition, there was also a

significant ( $P \leq 0.05$ ) increase in the shelf life of tomato fruits varieties. Adsorption of biocontrol agents on chitosan-silica nanocomposites enhanced their efficacy on growth, ripening and shelf life (Tables 4.13 and 4.14).

**Table 4.13: Days to Flowering and Ripening of Fruits in Tomato Hybrids Treated with Bionanocomposites**

Treat	Anna F1	Chonto F1	Anna F1	Chonto F1
CISNC-AMF	24 a	26 a	63 a	64 a
CISNC-EM	25 a	27 a	63 a	65 a
CISNC-BS	25 a	27 a	64 a	66 ab
CISNC-TV	25 a	28 ab	64 a	67 b
Chitosan immobilized silica nanocomposite (CISNC)	26 b	29 b	65 ab	67 b
Chitosan immobilized silica nanoclay (CINC)	26 b	29 b	65 ab	67 b
CISNC-Phage	27 b	29 b	66 b	67 b
Glomus mosseae (AMF)	27 b	29 b	66 b	68 c
Effective microorganisms (EM)	27 b	30 c	66 b	68 c
Bacillus subtilis (BS)	28 c	30 c	66 b	68 c
Trichoderma viride (TV)	28 c	32 cd	66 b	70 d
Chitosan nanoparticles	28 c	32 cd	68 c	70 d
Mesoporous silica nanoparticles (MSN)	28 c	32 cd	69 c	70 d
Chitosan	28 c	32 cd	69 c	69 cd
Chitin	28 c	32 cd	72 d	74 e
Phage	28 c	33 d	72 d	74 e
Control (Acetic acid)	29 d	34 d	72 d	75 e
Control (Distilled water)	29 d	35 e	74 de	75 e

Means followed by the same letter along a column are not significantly different. LSD<sub>0.05</sub> Protected

**Table 4.14: Shelf Life (Days) of Tomato Fruits Treated with Bionanocomposites**

Treatment	Theta tea factory	JKUAT	Cocopeat
Control (Distilled water)	10.0 a	7.0 a	5.7 a
Control (Acetic acid)	10.7 a	8.0 a	5.4 a
Bacillus subtilis (BS)	11.2 a	10.4 b	9.4 b
Trichoderma viride (TV)	11.2 a	10.1 b	9.7 b
Effective micro-organisms (EM)	13.2 b	12.1 c	10.6 bc
Mesoporous silica nanoparticles (MSN)	14.3 bc	11.8 c	10.2 bc
Phage	14.7 bc	22.5 d	9.0 b
Nanoclay	15.2 c	21.8 d	13.3 c
Glomus mosseae (AMF)	24.3 d	23.4 d	16.2 d
CISNC-AMF	24.3 d	23.9 de	18.4 e
Chitosan	24.3 d	23.1 d	16.8 d
CISNC-TV	24.3 d	24.5 e	16.9 d
CISNC-BS	25.5 e	23.0 d	17.4 de
Chitosan nanoparticles	26.0 e	24.0 e	17.5 de
CISNC-Phage	25.5 e	23.9 d	16.2 d
Chitosan immobilized silica nanocomposite (CISNC)	26.0 e	24.0 e	16.3 d
CISNC-EM	27.3 f	24.5 e	20.6 f
Chitosan immobilized nanoclay (CINC)	26.0 e	23.0 d	15.8 d

Means followed by the same letter along a column are not significantly different. LSD<sub>0.05</sub> Protected

#### 4.4 Discussion

##### 4.4.1 Determination of Effective Concentration (EC) of Chitosan Immobilized Silica Nanocomposite (CISNC) Gel

Validating effectiveness of CISNC gel on *R. solanacearum* inhibition, tomato seed germination, wilting of tomato plants, elicitation of resistance and tomato fruit shelf life was an important step towards synthesis of a bionanocomposite pesticide. This was achieved by determination of the effective concentration (EC) with significant ( $P \leq 0.05$ ) effects on bacterial inhibition, tomato wilt incidences, elicitation of chitinase and postharvest shelf life of harvested tomato fruits (Table 4.1). From the study, a

concentration of 0.5% reduced *R. solanacearum* colony by 18.7%, germination was at 77.9%, chitinases 2.029 nm, wilt incidence at 31.11 and shelf-life prolonged to 20.1 days. In comparison, a concentration of 10% resulted in 75.3% reduction in inhibition, seed germination of 82.9%, chitinases elicited to 2.081 nm, wilt incidence reduced by 33.8% and shelf-life enhanced to 21.7 days. The 10% concentration of CISNC was not significantly ( $P \leq 0.05$ ) different from the 20-50% concentration in *R. solanacearum* inhibition, seed germination, chitinases elicitation, wilt incidence and shelf life of treated fruits. Thus adoption of 10% as the EC was based on the 5 parameters tested and the fact that too high concentration would be economically untenable and may imbalance other ecological aspects when copious amounts of reagents are added to the rhizosphere (Sharp, 2013).

#### **4.4.2 Colonization of Roots by Biocontrol Agents**

Beneficial microbial root colonization is associated with root hairs development in most crops. The root hairs are colonized internally or externally by these microbes with evidence of hyphal, vesicular and arbuscular structures. Colonization of plant roots by beneficial micro-organisms enhances establishment of mycorrhizal structures (Mandal *et al.*, 2013).

Park., Paul., Kim., Nam., Lee., Choi and Lee (2007) observed that, most beneficial microbes act as mycorrhiza-helpers enhancing mycorrhizal colonization and frequency. The interaction of the saprophytic plant growth promoting rhizobacteria and/or fungi (PGPR/F) and the symbiotic mycorrhiza improved the biotic activity in the rhizosphere. The interaction results in antagonism of pathogens by increased competition for space and nutrients (Gholami, Shahsavani, Nezarat, 2009). Tomato plant is a mycorrhizal “friendly plant” hence, *Glomus mosseae* readily colonized the root hairs. Mycorrhiza fungi enhances root establishment and root damage compensation increasing nutrient uptake and overcoming soil borne pathogens and pests thus, reduced tomato wilt

incidences in treatments colonized by the biocontrol agents (Hodge, 2000) (Tables 4.3, 4.4 and Plate 4.1). In related studies, critical analysis of mycorrhiza colonized roots showed that growth of pathogens was only restricted to the epidermis and cortical tissues. Conversely, in diseased non-mycorrhizal roots, the pathogens infected even the stele. Mycorrhizal colonized roots also structurally disorganized and inhibited pathogen development (Barea, Azcon, Azcon-Anguilar, 2002).

#### **4.4.3 Elicitation of Resistance in Tomato by Bionanocomposites**

Plant materials for analysis were taken 8 weeks after transplanting to ensure that microbial colonization and effect of bionanocomposites had fully taken place. The enhanced resistance was expressed by the elevated of chitinase and glucanase concentrations (Table 4.4 and 4.5). The two hydrolytic enzymes are related to plant resistance as they change with pest attacks or when exposed to resistance eliciting agents (Jach *et al.*, 1995). The study showed high correlation between the induced chitinase and bacterial wilt incidences in the two tomato varieties (Table 4.6). Garcia-Garrido and Ocampo (2002) demonstrated that, some plant genes and biochemicals are associated with plant defense response. Mycorrhizal structures such as the hyphae, vesicles and arbuscules induced expression of some pathogenesis related genes hence, plants colonized by mycorrhiza has elevated defense related genes and enzymes. Chitinase and glucanase enzymes are synergistically induced during attack by pathogens and/or resistance elicitors. Total chitinase activity is higher in mycorrhizal friendly plants more so when colonized by the root-fungus complex than non-mycorrhizal plants and their controls. Confirming the above observations, Sambrook, Fritsch & Maniatis (1989) found out that, constitutive activities of chitinase and glucanase were several folds lower in wheat leaves before treatment with elicitors. The enzymes were elevated significantly ( $P \leq 0.05$ ) upon treatment with *Stagonospora nodorum* isolates with high virulence.

However, Mandal *et al.* (2013) opined that the enzymes were non-specific defense response in plants. This was quite inconsistent as there was evident and systematic reduction of disease symptoms in tomato plants with the elevated enzymes in this study. This resulted in the enzymes being referred to as bioprotector agents (Jongedijk *et al.*, 1995). Participation of hydrolytic enzymes; chitinase and glucanase in defense response of plants has also been described by Jongedijk *et al.* (1995). This has been attributed to the fact that, most pathogenic bacteria and fungi contain 1, 3 B-glucans, chitin and other substrates of these enzymes as cell wall components. These enzymes effectively restrict growth of fungi and bacteria as they have lysozyme activity. Infection of healthy plants by pathogens is also associated with rapid activation of the corresponding gene that is, chitinase and/or glucanase gene(s) around the necrotic area in a leaf. Though chitinases and glucanases act synergistically in host plant defense and they employ different mechanisms to fight the pathogens (Soad *et al.*, 2013). For instance, while the chitinase enzyme catalyse the cleavage of a bond between C<sub>1</sub> and C<sub>4</sub> of two consecutive N-acetyl-D-glucosamine monomers of chitin, glucanase enzyme catalyse the cleavage of B,1-3 glucans. The two compounds are ubiquitous in most pathogens (Neerja, Anil, Purushotham, Suma, Sarma, Moers-chbacher & Podile, 2010). Jongedijk *et al.* (1995) demonstrated that, when chitinase is released, it induces copious biosynthesis of chitinases, glucanases, catalyses and other defense related enzymes. Also plants transformed with the two genes i.e. chitinase and glucanase are observed to have higher resistance to most pathogens than those transformed with the either of those genes (Livio, Anna & Dario, 2006; Pratibha *et al.*, 2012). This was consistent with the current study, where there was a strong correlation between the concentration of the chitinase and glucanase biochemicals in tomato plants with less wilting incidences (Table 4.2; Plate 4.1).

#### **4.4.4 Bacterial Wilt Incidence and Severity**

Combination of several resistance elicitor agents such as silica, nanoclay, chitosan and biocontrol agents known as co-inoculation resulted in highest significant ( $P \leq 0.05$ ) effect against wilt in this study (Table 4.7). This resistance was caused by competition of colonization sites, carbon components and induction of systemically induced resistance for disease suppression (Algam *et al.*, 2010). Use of chitosan in the nanocomposite carrier enhanced the biocontrol agents' efficacy against the pathogen. Thus, combination of chitosan nanocomposite and microbial antagonists, such as the *B. subtilis*, effective micro-organisms, *T. viride*, *G. mosseae* and *R. solanacearum*-phage, enhanced their efficacy. Chitosan acts as a good carrier material due to high concentration of polysaccharides. Chitosan and its derivatives were also degraded producing pathogen repellents like ammonia which predisposed the *R. solanacearum* to the emboldened biological antagonists making the adsorbed micro-organisms more efficacious in controlling the pathogen as observed in this study. However according to Pal and Spadden (2006), biocontrol agents are more likely to be preventive than therapeutic in disease control thus, their potential should be harnessed by seed priming and/or pre-treatment before transplanting. The biocontrol agents were found to be more efficacious in seed primed seedlings while chitosan and its derivatives acted better as a soil drench (Prevost *et al.*, 2006). Interestingly, substitution of mesoporous silica with nanoclay did not result in significant ( $P \leq 0.05$ ) difference of the parameters tested i.e wilt incidences. This was attributed to the fact that clay contains substantial quantities of silica in composition (over 90% silica) (Saldajeno & Hyakumani, 2011; Pinto, Do Nascimento, Gomes, da Silva & Miranda, 2012).

#### **4.4.5 Effect of Bionanocomposites on Tomato Yield**

Tomato yield was increased significantly ( $P \leq 0.05$ ) when bionanocomposites were used (Table 4.9 and 4.10). The bionanocomposite contained silica which greatly improves

plant performance and productivity. Silica increases chlorophyll content (Jian, 2004). Effects of silica deposited in leaves on improving photosynthetic potential and efficiency by opening angle of leaves, keeping the leaf erect, and decreasing self-shading have been reported in rice, barely, wheat and sugarcane (Soratto *et al.*, 2012). Application of silica also improves photosynthetic capacities of crops' by the enlarged size of chloroplasts and the increased number of grana in leaves (Yang, 2010). The increased yield was also associated with beneficial microbial inoculation of the seedlings. For instance, mycorrhiza fungi have been found to increase plant growth, chlorophyll content, phosphorous content and resistance to cultural and environmental stresses (Gaur, Gaur & Adholeya, 2000). These biocontrol agents enhance biosynthesis processes, growth and development, greater leaf area and higher yield per plant (Schemidt, Domonkos, Sumalan & Biro, 2010). Plant growth promoting rhizobacteria and fungi, such as bacillus, effective micro-organisms, trichoderma and mycorrhiza influences root exudation of host plants which helps in solubilization of P and promotion of a sustainable nutrient supply to crops through mineralization thus higher yield (Boer, Folman, Summerbell & Boddy, 2005). Finally, chitosan contains high carbon content which can stimulate growth of beneficial microbes resulting in higher microbial activity in the rhizosphere thus increased nutrients for plant uptake (Gaur *et al.*, 2000). Cao *et al.* (2013) found out that, chitosan contains oligosaccharides that act on plants as phytohormones which increase plant growth and development. It also promotes availability and uptake of water and essential nutrients by adjusting osmotic pressure (Li *et al.*, 2010).

#### **4.4.6 Total Organic Carbon Accumulation in the Soil**

Application of biocontrol agents and organic polymers increases the microbial activity in the rhizosphere (Kubata *et al.*, 2005). Use of organic polymers as carriers increased the longevity of microbes in the soil and their efficacy in root hairs colonization. Adsorption of biocontrol agents on chitin derivatives had a positive effect of providing the microbes

with substrate for utilization to obtain energy and minerals before adapting to the rhizosphere. Microbial activity increases soil organic matter which is expressed as percent carbon, thereby affecting the soil physical and chemical properties. The microbial activity increases soil fertility by providing cation exchange sites and acting as a reserve for plant nutrients which are slowly released upon mineralization. According to Gray and Smith (2005), there exists a strong correlation between soil organic matter and soil fertility. The low carbon content in the control was attributed to continued cultivation of soil with addition of synthetic fertilizers reducing the microbial diversity and numbers. This resulted in soil degradation, increased soil acidity and reduced soil fertility (Vahjen, Munch & Tebbe, 1995).

#### **4.4.7 Effect of Bionanocomposites on Soil pH**

Application of bionanocomposites had an effect on the soil pH in the long run (Table 4.12). Chitosan had a higher effect on the soil pH than chitin, attributed to the ease of polymer solubility. This is because, deacetylation of chitin into chitosan reduces the strength of bonds and makes the polymer polar, and thus chitosan is easily broken down (Prevost *et al.*, 2006). The polymer gradually increased the rhizosphere soil pH in this study, due to the released ammonia during breakdown of the nitrogen rich chitinous substrate (Rodrigo *et al.*, 2006). Regulation of soil pH is important for optimal microbial colonization. For instance, acidic soils inhibit the establishment of plant growth promoting fungi, while alkaline soils reduce colonization by the plant growth promoting rhizobacteria. A fairly neutral soil pH has the effect of enhancing development of both fungal and bacterial beneficial microbes. This promotes diversity of soil microbial communities a desired property in soil fertility and crop productivity (Barea *et al.*, 2002).

#### **4.4.8 Effect of Bionanocomposites on Flowering, Ripening and Shelf Life of Tomato Fruits**

The accelerated growth, flowering and increased shelf life of the 2 tomato varieties observed in the study was attributed to nutritional, antimicrobial and physiological effect of bionanocomposites (Table 4.13 and 4.14). Silica for instance, influences nutrients such as N, P, K and Ca uptake in tomato. The macro nutrients are associated with growth and development therefore any activity that enhances their absorption increases development. Calcium helps in formation of firm fruits by combining with pectins in the cell wall. High concentration of silica in tomato increases the betacarotene and lycopene contents, the 2 are associated with tomato fruit quality (De Pascale, Maggio, Foglianov, Ambrosino & Ritieni, 2001). Also, silica contained in the nanocomposite, played an important role in modifying the physiology of tomato crops and fruits (Jian, 2004). This helped tomato plants and fruits in this study cope well with both biotic and abiotic stress. Soluble silica penetrates cell wall and accumulates around the epidermis, conferring strength and turgor. The compound also forms a gel and associates with calcium and pectins to stabilise cell walls thus improving shelf life and quality of fruit. Silica also enhances disease resistance which in turn decreases postharvest rotting in agricultural produce (Prado & Natale, 2005).

Secondly, most beneficial microbes also known as plant growth promoting rhizobacteria and fungi promotes plant growth directly by either facilitating resource acquisition such as phosphate solubilisation, sequestering iron, modulating phytohormone levels e.g. Cytokinins, gibberellins, indoleacetic acid, ethylene. Indirectly the microbes enhance growth by decreasing the inhibitory effects of the pathogenic agents on plant growth and development (Glick, 2012). Beneficial microbes such as lactic acid bacteria (LAB), effective micro-organisms and *Bacillus subtilis* have a preservation effect on fresh produce (Soad *et al.*, 2013). Combination of biocontrol agents with essential oils like thyme and other materials with antimicrobial properties such as chitosan reduced the

pathogenic agents significantly ( $P \leq 0.05$ ) (Lee *et al.*, 1999). The prolonged shelf life of tomato fruits by biocontrol agents' treatment of plants is due to the effect on cellular integrity. This is achieved through good nutrition and reduced pre-harvest damage by pathogens which lead to softening aspect associated with spoilage in fruits (Lucas-Garcia, Probanza, Ramos, Ruiz-Palomino & Gutierrez, 2004; Soad *et al.*, 2013).

Finally, chitosan is associated with plant growth and development and also post harvest physiology. This is due to the nutritional role of the substance by providing nutrients and increased plant vigour (Gupta, 2011). The role of chitosan in post-harvest treatment of fruits cannot be overemphasized due to its antimicrobial effects. Plants treated with chitosan accumulate chitosan oligosaccharides which confer beneficial properties to produce. Such properties include; firm cell walls and membranes, reduced attack by pests in the field and reduced rate of respiration. Low respiration rate in climacteric fruits is due to degradation of chitosan which results in the release of nitric oxide (NO), the gas is unstable and combines with oxygen in the atmosphere around the fruits hence reducing the cell activities. The gas also limits hydrogenation of ethane ( $C_2H_6$ ) to ethylene ( $C_2H_4$ ) reducing senescence (Payasi & Sanwal, 2010). It particularly inhibits release of ethylene in the field which ensures the fruit attains physiological maturity (Cheng, Yang, Lu, Jia & Duan, 2009). This effect makes chitosan an ideal compound in production of high quality fruits as observed in this study. The bionanocomposites extends shelf life of fresh produce by suppressing respiration, transpiration and microbial growth by decreasing moisture and weight loss through enhancement of the cell membrane integrity reducing electrolyte leakages (De Pascale *et al.*, 2001).

## CHAPTER FIVE

### DEVELOPMENT OF A DIAGNOSTIC KIT FOR THE DETECTION OF *Ralstonia solanacearum*

#### ABSTRACT

Precision in pathogen detection has been made possible by advances in plant pathology, biotechnology and nanotechnology. For instance, polymerase chain reaction (PCR) and fluorescent kits have been developed to detect diseases. On-farm utilization of the aforementioned technologies has been limited by the expertise required and cost. Colorimetric nanoprobe have been applied in detection of water borne pathogens and heavy metals. This study entailed development of nylon-ferrous oxide chitosan-silica nanoprobe for detection of *R. solanacearum* pathogen. Electrospun nanofibres were used as support for ferrous oxide chitosan immobilized silica nanocomposite (FeOCISNC) gel. The materials were selected due to their compatibility, large surface area for microbial adsorption and high affinity of iron by *R. solanacearum* bacteria. Optimization experiments were carried out to determine the concentration of components and pH that yielded highest iron oxide nanoparticles (FeONPs). There was significantly high yield ( $P \leq 0.05$ ) when a ratio of 2:3 (v/v) for green tea extract to iron chloride solution and a pH of 6 were used. Synthesized composites were characterized using X-ray powder diffraction (XRD). The resulting nanomaterials had crystallite sizes of 3.96, 5.00 and 11.60 nm for FeONPs, FeOCISNC and nylon-FeOCISNC respectively. Detection of *R. solanacearum* was marked by colour change of the nanoprobe from grey to brown when placed in the pathogen suspension. This was also corroborated by XRD characterization; the nanoprobe adsorbed pathogen had a crystallite size of 14.75 nm. Additionally, the time required for optimal adsorption of FeOCISNC gel and pathogen inoculums on the nylon nanofiber and nylon-FeOCISNC probe respectively was determined using optical densities of the suspensions after adsorption. There was no

significant difference ( $P \leq 0.05$ ) in the optical density (O.D) of FeOCISNC gel when nylon nanofibres were immersed for 8 hr, 16 and 48 hr. Also, the O.D of the pathogen suspension was not significantly different ( $P \leq 0.05$ ) after 5, 30 and 60 min which validated the observation that the intensity of change in colour from grey to brown on the nanoprobe was not visually different within the same periods of time. The colour change was attributed to the mineralization of iron oxide in the nanoprobe which was caused by disruption of the pathogen membrane by glucosamine units in chitosan followed by complexation and absorption of iron. Absorption of iron from the nanocomposite was due to the high affinity for iron by the bacteria. Combination of ferrous oxide and chitosan silica nanocomposites gel produced a rapid, precise and user friendly tool for detection of the lethal *R. solanacearum* pathogen. The precise detection will consequently form basis for the pathogen control.

## 5.1 Introduction

Crop losses can be ameliorated and specific treatments developed to control the pathogens if the diseases are accurately diagnosed and identified prior to spreading. The conventional methods of identifying plant pathogens have been through physical observation which is only possible after damage has been done to the crop limiting effectiveness of the remedial strategies. To save plants from irreparable damage by pathogens, farmers have to identify an infection before the disease manifests using a disease diagnostic kit (KHDP, 2007; KHCP, 2012).

Development of disease diagnostic kits has been made possible by advances in molecular biology, plant pathology, and biotechnology (Chilvers, 2012). The kits are designed to detect plant diseases early, either by identifying the presence of a pathogen in the plant or the molecules produced by either the pathogen or the plant during infection (Michailides *et al.*, 2005; Chaumpluk *et al.*, 2012). These techniques are rapid and accurate in detecting pathogens. For instance, polymerase chain reaction (PCR) kits

have been developed to detect black Sigatoka disease in banana (Kumlachew, 2014), *Phytophthora infestans* in potato and *Fusarium* in cotton (Tim *et al.*, 2008). Also, enzyme-linked immunosorbent assay (ELISA) method has been used in the detection of viruses (Nam, Jang & Groves, 2007; Leufen *et al.*, 2014). However the adoption of these diagnostic kits has been limited by high initial and maintenance costs and farmers' limitation on technical knowhow. Thus the need for development of low cost, farmer friendly and low maintenance pathogen diagnostic kits using nanotechnology (Artz, Avery, Jones & Killham, 2006; Agasti *et al.*, 2010; Kang *et al.*, 2014; Susanne *et al.*, 2014).

Recently, there has been intensified research on the use of nanocolorimetric probes in detecting water borne pathogens where molecules of biotic and abiotic origin bind selectively to the analyte with concomitant change in color (Bargossi, Fiorini, Montalti, Prodi & Zaccheroni., 2000). Although the technology of nanocolorimetric detection is still not fully developed, it is becoming popular due to its simplicity, rapidity and sensitivity (Chi *et al.*, 2010). Colorimetric nanoparticles become effective when supported by polymers preferably the nanofibres which offer a large surface area that allow exposure to analytes, resulting in increased sensitivity. Various polymeric materials have been used, for instance, cellulose and other polysaccharides (Melinka, 2014). However, nylon nanofibres are superior due to their useful properties such as high strength, surface energy, surface reactivity, thermal and electrical conductivity (Yang, He, Xu & Yu, 2009). Nanomaterials exhibit unique mechanical, optical, magnetic and electronic properties as a result of their nanoscale dimensions (Chi *et al.*, 2010).

## 5.2 Materials and Methods

### 5.2.1 Experimental Site and Design

The experiments were carried out in Jomo Kenyatta University of Agriculture and Technology at the departments of Horticulture and Chemistry. The experiments were laid on a completely randomized design and replicated three times. The tests were done under sterile conditions in growth chambers and/or lamina flow.

### 5.2.2 Preparation of Green Ferrous Oxide Nanoparticles (FeONPs)

#### Method I

Iron oxide nanoparticles were synthesized using tea extracts. The extracts were prepared by bringing to boil 60.0 g of green tea-POF grade (KTDA-Kangaita Tea Factory Ltd, Kenya) in 1 L of distilled water. The extract was left to cool for 1.0 hr then vacuum-filtered. Separately, a solution of 0.10 M iron chloride ( $\text{FeCl}_2$ ) (Sigma Aldrich UK) was prepared by adding 19.9 g of solid  $\text{FeCl}_2 \cdot 4\text{H}_2\text{O}$  in 1.0 L of distilled water. The green tea extract was carefully added to the  $\text{FeCl}_2$  (aq) contained in a conical flask and agitated for 5 min using rotary shaker after which 1.0 M sodium hydroxide (Sigma Aldrich UK) solution ( $\text{NaOH}$  (aq)) was used to adjust the pH to 6.0. The mixture was then agitated for another 6 hr with formation of FeONPs being marked by appearance of an intense black precipitate. The mixture was centrifuged at 3500 rpm for 10 min, the supernatant was discarded and the residue rinsed with ethanol (70%) before being dried on a hot plate at 80 °C for 24 hr in a fume hood (Shahwan *et al.*, 2011).

#### Method II

For comparative purposes, FeONPs chemical synthesis method by Yuvakkumar, Elango, Rajendran and Kannan (2011) was used.

### **5.2.2.1 Quantitation and Characterization of Ferrous Oxide Nanoparticles (FeONPs)**

Iron oxide nanoparticles obtained by the two methods were quantified using Atomic Absorption Spectrophotometer (AAS, SHIMADZU) and characterized using Manniflex II Desktop X-ray powder diffractometer (XRD, Rigaku) machine with a radiation of wavelength  $1.5418\text{\AA}$  at scan range of  $1\text{--}120^\circ$  at a scanning rate of  $1^\circ/\text{min}$  with a step size of  $0.04^\circ$  (Glavec., Klabunde., Sorensen., Hadjipanayis, 1995). Estimation of crystallite sizes of the FeONPs was done using the Scherrer equation;

$D = \frac{K\lambda}{\beta \cos\theta}$ . Where, D is the crystallite size,  $\lambda$  is wavelength of X-ray,  $\beta$  is full width and half maxima value and  $\theta$  is Bragg's angle (Cullity & Stock (2001)).

Elemental analysis of the nanocomposites was done using the X-ray fluorescence (XRF) technique (Blank & Eksperiandova, 1997).

### **5.2.3 Synthesis of Ferrous Oxide Chitosan Immobilized Silica Nanocomposite (FeOCISNC)**

Chitosan immobilized silica was synthesized following the sol-gel centrifugation method. The green synthesized iron oxide nanoparticles were added to the CISNC gel in a rotary shaker until colour changed to grey. The mixture was stirred for 1 hr to form a homogenous mixture (Shrifian-Esfahni, Salehi, Nasr-Esfahni & Ekramian, 2015).

### **5.2.4 Synthesis of Nylon-FeOCISNC (Nanoprobe)**

Electrospun nylon fibres (200 nm) (Rhodes University, South Africa) were placed in a beaker containing the ferrous oxide CISNC gel for 4, 8, 12, 24, 48 hr to allow adsorption of the gel on the nylon nanofibres. The nylon nanofibres adsorbed with FeOCISNC were

then dried on petridishes in a sterilized lamina flow at 25 °C for 24 hr before storage in a refrigerator at 10 °C (Mafuma, 2013).

### **5.2.5 Characterization of Nylon-FeOCISNC (Nanoprobe) Using XRD**

The synthesized nylon ferrous oxide CISNC were characterized using X-ray diffraction machine with a radiation of wavelength  $1.5418\text{\AA}$  at scan range of 1- 120° at a scanning rate of 1°/ min with a step size of 0.04°. The obtained diffractograms confirmed formation of the nanocomposite (Jolanta *et al.*, 2010).

### **5.2.6 Isolation and Identification of *R. solanacearum* and *F. oxysporum***

Diseased hybrid tomato plant material was obtained from a greenhouse in Thika, Kiambu County in an area heavily infected by the disease (KHDP, 2007). The plants were thoroughly washed to remove dirt and dipped in 1% chlorox for sterilization. The lower stem was cut into small pieces of 5 cm each then cut longitudinally and placed in a 1 ltr beaker containing distilled water to allow flow of bacterial exudates. The obtained bacteria were cultured in a sterilized growth chamber for 48 hr at 32 °C on 20 ml nutrient-TZC agar contained in a petridish. *F. oxysporum* pathogen was also isolated from an infested greenhouse soil and cultured on PDA agar at 25 °C for 96 hr (Denny & Hayward, 2001). The colonies were observed using a hand lens and light microscope (French, Gutarra, Aley & Elphinstone, 1995).

### **5.2.7 Colorimetric Tests of the Nanoprobe in *R. solanacearum* Suspension**

*R. solanacearum* culture was standardized to 3.000 O.D and a stock suspension of  $10^{12}$  fungal spores of *F. oxysporum* were prepared and placed in 50ml beakers. Nylon ferrous oxide CISNC probes were placed in the suspensions for 5, 30 and 60 min, then placed on a petridish. Control involved placing the nanoprobe in distilled water, while

another test involved placing the probe in a *F. oxysporum* suspension. The tests were carried out under sterile conditions in a lamina flow.

### **5.2.8 Elemental analysis of the Nanocomposites using the X-Ray Fluorescence (XRF) Technique**

Energy dispersive x-ray fluorescence spectrometer (EDXRF) unit, JSX-3202-M was used for elemental analysis of the nanocomposites products using the x-ray fluorescence (XRF) technique. The sample analysis involved mixing the sample in a mixer to make it homogeneous then placing the sample in the sample holder (Blank & Eksperiandova, 1997; Cullity & Stock, 2001).

### **5.2.9 Validation of the Colorimetric Nanoprobe using PCR and Conventional Techniques**

To obtain DNA from the isolated and morphologically identified microbes, the cells were cultured on TZC nutrient agar and potato dextrose (PDA) for *R. solanacearum* and *F. oxysporum* respectively. The cultured inocula were added to distilled water to form suspensions. The suspensions were standardized to an optical density (O.D) of 3.000 observed at 600 nm on Uv-vis. DNA was extracted following the CTAB extraction method and then stored at -20°C (Kumlachew, 2014). The polymerase chain reaction (PCR) was carried out using touchdown procedure. The primers were a 20 mer forward primer –GAA CGC CAA CGG TGC GAA CT-, and reverse –GGC GGC CTT CAG GGA GGT C- and Forward primer (5'- ATGGGTAAGGAAGGACAAGAC-3') and the reverse primer (5'-GGAGAGTACCAGTGCATCATGTT-3') for virulent *R. solanacearum* and *F. oxysporum* strains respectively. The samples were cooled at 4 °C and subjected to electrophoresis on a 1.5% agarose gel in 1X TAE buffer (40 mM Tris acetate and 1.0 mM EDTA), photographs of the images were taken under ultra-violet

(UV) light. The obtained ladders were interpreted using base pair amplicons for pathogen detection (Chilvers, 2012).

### 5.2.10 Data Analysis

The data of iron oxide yield and adsorption of *R. solanacearum* pathogen on the nanoprobe were subjected to analysis of variance (ANOVA) and means compared by Fischer's Least Significant Difference ( $LSD_{0.05}$ ). The X-ray diffractograms were interpreted as depicted by the peaks. Linear fits were also drawn to show the trends for adsorption of FeOCISNC on the nylon nanofibres and yield of iron oxide at different conditions (Jolanta *et al.*, 2010; Yuvakkumar, Elango, Rajendran & Kannan, 2011).

## 5.3 Results

### 5.3.1 Green Synthesis of Iron Oxide Nanoparticles (FeONPs)

The reaction of green tea extract and hydrated iron chloride resulted in formation of iron oxide. Results of obtained are corroborated by linear fit in Figure 5.1 and the variation in mean yield per treatment depicted in Table 5.1.

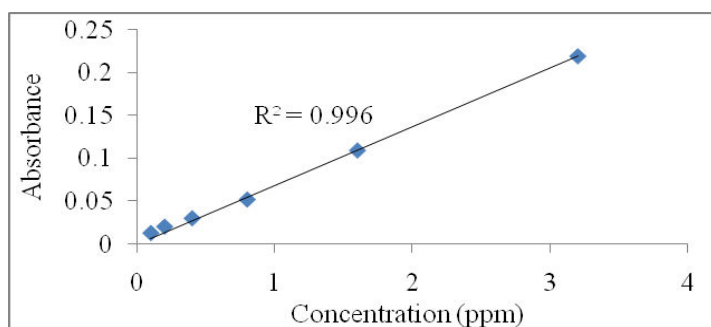


**Figure 5.1: Linear Fit of Absorbance of Oxide Iron Nanoparticles versus Concentration**

The linear fit showed a strong correlation between absorbance resulting from yield of iron oxide nanoparticles (FeONPs) and concentration of reagents. Absorbance was also affected by the pH since sodium hydroxide was added to raise the pH in order to achieve higher iron oxide yield.

**Table 5.1: Yield (ppm) of FeONPs from Iron Chloride and Green Tea Extracts (Te)**

Treatments			FeONPs Yield (ppm)
Conc. of FeCl <sub>2(aq)</sub> (M)	Ratio (TE:FeCl <sub>2(aq)</sub> )	pH	
0.5	2:3	3	124.5 a
1.0	2:3	3	140.5 b
2.0	2:3	3	142.1 b
0.5	3:2	3	122.3 a
1.0	3:2	3	131.7 a
2.0	3:2	3	138.2 b
0.5	2:3	6	136.7 b
1.0	2:3	6	154.8 c
2.0	2:3	6	160.3 c
0.5	3:2	6	126.7 a
1.0	3:2	6	146.1 b
2.0	3:2	6	152.9 c
0.5	2:3	8	123.1 a
1.0	2:3	8	132.6 b
2.0	2:3	8	144.9 b
0.5	3:2	8	116.1 a
1.0	3:2	8	122.8 a
2.0	3:2	8	131.9 b

The ratios (v/v) represent iron oxide to green tea extract (TE); Means followed by the same letter are not significantly different at  $P \leq 0.05$ . Protected

### 5.3.2 Characterization of Nylon-ferrous Oxide Chitosan Immobilized Silica Nanoprobe (nylon-FeOCISNC) using Uv-vis and XRD

Development of nylon-ferrous oxide CISNC was confirmed by change in optical density (Uv-vis) of the FeOCISNC gel after nylon nanofibres were placed in the composite gel as indicated in Figure 5.2. The diffractograms of the nylon-ferrous oxide CISNC were also used to indicate formation of the nanopathogen probe due to change in the diffractograms of the original materials as shown in Figures 5.3 and 5.4. The same was observation was made when the composites were observed under a compound microscope indicated in Plate 5.1.

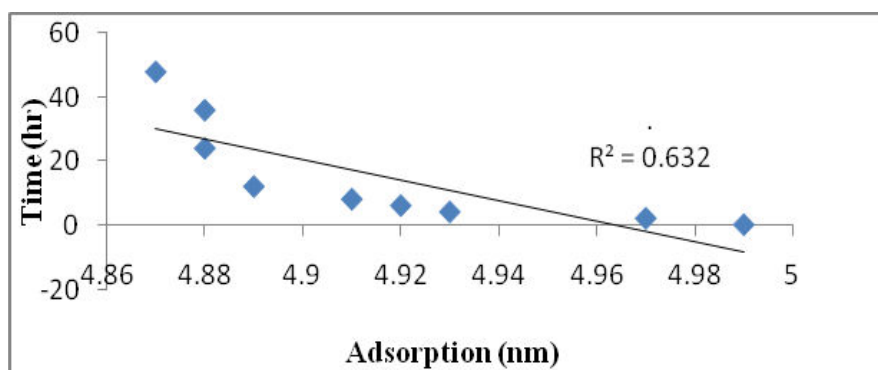


**Figure 5.2: Change in optical density of Ferrous Oxide Chitosan Immobilized Silica Nanocomposite (FeOCISNC) due to Adsorption by Nylon Nanofibres**

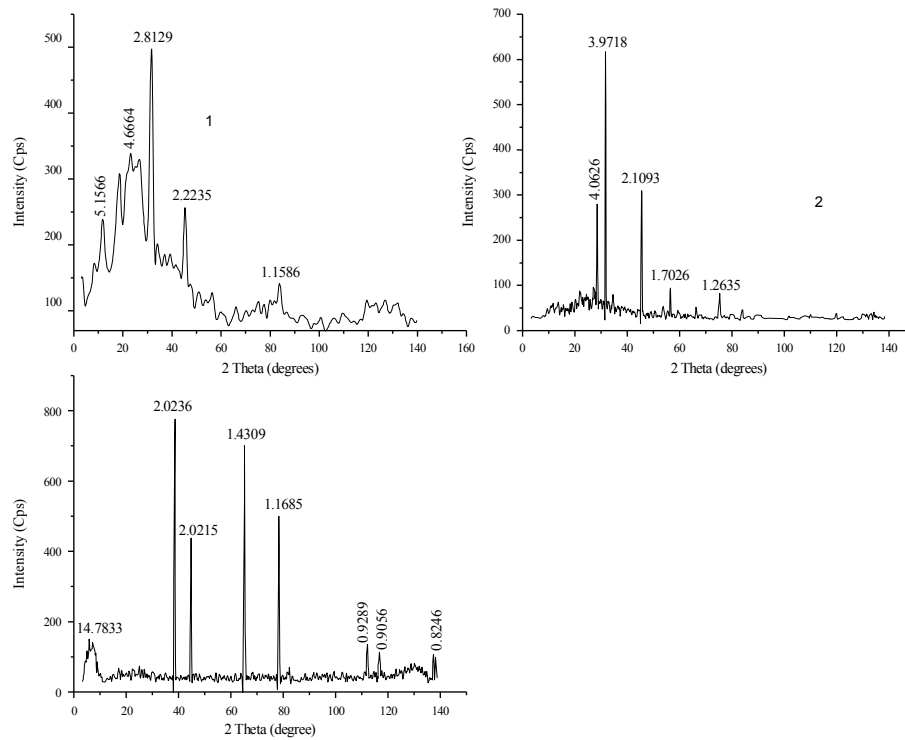


**Figure 5.3: X-ray diffractograms for CISNC, FeONPs and FeOCISNC**

Key: 1- Chitosan immobilized silica nanocomposite (CISNC), 2- Ferrous oxide nanoparticles (FeONPs) and 3- Ferrous oxide CISNC.

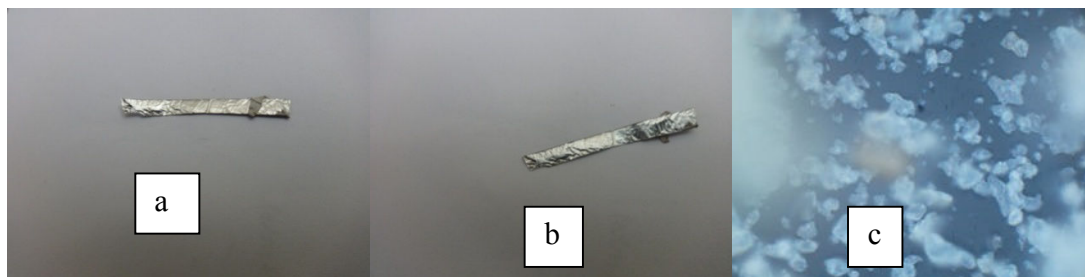


**Plate 5.1: Compound Microscope Images for Nylon Nanofibres, Nylon-Ferrous Oxide CISNC and FeOCISNC**

a- Nylon nanofibers, b- Nylon nanofibers adsorbed with FeOCISNC and c- FeOCISNC

### 5.3.3 Characterization of Nanocomposites using x-ray Florescence (XRF)

Analysis of the individual compounds and nanocomposites indicated notable change in the constituent elements. The ratios of C, H, N and S changed clearly in the process of forming a complex composite (Table 5.2).

**Table 5.2: Elemental Analysis of the Nanoprobe**

Substance	%			
	C	H	N	S
Chitin	42.35	6.627	5.8	0.153
Chitosan	34.07	6.49	4.29	0
CISNC	23.64	5.405	4.87	3.4
FeOCISNC	23.52	4.792	4.14	1.852
Nylon nanofibres	12.22	1.179	2.24	0.269
NyFeOCISNC	29.75	6.712	6.76	1.796
NyFeOCISNC-R. solanacearum	45.31	8.404	7.41	2.536

### 5.3.4 Colorimetric Tests of Nylon-ferrous Chitosan Immobilized Silica Nanoprobe

There was significant ( $P \leq 0.05$ ) reduction in the optical density of *R. solanacearum* when the nanoprobe was placed in the suspension as shown in Table 5.3. Nylon-ferrous oxide chitosan immobilized silica nanocomposite had the least O.D after adsorption of *R. solanacearum*, an indication that formation of nanocomposite increased adsorption of the pathogen significantly ( $P \leq 0.05$ ). Adsorption of the pathogen was also indicated by colorimetric visible change in the nanoprobe (Plate 5.2). In addition, the same findings were corroborated using X-ray diffractograms shown (Figure 5.4). There was no significant ( $P \leq 0.05$ ) difference in concentration of *F. oxysporum* after 8 hr of placing the nanoprobe in the suspension of *F. oxysporum* and also there was no notable colour change.

**Table 5.3: Change in Concentrations of Residual *R. Solanacearum* and *F. oxysporum* Suspensions after Adsorption on the Nanoprobe**

Treatment	Change in concentration
CISNC- <i>R. solanacearum</i>	0.065 a
Nylon nanofibers- <i>R. solanacearum</i>	0.069 a
Iron oxide nanoparticles- <i>R. solanacearum</i>	0.285 b
Nylon ferrous oxide nanoparticles- <i>R. solanacearum</i> (6 hr)	0.307 c
Nylon ferrous oxide nanoparticles- <i>R. solanacearum</i> (8 hr)	0.453 de
Nylon ferrous oxide nanoparticles- <i>R. solanacearum</i> (48 hr)	0542 e
Nylon ferrous oxide nanoparticles- <i>F. oxysporum</i> (6 hr)	$10^2$ a
Nylon ferrous oxide nanoparticles- <i>F. oxysporum</i> (8 hr)	$10^4$ b
Nylon ferrous oxide nanoparticles- <i>F. oxysporum</i> (48 hr)	$10^4$ b

Means followed by the same letter along a column are not significantly different. LSD<sub>0.05</sub> Protected

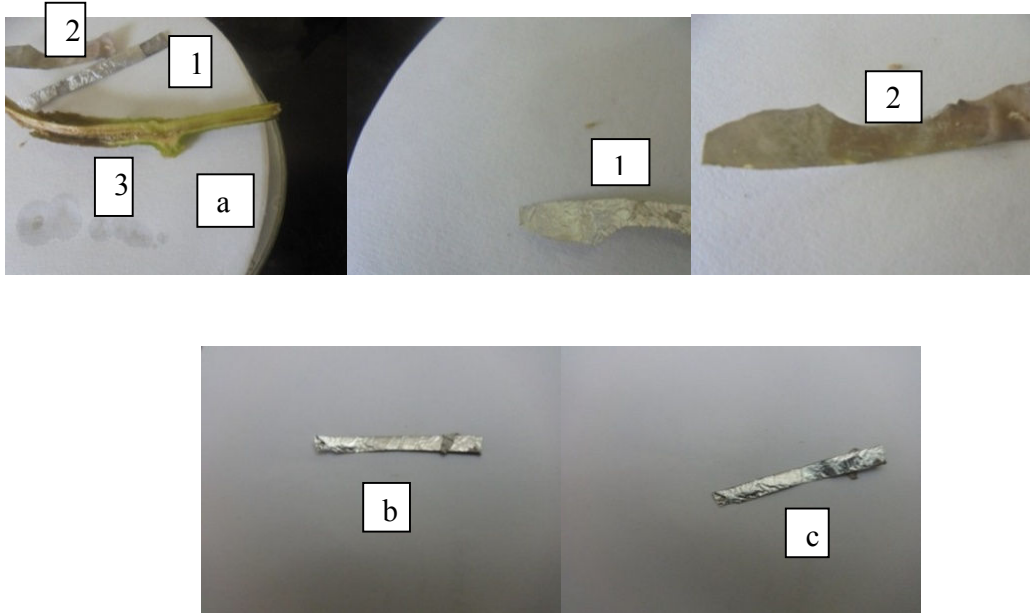


**Plate 5.2: Images of Nylon-Ferrous Oxide Chitosan Immobilized Silica Nanocomposite Colorimetric Probe**

1 and 2 represents nylon-ferrous oxide chitosan immobilized silica nanocomposites (grey) and nylon-ferrous oxide chitosan immobilized silica nanocomposite treated with *R. solanacearum* (brown) respectively and 3 tomato stem infected with the *R. solanacearum*, b - Nylon ferrous chitosan immobilized silica nanocomposite adsorbed with *F. oxysporum*, c - Nylon ferrous chitosan immobilized silica nanocomposite immersed in distilled water.

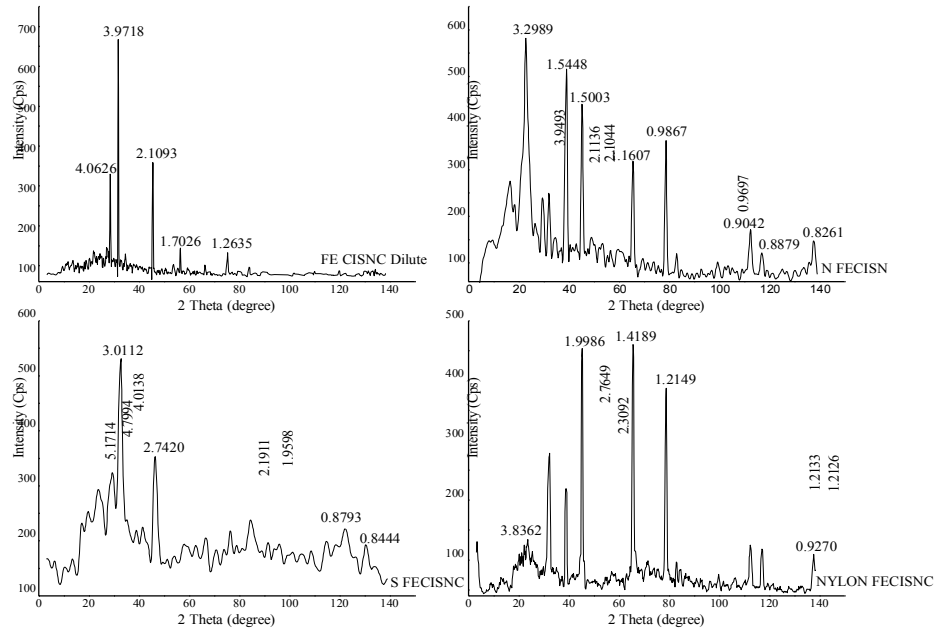


**Figure 5.4: X-ray Diffractograms for i-Nylon nanofibre ii-CISNC and iii-Nylon-ferrous oxide CISNC**

**Table 5.4: Crystallite Sizes of Synthesized Nanocomposites**

Substance	FWHM	$\lambda$ (nm)	$2\theta$ (deg)	Crystallite size (nm)
CISNC	0.31	1.5418	45.47	4.80
FeONPs	0.35	1.5418	46.26	4.30
Nylon nanofibres	0.13	1.5418	45.34	11.57
FeOCISNC	0.33	1.5418	65.58	5.00
Nylon-feOCISNC	0.33	1.5418	137.49	11.60
Nylon-feOCISNC- <i>R. solanacearum</i>	0.26	1.5418	137.56	11.75

Key: Iron oxide nanoparticles (FeONPs), Ferrous oxide chitosan immobilized silica nanocomposite (FeOCISNC), nylon nanofibres, nylon-ferrous oxide chitosan immobilized silica nanocomposite (nylon-FeOCISNC) and nylon-ferrous oxide chitosan immobilized silica nanocomposite adsorbed with *R. solanacearum* (nylon-FeOCISNC-*R.s*).

### 5.3.5 Validation of the Colorimetric Nanoprobe using PCR and Conventional Techniques

The isolated *R. solanacearum* and *F. oxysporum* used to test the colorimetric nanoprobe were confirmed using morphological and molecular characterization plate 5.3.

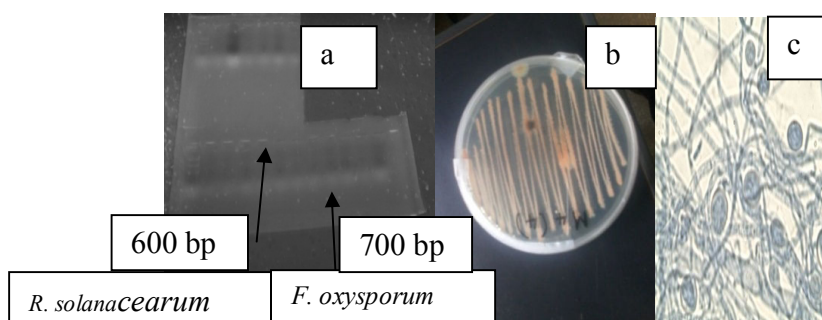


**Plate 5.3:** Gel image of a- *R. solanacearum* and *F. oxysporum* (PCR), b- *R. solanacearum* on TZC agar, c- chlamydospores of *F. oxysporum* (x 400).

## 5.4 Discussion

### 5.4.1 Green Iron Oxide Nanoparticles (FeONPs) Synthesis

The linear fit showed a strong correlation between absorbance resulting from yield of iron oxide nanoparticles (FeONPs) and concentration of reagents. Absorbance was also affected by the pH and sodium hydroxide was added to raise the pH in order to achieve a higher yield of iron oxide (Figure 5.1) and Table 5.1). Optimal yield of iron oxide was attained at a pH of 6 and when the concentration of iron chloride solution was higher than that of green tea extract (v/v) (Gulcin 2006; Ling *et al.*, 2011). The pH of the mixture affects reduction of iron oxide by tea extracts due to concentration of hydrogen ions. Very high hydrogen ions associated with low pH makes the solution unable to gain protons inhibiting the reduction process (Peterson *et al.*, 2005; Nadagouda, Castle, Murdock, Hussain & Varma, 2010). On the other hand, low concentration of hydrogen ions is associated with high pH which enhances gain of protons. This results in the

reduction process and high yield of iron oxide from the iron chloride solution. Additionally, the ratio of iron chloride to green tea extract affected the yield of iron oxide due to the fact that, provided iron chloride is not limiting, then the reduction by the green tea was not inhibited resulting in higher yield of iron oxide (Leung, Yakun, Chen, Zhang, Hang & Chen, 2001).

The ability of tea extracts and hydrated iron chloride to form iron oxide nanoparticles was attributed to the reducing effect of green tea liquor. This is because, tea is rich in polyphenols which are known for their reducing effect (Pereira, Korndorfer, Vidal & Camargo, 2009). Plant phenolic compounds cause redox reactions when mixed with reactive substances due to hydrogen donation, oxygen removal and chelation of metals (Wang & Helliwell, 2001; Prasad *et al.*, 2009). The outcome was in agreement with Carmen, Artacho and Gime'nez (2006); Karori., Wachira, Wanyoko and Ngure (2007), that tea extracts are strong reducing agents and that the reducing effect decrease when tea is oxidized before drying. Therefore, green tea also known as non-oxidized or non-fermented tea possesses good reducing properties. Koech *et al.* (2001); Dutta, Mahapatra and Datta (2011) found out that oxidation of tea is a chemical process, which results in formation of theaflavins and thearubigins a process that is not reversible. This process is environmentally safe, unlike other reducing agents such as sodium borohydride which is carried out in a fume chamber due to the toxic fumes emitted (Yuvakkumar *et al.*, 2011). The compound is also highly corrosive and flammable thereby posing a potential hazard during utilization (Shahwan *et al.*, 2011). Another advantage of using tea extracts in synthesis of the iron nanoparticles is the impartation of steric stabilization resulting in electrostatic repulsion which hinders aggregation of the nanoparticles (Sun, Li & Cao, 2007).

## **5.4.2 Characterization of Nylon-Ferrous Oxide Chitosan Immobilized Silica Nanoprobe (Nylon-Feocisnc) using X-Ray Fluorescence, Uv-Vis Spectrophotometer and X-Ray Powder Diffractometer**

### **5.4.2.1 Characterization of Nanoprobe using X-Ray Fluorescence (XRF)**

Analysis of the composites using the XRF technique was preferred due to rapidity, accuracy, non destructive and limit of detection in the range of few part per million (ppm) of most elements (Al-Eishaikh & Kadachi, 2006; Ida, Segawa, Tohyama & Kawai, 2005). Sample preparation for XRF analysis is also relatively simple and require less time. Change in the elemental composition of C, H, N and S was attributed to complexation and formation of composites (Table 5.2). For instance, deacetylation and functionalization of chitosan reduced the C/N ratio due to loss of acetyl groups (Slabaugh, 2004). Complexation of iron oxide nanoparticles (FeONPs) with chitosan immobilized silica nanocomposite (CISNC) resulted in displacement of some constituent elements in order to accommodate the compound, while reaction of the nylon-ferrous oxide CISNC (nanoprobe) with the *R. solanacearum* bacteria resulted in increased C, H, N and S due to integration of organic material into the nanomatrix. Adsorption of bacteria onto the nanoprobe was due to rupturing of bacterial cells that interacted with the ammonia cations in the CISNC by H-bonding, hence demonstrating relatively higher adsorption. In the process, the bacterial cell that possess very high affinity for iron, complexes with the iron oxide nanoparticles in the nanoprobe. This reaction results in increased C, H, N and S in the composite due to the increased organic matter from the adsorbed bacteria (Lawton, Cornish & MacDonald, 1998).

### **5.4.2.2 Characterization of Nanoprobe using Uv-Vis Spectrophotometer**

Adsorption of iron oxide chitosan immobilized silica nanocomposite (FeOCISNC) gel on nylon nanofibers resulted in reduced gel viscosity (Figure 5.2). This was in

agreement with previous studies by Li, Bellan, Craighead and Frey (2006) where, when nylon nanofibers were placed in a gel containing chitosan, silver and nickel, there was a significant decrease in viscosity of the solution. The decrease in viscosity was attributed to removal of some constituent elements through adsorption of polar particles. Further, nylon nanofibers offer good support due to their large surface area and rigidity making it possible to adsorb the nanocomposites. The nylon nanofibres also offer a large surface area for probing the pathogen suspension increasing sensitivity of the probe in diagnostics (Safavi & Abdollahi, 1999; Wan, Ngah, Ghani & Kamari, 2005; Agasti *et al.*, 2010).

#### **5.4.2.3 Characterization of Nanoprobe using X-Ray Diffractometry**

There was notable change in diffractograms after synthesis of nanocomposites. The crystallite sizes of the composites changed after adsorption. The synthesized iron oxide nanoparticles had only two visible peaks which changed to six prominent peaks when the nylon-ferrous oxide chitosan immobilized silica nanocomposites were formed. The d-spacing (nm), 2-theta ( $\Theta$ ) and full width and half maxima values (FWHM) were changed after adsorption. The major diffraction peak was at 32 (66) and minor peak at 46 (20) conforms to previous studies where iron oxide nanoparticles were synthesized through chemical precipitation method (Figure 5.3). The diffraction peaks are attributed to the spinel structure of iron oxide (Jiang, Yang, Vachet & Xing, 2010). However, chemical modification of iron oxide nanoparticles with chitosan did not affect the crystal structures since the major peaks at  $2\Theta$ , 39 (225), 29 (47), 45 (147), 65 (134) and 78 (144) correspond to 8.3840 Å lattice only, though careful analysis indicated physical modifications attributed to the inclusion of chitosan matrix (Goycoolea, Higuera-Ciapara & Alonso, 2008). Nylon nanofibre had only two prominent peaks while the resulting composites indicated changes in peaks (Figure 5.4). It was noted that formation of nylon-ferrous oxide chitosan immobilized silica nanocomposite resulted in more peaks attributed to the physisorption nature of compounds in the nanocomposite. The nylon

nanofibers spectra showed characteristic peaks at 2-theta 32.64 and 46.26° but were shifted to 29.8, 39.12, 45.32, 65.58, 78.525, 112.21 and 137.49° in nylon-ferrous oxide chitosan immobilized silica nanocomposite suggesting formation of inter and intra-molecular hydrogen bonds in the presence of additional compounds. There was also a significant change in d-spacing of the compounds, the d-spacing increased with adsorption of materials. The iron oxide nanoparticles were also characterized by two prominent peaks at 31.7 and 45.47° attributed to crystallinity of the particles (Table 5.4). Adsorption of *R. solanacearum* also altered crystallinity of the nanoprobe. This resulted in slight peak modifications at 29.8, 39.12, 45.32, 65.58, 78.52, 112.21 and 137.49° to 32.27, 38.98, 45.20, 65.55, 78.63, 112.38 and 137.56° for the nylon-ferrous oxide chitosan immobilized silica nanocomposite and nylon-ferrous oxide chitosan immobilized silica nanocomposite-*R. solanacearum* respectively confirming that complexation may have taken place after adsorption bacterial pathogen by the nanoprobe (Nadagouda *et al.*, 2010).

### **5.4.3 Science of Formation of Nylon Ferrous Oxide Chitosan Immobilized Nanoprobe**

Formation of ferrous oxide chitosan immobilized silica nanopcomposites was vital in ensuring that agglomeration of the synthesized iron oxide nanoparticles does not happen and that the particles aggregate only in the presence of the analyte. Adsorption of iron nanoparticles on chitosan was possible due to the oxidizing effect of chitosan attributed to the amino group charge in chitosan, binding energy of nitrogen, hydrogen and silicate hydroxide (Budnyak, Tetykh & Yanovska, 2013). The binding also known as chelation is based on mineralization of magnetite in chitosan hydrogel (Bargossi *et al.*, 2000; Qian *et al.*, 2002). According to Budnyak *et al.* (2013), chitosan is considered as an effective chelation and aggregating agent that can enhance formation of a complex. Also the hydroxyl (-OH) group of chitosan interact with the iron oxide ions resulting in a stable and well dispersed colloidal suspension. The coulomb repulsion between the iron

nanoparticles played a major role in dispersivity of particles. Silica nanoparticles improved the mechanical properties of the nanoprobe. This property was desirable in the nanoprobe as the strength imbued by silica enhanced ability of the probe to absorb pathogen inoculum until the colour changed. Mesoporous silica nanoparticles used in this study offered a large surface area due to its extensive mesoporosity providing a large surface for harbouring iron oxide and chitosan nanoparticles (Joshi, Biswas, Sarvanan & Mukhopadhyay, 2012). Utilization of silica nanoparticles in enhancing the hydrogel strength had been previously done by Grattner and Teller (1999) resulting in materials with high strength and large adsorbing surfaces. Adsorption of the ferrous oxide chitosan immobilized silica nanocomposite on nylon nanofibers resulted in formation of a solid nanoprobe which is more effective than wet chemisorption mode of pathogen detection. Solid probes are easy and ideal under field conditions. The modification also increased the lifespan of the nanocomposite probe. The complex nanocomposite therefore, has much superior properties compared to conventional one (Chassary, Vincent & Guibal, 2004). Nylon-6 electrospun nanofiber mats resulted in a strong nanoprobe due to reinforcement of the ferrous oxide CISNC gel by materials with high tensile strength and toughness, such as the melamine–formaldehyde (MF) resin derived nylon nanofibres (Wan *et al.*, 2005; Yang *et al.*, 2002; Zhang, Guo & Cui, 2009). The reinforcement altered the morphology and mechanical properties of the composites resulting in better adsorption and wetting characteristics (Butola, Joshi & Kumar, 2010; Bhattacharyya & Joshi, 2010).

#### **5.4.4 Colorimetric Effect of the Nanoprobe**

The colorimetric effect observed during the nanoprobe-pathogen interface was due to reaction of iron oxide contained in the nanoprobe matrix with the pathogen (Safavi & Abdollahi, 1999; Wan, Ngah, Ghani & Kamari, 2005; Agasti *et al.*, 2010). *R. solanacearum* possess a high affinity for iron particularly in instances of interface (Miethke & Marahiel, 2007; Auffan *et al.*, 2008). This is through mechanisms such as;

development of siderophores, complexation and chelation. Siderophores are low molecular weight ferric ion specific chelating agents developed by haemaphitic microbial agents used for availing the mineral to the microbial cell. These structures are related to pathogenic virulence and are hydroxamates or catechols. Complexation or chelation of siderophores with iron oxide results in a colorimetric reaction. This formed the basis for formation of the nanoprobe (Lawton *et al.*, 1998). According to Lifeng, Zirong, Xia, Caihong and Xiangfei, 2004; Hutchison, 2008, the colour change in the nanoprobe can also be caused by reduction of iron oxide nanoparticles and formation of a complex with the bacterial cell. Iron is a nutritionally essential trace element playing a major role in metabolic processes of most micro-organisms with bacterial cells having high absorption effect (Michailides *et al.*, 2005; Amemiya, Arakaki, Staniland, Tanaka & Matsunaga, 2007). Justifying the current study Sun, Lu and Gao (2010), found out that *R. solanacearum* had the highest absorption capacity for iron compared to other microbes such as *B. subtilis*, *S. aureus*, *E. coli* and *F. oxysporum*. This was therefore attributed to the colorimetric change observed when the nanoprobe was placed in a suspension of *F. oxysporum* which did not result in a notable colour change, making the nanoprobe an effective tool for differentiating the two pathogens which are characterized by similar symptoms of wilting in infected plants (Rosi & Mirkin, 2005; Sun *et al.*, 2008; Sun, Liu & Qu, 2009).

#### **5.4.5 Validation of the Colorimetric Nanoprobe using Polymerase Chain Reaction (PCR) and Conventional Techniques**

Micro-organisms have unique and distinct morphological and molecular characteristics. The *R. solanacearum* was characterized morphologically by observing the colour and shape of colonies after culturing in tetrazolium chloride (TZC) media (Plate 5.2). Further, *F. oxysporum* was confirmed by the presence of chlamodospores under a compound microscope. The morphological characterization was ascertained by employing molecular techniques whereby amplification of genomic DNA confirmed the

microbes. Touchdown PCR procedure ensures that primers avoid amplifying nonspecific sequences. The annealing temperature during a polymerase chain reaction determines the specificity of primer annealing. The melting point of the primer sets the upper limit on annealing temperature where very specific base pairing between the primer and the template occurs because at low temperatures primers bind less specifically resulting in nonspecific sequences. Thus at higher annealing temperatures, there is more specificity and obscurity is eliminated resulting in an accurate detection of the DNA of interest (Hecker & Roux, 1996). The DNA of isolated *R. solanacearum* was in the range of 630 bp which is found mainly in the virulent strains (Alka, Abhinav, Chakrabarti, Wamik, Durai & Khurana, 2011; Fujiwara, Kawasaki, Usami, Fujie & Yamada, 2008). The virulent strains of *F. oxysporum* occurs around 700 bp. However, the procedure unlike the colorimetric nanoprobe is time consuming, labourious and requires a high level of precision and expertise which may not be tenable under normal field conditions applicable to an ordinary farmer in sub-Saharan Africa (SSA). The other method of milky exudates is only applicable in heavily infected tomato plants with high bacterial load freely flowing from the cut stem into a beaker containing distilled water (Kim *et al.*, 2003). Further, observation of wilting leaves and plants as done by most farmers may not precisely differentiate between wilting caused by bacteria (*R. solanacearum*) and one caused by fungi (*F. oxysporum*), complicating the disease management (Jahanshir & Dzhililov, 2010).

## CHAPTER SIX

### GENERAL DISCUSSION, CONCLUSIONS AND RECOMMENDATIONS

#### 6.1 General Discussion

Application of biocontrol agents using chitosan-silica nanocomposite carriers enhances their efficacy. The choice of chitosan and silica nanocomposite as a carrier material in this study was due to biocompatibility, ease of functionalization of the substances, non-polluting effects and efficacy in disease control. The high quantity of functional bonds such as amino, hydroxyl and silanol groups played a significant role in choice of the materials. It has been proven that chitosan is an effective bioadsorbent material towards most substances. Use of silica in the hybrid formation, was due to the advanced surface stability in the acidic medium, highly functionalizable surface, good kinetics, thermal stability, resistance to microbial attack and low cost. The formed hybrid nanocomposite material chitosan-silica combined the superior properties of the two substances. In addition, the nanoparticle moieties increased the surface area for adsorption and also resulted in particles that easily penetrated the plant epithelial membranes.

The technology of delivering biocontrol agents by adsorbing them on chitosan silica nanocomposites, though new, holds a great promise in control of the devastating and persistent bacterial wilt disease in tomato. The nanocomposite carriers increased efficacy of the biocontrol agents significantly in terms of increased resistance induction, plant vigour, yield, total organic carbon accumulation, beneficial microbes' root hairs colonization and post harvest shelf life. The bionanocomposite therefore, enhances tomato value chain through high yield, increased plant resistance to bacterial wilt disease and reduced postharvest losses by longer shelf life.

Colorimetric nanoprobe have successfully been used to detect various substances in analytes. These probes are preferred as they do not require specialized skills for use, are

specific and rapid in analysis. Formation of nylon ferrous oxide nanoprobe was due to ionic chelation and electrostatic coulomb interactions. Iron oxide nanoparticles were responsible for the colour change of the nanoprobe a process known as colorimetric. The iron nanoparticles were synthesized using green tea extracts to prevent aggregation of the particles before utilization. The nanoprobe is effective in detection of *R. solanacearum* in a suspension due to the high affinity of the bacteria for iron. The nanoparticles also provided a large surface area for interface increasing effectiveness of the nanoprobe. The developed colorimetric nylon-ferrous oxide chitosan-silica nanoprobe is therefore; user friendly, relatively cheaper and effective in detection of the *R. solanacearum*. Therefore, use of nanocomposites portends a new frontier in disease control where precise pathogen detection will precede control. In this system, there is accurate pathogen detection, precise delivery of control agents and elicitation of disease resistance. This is an effective three pronged approach in plant disease management.

## **6.2 Conclusions**

The presence of functional groups such as hydroxyl, amino and silanol groups in chitosan and silica were attributed to the ease of immobilization of chitosan on mesoporous silica or nanoclay in the formation of chitosan immobilized silica nanocomposite carrier. The two compounds have large surfaces and are easily functionalized in the formation of the nanocomposite. The overall positive charge was attributed to the sorption property of the nanocomposite carrier which made it easier for the polar microbes to be adsorbed on the carrier. The change in sorption properties of the nanocomposite carrier under different pH conditions allowed adsorption and desorption of the biocontrol agents making the chitosan immobilized silica nanocomposite an ideal carrier material.

The attained complex after adsorption of biocontrol agents on the CISNC known as bionanocomposite had superior pathogen inhibitory effect and enhanced tomato wilt

resistance, yield, post harvest shelf life and rhizosphere health of tomato. Due to the numerous materials used in synthesizing the bionanocomposite, it acted both as a pesticide and fertilizer on tomato. The Substitution of mesoporous silica nanoparticles (MSN) in the nanocomposite with nanoclay in the development of the bionanocomposite was desirable in sustainable production of the product.

Finally the synthesized nylon ferrous oxide chitosan immobilized silica nanoprobe employed the colorimetric mechanism in pathogen detection. This was characterized by concomitant and unique colour change from grey to brown.

### **6.3 Recommendations**

1. Chitosan immobilized silica nanocomposites are effective carrier materials for biocontrol agents (BCAs) and enhance their efficacy. The bionanocomposites are good resistance elicitors in tomato plants for the control of bacterial wilt. Application of these bionanocomposites is recommended in enhancing plant resistance.
2. Nylon-ferrous oxide chitosan immobilized silica nanocomposite probe is an effective pathogen diagnostic tool for *R. solanacearum*. The probe is a rapid, simple and accurate pathogen detection tool with detection manifested in form of colour change. The probe is therefore recommended for use to enhance pathogen detection prior to control.
3. Trials for the bionanocomposites as a control for other diseases and plants in the solanaceae family and use of the nanocolorimetric diagnostic probe to test other bacterial diseases in solanaceae family are recommended.
4. There is need for testing effect of bionanocomposites in enhancing post harvest shelf life of other climacteric fruit such as bananas, strawberries and apples.

## REFERENCES

- Agasti, S., Rana, S., & Park, M. (2010). Nanoparticles for detection and diagnosis. *J. Adv Drug Delivery Rev.*, 62, 316–328.
- Agrios, G. (2005). *Plant pathology*. (5<sup>th</sup> ed.), NY: Academic press.
- Algam S., Xie, G., Li, B., Yu, S., Su, T., & Larsen, L. (2010). Effects of paenibacillus strains and chitosan on plant growth promotion and control of *R. solanacearum* wilt in tomato. *J. Plant pathol*, 92(3).
- Al-Eshaikh, M.A., & Kadachi, A. (2006). Toxic heavy metal analysis in residential paint using X-ray fluorescence (XRF) technique. In: Proceedings of the 12th International Conference on Machine Design and Protection, September 5–8, Kusadast, Turkey
- Alka, G., Abhinav, G., Chakrabarti, S., Wamik, A., Durai, S., & Khurana, S. (2011). Identification of *Ralstoniasolanacearum* using conserved genomic regions. *International Journal for Biotechnology and Molecular Biology Research*, 2(1), 23-30.
- Ambrorabe, E., Bonmort, J., Fleurat-Lessard, P., Roblin, G. (2008). Early events induced by chitosan on plant cells. *J. Exp Bot*, 59, 2317-2324.
- Amemiya, Y., Arakaki, A., Staniland, S., Tanaka, T., & Matsunaga, T. (2007). Controlled formation of magnetite crystal by partial oxidation of ferrous hydroxide in the presence of recombinant magnetotactic bacterial protein Mms6. *J. Biomaterials*, 28(35), 5381-5389.

- Artz, R., Avery, L., Jones, D., & Killham, K. (2006). Potential pitfalls in the quantitative molecular detection of *Escherichia coli* 0157:H7 in environmental matrices. *Canadian Journals of Microbiology*, *52*, 482-488.
- Auffan, M., Achouak, W., Rose, J., Roncato, M., Chane'ac, C., Waite, D., ..., Bottero, J. (2008). Relation between the redox state of iron-based nanoparticles and their cytotoxicity toward *Escherichia coli*. *J. Environ. Sci. Technol*, *42*, 6730–6735.
- Balakhina, T., & Borkowska, A. (2013). Effects of silica on plant resistance to environmental stresses. *J. International Agrophysics*, *27*, 225-232.
- Balogh, B., Jones, J. B., Iriarte, F. B., & Momol, M. T. (2010). Phage therapy for plant disease control. *J. Curr. Pharm. Biotechnol*, *11*, 48–57.
- Barea, J., Azcon, R., & Azcon-Anguilar, C. (2002). Mycorrhizosphere interactions to improve plant fitness and soil quality. *Antonie Van Leeuwenhoek* *81*, 343-351.
- Bargossi, C., Fiorini, M., Montalti, M., Prodi, L., & Zaccheroni, N. (2000). *Coord. Chem. Rev.*, *208*, 17-32.
- Bhattacharyya, P., & Joshi, M. (2012). Functional Properties of Microwave Absorbent Nanocomposite Coatings based on Thermoplastic Polyurethane-based and Hybrid Carbon-based Nanofillers. *Polymers for Advanced Technologies*, *23*(6), 975-983.
- Blank, A.B., & Eksperiandova L.P. (1997). Specimen Preparation in X-ray Fluorescence Analysis of Materials and Natural Objects. *Wiley-Interscience* (Abstract).

- Boer, W., Folman L., Summerbell, R., & Boddy, L. (2005). Living in a fungal world: impact of fungi on soil bacterial niche development. *FEMS Microbiology Review*, 29, 795-811.
- Butola, B., Joshi, M., & Kumar, S. (2010). Hybrid OrganicInorganic POSS (Polyhedral Oligomeric silsesquioxane)/Polypropylene Nanocomposite Filaments, *Fibers and Polymers*, 11(3), 1137-1145.
- Budnyak, M., Tetykh A., & Yanovska, S. (2013). Chitosan and its derivatives as sorbents for effective removal of metal ions. *Surface*, 5(20), 118-34.
- Cao, W.L., Jing, D.H., Li, J.M., Gong, Y.D., Zhao, N.M., & Zhang, X.F. (2005). Effects of the degree of deacetylation on the physicochemical properties and Schwann cell affinity of chitosan films. *J. Biomater. Appl.*, 20, 157-177.
- Cao, B., Xu, & Shi, J. (2013). Effects of silica on growth, photosynthesis and transpiration of tomato, *Plant Nutrition and Fertilizer Science*, 19(2), 354–360.
- Carmen, C., Artacho, R., & Giménez, R. (2006). Beneficial Effects of Green Tea-a Review, *Journal of the American College of Nutrition*, 25, 79-99.
- Champoiseau, P., Allen, J., & Momol, T. (2009). Description and strategies for best management of *Ralstonia solanacearum* Race 3 biovar 2 as a casuse of bacterial wilt of tomato. Proceedings of the 24<sup>th</sup> Annual Tomato Disease Workshop held on November. 3-5, State College, Pennsylvania, 1-35.
- Chassary, P., Vincent, T., & Guibal, E. (2004). Metal anion sorption on chitosan and derivative materials: a strategy for polymer modification and optimum use. *React Funct Polym.*, 60, 137-49.

- Chatelet, C., Damour, O., & Domard, A. (2001). Influence of the degree of acetylation on some biological properties of chitosan films. *Biomaterials*, *22*, 261-268.
- Chaumpluk, P., Chaiprasart, P., & Vilaivan, T. (2012). Postharvest Non-destructive Determination of Fruits: A Model on Fruit Maturity Assay via Biosensor Based on Colorimetric Change of Gold Nanoparticles. *Acta Hortic.*, *945*, 205–211.
- Cheng, G., Yang, E., Lu, W., Jia, Y., & Duan, X. (2009). Effect of nitric oxide on ethylene synthesis and softening of banana fruit slice during ripening. *J. Agric. Food Chem.*, *57*, 5799-5804.
- Chi, H., Liu, B H., & Guan, G (2010). A simple, reliable and sensitive colorimetric visualization of melamine in milk by unmodified gold nanoparticles. *Analyst.*, *135*, 1070–1075.
- Chilvers, M. (2012). Molecular Diagnostics in Plant Disease Diagnostic Clinics. What's the Status? Fungal Genome. *Biol.*, *102*, 10.4172/2165-8056.
- Choi, S. (1990). Interval estimation of the LD50 based on an up-and-down experiment. *Biometrics*, *46*, 485 -492.
- Choong, J., & Wolfgang, H. (2003) "Chemical modification of chitosan and equilibrium study for mercury ion removal" *Water Research*, *37*(19), 4770–4780.
- Christian, P., Kammer, F., & Baalousha (2008). Nanoparticles: structure, properties, preparation and behavior in environmental media. *Ecotoxicology*, *17*(5), 326-343.

- Christos, A., Damalas, I., & Eleftherohorinos, I. (2011). "Pesticide Exposure, Safety Issues and Risk Assessment Indicators". *International Journal of Environmental Research and Public Health*, 8(5), 1402–19.
- Costa, M., Silva, S., Tavarina, K., & Pintado, M. (2013). Study of the effects of chitosan upon streptococcus mutans adherence and biofilm formation. *Anaerobe*, 20, 27-31.
- Cullity, B., & Stock, S. (2001). Elements of X-Ray Diffraction, 3rd ed., *Prentice-Hall Inc.*, 167-171
- Currie, A., & Perry, C. (2007). Silica in plants: biological, biochemical and chemical studies. *Ann. Bot.*, 100, 1383–1389.
- Datnoff, E., Deren, W., & Snyder, H. (1997). Silica fertilization for disease management of rice in Florida. *Crop Protection*, Oxford 16(6), 525-531.
- Dennis, G., Harrison, W., Agnes, K., & Erastus, G. (2016). Effect of Biological Control Antagonists Adsorbed on Chitosan Immobilized Silica Nanocomposite on *Ralstonia solanacearum* and Growth of Tomato Seedlings. *J. Advances in Research*, 6(3), 1-23.
- Denny, T.P., & Hayward, A. C. (2001). Gram-negative bacteria: *Ralstonia*. Pages 151-174 in: *Laboratory guide for identification of plant pathogenic bacteria*, 3<sup>rd</sup> ed. Schaad, NW; Jones, JB; Chun, W, eds. APS Press, St. Paul, M. N. CABI/EPPO. 1999.
- De Pascale, S., Maggio, A., Foglianov, V., Ambrosino, P., & Ritieni, A. (2001). Irrigation with saline waer improves carotenoids content and antioxidant activity of tomato. *J. Hort. Sci. Biochem.*, 76, 447-453.

- Domszy, J., & Roberts, G. (1985). Evaluation of infrared spectroscopic techniques for analyzing chitosan. *Makromol. Chem.*, 186, 1671-1677.
- Dutta, P., Rayikumar, M., & Dutta, J. (2002). Chitin and chitosan for versatile applications. *J. Macromolecular sc.*, 42(3), 307-354.
- Dutta, A., Mahapatra, S., & Datta, J. (2011). *Int. J. Hydrogen Energy*, 36, 14898-14906.
- Dzung, N., Minh, H., & Van Nguyen, S. (2013). Study on chitosan nanoparticles on biophysical characteristics and growth of Robusta coffee in green house. *Biocatalysis and Agricultural Biotechnology*, 2(4), 289–294.
- El-Hadrami, A., Adam, L., El-Hadrami, I., & Daayf, F. (2010). Chitosan in plant protection. *Mar drugs*, 8(4), 968-987.
- Elphinstone, J., Stanford, H., & Stead, D. (1998). Detection of *Ralstonia solanacearum* in potato tubers, *Solanum dulcamara* and associated irrigation water. In. Bacterial Wilt Disease: Molecular and Ecological. Aspects (Ed. Prior P, Allen C and Elphinstone J), *Springer Verlag*, Berlin German 133-139.
- Food and Agricultural Organization (FAO). (2012). Statistical Database. Retrieved from <http://www.faostat.fao.org>
- Food and Agricultural Organisation of the United Nations Statistics (FAO) 2013. Retrieved from: <http://faostat.fao.org/site/291/default.aspx>.
- Fintrac Inc., USAID-KHDP (2009). Kenya Horticultural Development Program October 2003-March 2009 Final Report.
- Fleming, C., & Wingender, J (2010). The biofilm matrix nature. *Rev. Microbiol.*, 8, 623-633.

- Freier, T., Koh, H., Kazazian, K., & Shoichet, M. (2005). Controlling cell adhesion and degradation of chitosan films by N-acetylation. *Biomaterials*, *26*, 5872-5872.
- French, E., Gutarra, I., Aley, P., & Elphinstone, J. (1995). Culture media for *Ralstonia solanacearum* isolation, identification and maintenance. *Fitopatologia*, *30*(3), 26-130.
- Fujiwara, A., Kawasaki, T., Usami, S., Fujie, M., & Yamada, T. (2008). Genomic characterization of *R. solanacearum* phage and its related pro-phage. *J. Bacteriol.*, *190*, 143-156.
- Fujiwara, A., Fujisawa, M., Hamasaki, R., Kawasaki, T., Fujie, M., & Yamada, T. (2011). Biocontrol of *R. solanacearum* by treatment with lytic bacteriophages. *Appl. Environ Microbiol.*, *77*, 4155-62.
- Garcio-Garrido, J., & Ocampo, J. (2002). Regulation of the plant defense response in arbuscular mycorrhizal symbiosis. *Journal of Experimental Botany*, *53*, 1377-1386.
- Gaur, A., Gaur, A., & Adholeya, A. (2000). Growth and flowering in *Petunia* hybrid, *Callistephus chinensis* and *Impatiens basamina* inoculated with mixed AM inocula or chemical fertilizers in a soil of low P fertility. *Scientia Hort.*, *84*, 151-162.
- Gholami, A., Shahsavani, S., & Nezarat, S. (2009). The effect of plant growth promoting rhizobacteria (PGPR) on germination, seedling growth and yield of maize. *Int. J. Biol. Life Sci.*, *1*, 35-40.
- Glick, B. (2012). Plant growth promoting bacteria: mechanisms and applications. *Scientifica*, *10*, 60-64.

- Goycoolea, F, Higuera-Ciapara, I., & Alonso, M. (2008). Chitosan-polysaccharide blended nanoparticles for controlled drug delivery, in *Handbook of Natural-based Polymers for Biomedical Applications*, Reis R. L., Neves N.M., Mano J. F., Gomes M. E., Marques A. P., and Azevedo H. S., Eds., 644–679.
- Grattner, C., & Teller, J. (1999). New types of silica-fortified magnetic nanoparticles as tools for molecular biology applications. *Journal of Magnetism and Magnetic Materials*, 8(15), 194.
- Government of Kenya. (2012). *National Horticulture Policy*. Ministry of Agriculture, Kilimo House, Nairobi: Government Printer.
- Gray, E., & Smith, D. (2005). Intracellular and Extracellular PGPR. Commonalities and distinctions in the plant-bacterium signaling processes. *Soil Biol. Biochem.*, 37, 395-412.
- Guan, J, Wang, J., & Shao, X. (2009). Seed priming with chitosan improves maize germination and seedling growth in relation to physiological changes under low temperature stress. *J. Zhejiang Univasce B.*, 10, 427-433.
- Gulcin, I. (2006). Antioxidant activity of caffeic acid (3, 4-dihydroxycinnamic acid). *Toxicology J.*, 217, 213-220.
- Guo, J., Tang S., Ju X., Ding Y., Liao S., & Song N. (2011). Effects of inoculation of a plant growth promoting rhizobacterium *Burkholderia* sp. D54 on plant growth and metal uptake by a hyperaccumulator *Sedum alfredii* Hance grown on multiple metal contaminated soil. *World Journal of Microbiology and Biotechnology*, 27, 2835–2844.

- Gupta, J. (2011). Protein S-nitrosylation in plants: photorespiratory metabolism and NO signaling. *Sci Signal*, *10*, 1126.
- Gupta, R. (2011). Origin of diderm (gram negative) bacteria: antibiotic selection pressure rather than endosymbiosis likely led to the evolution of bacterial cells with two membranes. *Antonie Van Leeuwenhoek* *100*(2), 171-82.
- Harish, P., Kittur, F., & Tharanathan, R. (2002). Solid state structure of chitosan prepared under different N-deacetylating conditions. *Carbohydr. Polym.*, *50*, 27-33.
- Hecker, K., & Roux, K. (1996). "High and low annealing temperatures increase both specificity and yield in touchdown and stepdownPCR". *Biotechniques*, *20*(3), 478–85.
- Helander, I., Nurmiaho-Lassila, E., Ahvenainen, R., Rhoades, J., & Roller S. (2001). Chitosan disrupts the barrier properties of the outer membrane of gram-negative bacteria. *International Journal of Food Microbiology*, *71*, 235-244.
- Hinkelmann, K., & Kempthorne, O. (2008). Design and Analysis of Experiments. I and II (2<sup>nd</sup> ed.). *Wiley*, 470, 38551-7.
- Hoag, G., Collins, J., Holcomb, J., Hoag, M., Nadagouda & Varma, R. (2009). Degradation of bromothymol blue by 'greener' nano-scale zero-valent iron synthesized using tea polyphenols, *J. Mater. Chem.*, *19*, 8671–8677.
- Hodge, A. (2000). Microbial Ecology of Arbuscular Mycorrhiza. *FEMS Microbiology Ecology*, *32*, 91-96.
- Hutchison, J. (2008). Greener Nanoscience: A Proactive approach to Advancing

- Applications and reducing implications of Nanotechnology. *ACS Nano.*, 2(3), 395-402.
- Ida, H., Segawa, T., Tohyama, S., & Kawai, J. (2005). Analysis of Painted Steel by Hand-held X-ray Fluorescence Spectrometer. Kyoto University, Skyo-Ku, Japan 606-8501.
- Iriarte, F., Obradovic, A., Wernsing, M., Jackson, L., Balogh, B., Hong, J. ...., Vallad, G. (2012). Soil-based systemic delivery and phyllosphere *in vivo* propagation of bacteriophages. *Bacteriophage*, 2(4), 215 - 224.
- Iriti, M., Pichi, V., Maffi, D., & Faoro, F. (2009). Chitosan in induced resistance: more chances than limits and vice versa? Proceedings of the 5<sup>th</sup> meeting of the IOBC working group induced resistance in plants against insects and diseases. 20-25.
- Jaber, Y., Mehanna, N., & Sultan, S. (2009). Determination of ammonium and organic bound nitrogen by inductively coupled plasma emission spectroscopy. *Talanta*, 78(4), 1298-1302.
- Jach, G., Gornhardt, B., Mundy, J., Logemann, J., Pinsdorf, E., Leah, R., Schell, J., & Maas, C. (1995). Enhanced quantitative resistance against fungal disease by combinatorial expression of different barley antifungal proteins in transgenic tobacco.
- Jacobsen, E., Daniel, M., Bergervoet-van, D., Huigen, D., & Ramanna, M. (1994). The first and second backcross progeny of the intergeneric fusion hybrids of potato and tomato after crossing with potato. *TAG Theoretical and Applied Genetics*, 88(2), 181-186.

- Jahanshir, A., & Dzhililov, S. (2010). The Effects of Fungicides on *Fusarium oxysporum* F. Sp. *Lycopersici* associated with fusarium wilt of tomato. *Journal of Plant Protection Res.*, 50(2).
- Jaworska, M., Sakurai, K., Gaudon, P., & Guibal, E. (2003). Influence of chitosan characteristics on polymer properties: I: Crystallographic properties. *Polym. Int.*, 52, 198-205.
- Jeon, J., Lee, S., Kim, H., Ahn, T., & Song, H. (2003). Plant growth promotion in soil by some inoculated microorganisms. *J. Microbiol.*, 41, 271–276.
- Jeong ,Y., Kim, J Kang, Y., Lee, S., & Hwang, I. (2007). Genetic diversity and distribution of Korean isolates of *R. solanacearum*. *Plant Disease*, 91, 1277-1287.
- Jian, F. (2004). Role of silica in enhancing the resistance of plants to biotic and abiotic stresses. *J. Soil science and plant nutrition*, 50, 11-18.
- Jiang, W., Yang, K., Vachet, R., & Xing, B. (2010). Interaction between oxide nanoparticles and biomolecules of the bacterial cell envelop as examined under Infrared Spectroscopy. *Langmuir*, 26, 18071-18077.
- Jolanta, K., Malgorzata, C., Zbignew, K., Anna, B., Krysztof, B., & Jorg, T. S. (2010). Application of spectroscopic methods for structural analysis of chitin and chitosan. *Marine Drugs*, 8, 1570-1577.
- Jones, J. (2007). Bacteriophages for plant disease control. *Annu. Rev. Phytopathol.*, 45, 245–262.
- Jones, J. (2012). Growing Tomato in the Greenhouse.

- Jongedijk, E., Tigelaar, H., Van Roekel, J., Bres-vloemans, S., Dekker, I., Van den Elzen, P..., & Melchers, L. (1995). Synergistic activity of chitinases and B, 1-3 glucanases enhances fungal resistance in transgenic tomato plants. *Euphytica*, 85, 173-180.
- Joshi, M., Biswas, D., Sarvanan, A., & Mukhopadhyay, R. (2012). Nylon 6/ Nanoclay filaments and their cords, *Journal of Applied Polymer Science*, 125, 224-234.
- Kailash A., Dilip K., & Vinod K. (2012). Seed-Borne Bacterial Diseases of Tomato (*Lycopersicon esculentum* Mill.) and their control measures: A review. *International Journal of Food, Agriculture and Veterinary Sciences*, 173-182.
- Kalpage, D., & Costa, D. (2014). Isolation of Bacteriophages and Determination of their Efficiency in Controlling *Ralstonia solanacearum* Causing Bacterial Wilt of Tomato. *Tropical Agricultural Research*, 26(1), 140 – 151.
- Karori, S., Wachira, F., Wanyoko, J., & Ngure, R. (2007). Antioxidant capacity of different types of tea products. *African Journal of Biotechnology*, 6, 2287-2296.
- Karungi, J., Kyamanywa, S., Adipala, E., & Erbaugh, M. (2011). Pesticide utilisation, regulation and future prospects in small scale horticultural crop production systems in a developing country, pesticides in the modern world - pesticides use and management, Dr. Margarita Stoytcheva (ed.), 307-459.
- Kenya Horticulture competitiveness project (KHCP)-USAID Report, 2012.
- Kenya Horticulture Development Project (KHDP) Report, 2007.

- Kim, S., Olson, T., Schaad, N., & Moorman, G. (2003). *Ralstonia solanacearum* race 3, biovar 2, the causal agent of brown rot of potato, identified in geraniums in Pennsylvania, Delaware, and Connecticut. *Plant Disease*, 87, 450.
- Kim, C., Nair, S., Kim, J., Kwak, H., Grate, W., Kim, H., & Gu, B. (2005). Preparation of biocatalytic nanofibers with high activity and stability via enzyme aggregate coating on polymer fibers. *Nanotech.*, 16, 3882-3888.
- Knaul, J., Kasai, M., Bui, V., & Creber, K. (1998). Characterization of deacetylated chitosan and chitosan molecular weight review. *Can. J. Chem.*, 76, 1699-1706.
- Koech, K., Wachira, F., Ngure, R., Wanyoko, J., Bii, C., Karori, S., & Kerio, L. (2001). Antioxidant, antimicrobial and synergistic activities of tea polyphenols. *African Crop Science Journal*, 22, 4, 837 – 846.
- Kolodynska, D. (2012). Adsorption characteristics of chitosan modified by chelating agents of a new generation. *Chem Eng J.*, 179, 33-43.
- Korbie, J., & Mattick, S. (2008). Touchdown PCR for increased specificity and sensitivity in PCR amplification. *Nat Protoc.*, 3(9), 1452-6.
- Krajewska, B. (2004). Applications of chitin and chitosan based materials for enzyme immobilizations: A review. *Enzyme and Microbial Tech.*, 35, 126-139.
- Kubata, M., Matsui, M., Chiku, H., Kasashima, N., Shimojoh, M., & Sakaguchi, K. (2005). Cell adsorption and selective desorption for separation of microbial cells by using chitosan immobilized silica. *Appl. Environ microbial*, 71(12), 8895-8902.

- Kumar, M. (2012). A review of chitin and chitosan applications. *React. Funct. Polym.*, *46*, 1-27.
- Kumlachew, A. (2014). Real-Time PCR and Its Application in Plant Disease Diagnostics Advances in Life Science and Technology. Retrieved from: [www.iiste.org](http://www.iiste.org)
- Lawton, L., Cornish, B., & MacDonald, A. (1998). Removal of cyanobacterial toxins (microcystins) and cyanobacterial cells from drinking water using domestic water filters, *Water Research*, *32*(3), 633–638.
- Li, F., & Ma, C. (2002). Effect of available silica in soil on cucumber seed germination and seedling growth metabolism. Beijing *Acta Horticulturae Sinica*, *29*(5), 433-437.
- Li, L., Bellan, L., Craighead, H., & Frey, W. (2006). Formation and properties of nylon-6 and nylon-6/montmorillonite composite nanofibers by electrospinning. *Polymer*, *47*, 6208-6217.
- Li, L., Deng, J., Liu, L., & Xin, L. (2010). Synthesis and characterization of chitosan-zinc oxide nanocomposite membranes. *Carbohydr. Res.*, *345*, 994-998.
- Li, X., Wen, F., Creran, B., Jeong, Y., Zhang, X., & Rotello, V. (2012). Colorimetric Protein Sensing Using Catalytically Amplified Sensor Arrays. *Small*, *8*, 3589-3592.
- Liu, H., Du, Y., Wang, S., & Sun, L. (2004). Chitosan kills bacteria through cell membrane damage. *Int J. Food microbial.*, *95*, 147-155.
- Lee, S., Choi, H., Doo, I., Oh, K., Choi, E., Schroeder-Taylor, A., Low, P., & Lee, Y. (1999). Oligogalaturonic acid and chitosan reduce stomatal aperture by

inducing the evolution of reactive oxygen species from guard cells of tomato and *Commelina communis*. *Plant Physiol.*, 121, 147–152.

- Lehn, J. (1995). *Supramolecular Chemistry: Concepts and Perspectives*. VCH. 262.
- Leung, L., Yakun, S., Chen, R., Zhang, Z., Hang, Y., & Chen, Z. (2001). Theaflavins in black tea and catechins in green tea are equally effective in antioxidant activity. *Journal of Nutrition*, 131, 2248-2251.
- Lifeng, Q., Zirong, X., Xia, J., Caihong, H., & Xiangfei, Z. (2004). Preparation and antibacterial activity of chitosan nanoparticles. *J. Carbohydrate Research*, 339, 2693–2700.
- Ling, R., Khizar, H., Yi, L., Eric, K., Shuqin, X., Chengsheng, J., Fang, Z., & Xiaoming, Z. (2011). Effect of ultrafiltration and fining adsorbents on the clarification of green tea. *Journal of Food Engineering*, 102, 321-326.
- Livio, T., Anna, P., & Dario, Z. (2006). PpEG4 is a peach endo-b-1, 4-glucanase Gene whose expression in climacteric peaches does not follow a climacteric pattern (2006). *Journal of Experimental Botany*, 57(3), 589–598.
- Lucas-Garcia, J., Probanza, A., Ramos, B., Ruiz-Palomino, M., & Gutierrez, F. (2004). Effect of inoculation of *Bacillus licheniformis* on tomato and pepper. *Agronomic J.*, 24, 169-176.
- Mafuma, T. (2013). *Immobilization of electric eel acetylcholinesterase on nanofibres electrospun from a nylon and chitosan blend*. MSc. thesis, Johannesburg: Rhodes University.

- Maksimov, I., Abigizgildina, K., & Pusenkova, L. (2011). PGPR as alternative to chemical crop protectors from pathogens (Review). *Appl. Biochem Microbial J.*, 47, 333-345.
- Mandal, S., Kar, I., Mukherjee, A., & Acharya, P. (2013). Elicitor induced defence responses in tomato against *R. solanacearum*. *The scientific world journal*.
- Maria, F., Rafael, F., Clara, P., & Diego, O. (2014). Increasing tomato fruit quality By enhancing fruit chloroplast function. A double-edged sword? *Journal of Experimerimental Botany*, 65(16), 4589–4598.
- Masinde, A., Anastacia, O., Kwambai, K., Thomas & Wambani, N. (2001). Evaluation of tomato (*Lycopersicon esculentum* L.) variety tolerance to foliar diseases at Kenya Agricultural Research Institute Centre-Kitale in North west Kenya, *African Journal of Plant Science*, 5(11), 676-681.
- Melinka, A., Mari, W., Markus, A., Anna, J., Hubert, K., Reidunn, B..., Georg, F. (2014). Tools and Strategies to Match Peptide-Ligand Receptor Pairs.
- Michailides, T., Morgan, D., Ma, Z., Luo, Y., Felts, D., Doster, M., & Reyes, H. (2005). Conventional and molecular assays aid diagnosis of crop diseases and fungicide resistance. *California agriculture*, 59(2), 115- 123.
- Miethke, M., & Marahiel, M. (2007). Siderophore-based iron acquisition and pathogen control. *Microbiol. Mol. Biol. Rev.* 71413-451.
- Ministry of Planning and National Development, Government of Kenya. (2008). United Nations Environmental Protection Agency Phasing out of Methyl bromide: National poverty survey.

- Monsatto website (2013). Tomato Anna F1 Hand book. Retrieved from: [http://www.Monsattoafrica.com/pdfs/tomato-annafl-growers hand book. Pdf](http://www.Monsattoafrica.com/pdfs/tomato-annafl-growers%20hand%20book.Pdf).
- Moussa, R. (2006). Influence of exogenous application of silica on physiological response of salt-stressed maize (*Zea mays* L.). *International Journal of Biology*, Toronto, 8(2), 293-297.
- Muriungi, S., Mutitu, E., Muthomi, J.W., & Muriungi, J. (2014). Efficacy of cultural methods in the control of *Rhizoctonia solani* strains causing tomato damping off in Kenya. *African Journal of Food, Agriculture, Nutrition and Development*, 14(2), 8776–8790.
- Musyoki, R., Omari, F., & Mwangi, T. (2005). *Evaluation of Elite Tomato Varieties in the Semi-arid regions of Eastern Kenya*. Nairobi: KARI Publication.
- Mylavarapu, R. (2009). UF/IFAS Extension Soil Testing Laboratory (ESTL) Analytical Procedures and Training Manual. Circular 1248, Soil and Water Science Department, Florida Cooperative Extension Service, Institute of Food and Agricultural Sciences, University of Florida.
- Nadagouda, M., Castle, A., Murdock, R., Hussain, S., & Varma, R. (2010). In vitro biocompatibility of nanoscale zerovalent iron particles (NZVI) synthesized using tea polyphenols, *Green Chem*, 12, 114–122.
- Nam, J., Jang K., & Groves, J. (2007). Detection of proteins using a colorimetric bio-barcode assay. *Nat Prot.*, 2, 1438–1444.
- Nasri, A., Zaki, M., Leonardis D., Ungphaiboon S., Sansongsak P., Rimoli G., & Trelli N. (2009). Chitosan/TPP and Chitosan/TPP-hyaluronic acid nanoparticles.

Systematic optimization of the preparative process and preliminary biological evaluation. *Pharm. Res.*, 26, 1918-1930.

- Neerja, C., Anil, K., Purushotham, P., Suma, K., Sarma, P., Moers-chbacher, B., & Podile, P. (2010). Biotechnological approaches to develop bacterial chitinases as a bioshield against fungal diseases of plants. *Crit. Rev. Biotechnol.*, 30, 231-241.
- Newman, M., Dow, J., & Daniels, M. (2001). Bacterial liposaccharides and plant-pathogen interactions. *Eur. J. plant pathol.*, 07, 95-102.
- Nguyen, M., & Ranamukhaarachchi, S. (2010). Soil-borne antagonists for biological control of bacterial wilt disease caused by *Ralstonia solanacearum* in tomato and capsicum. *Journal of Plant Pathology*, 92(2), 385-395.
- Noor, H. (1999). Sanitary and phytosanitary measures (SPS) and their impact on Kenya. *Eco news Africa*. 2-15.
- Obradovic, A., Jones, J., Olson, S., Jackson, L., & Balogh, B. (2005). Integration of biological control agents and systemic acquired resistance against bacterial spot on Tomato. *Plant Dis.*, 89, 712-6.
- Odame, P. (2009). *Manual on Greenhouse Technology*. Nairobi: Essensho Company Ltd.
- Ogawa, K., & Yui, T. (1993). Structure and function of chitosan. 3. Crystallinity of partially N-acetylated chitosans. *Biosci. Biotech. Bioch.*, 57, 1466-1469.

- Pab, E., Retuert, J., Quijada, R., & Zarate, A. (2004). TiO<sub>2</sub>–SiO<sub>2</sub> mixed oxides prepared by a combined sol–gel and polymer inclusion method. *Microporous Mesoporous Mater*, *67*, 195–203.
- Pal, K & Mc Spadden, B. (2006). Biological control of plant pathogens. *Plant Health Instr.*, 1117-02.
- Park, K., Paul, D., Kim, Y., Nam, K., Lee, Y., Choi, H., & Lee, S. (2007). Induced Systemic Resistance by *Bacillus vallismortis* EXTN-1 Suppressed bacterial wilt in tomato caused by *R. solanacearum*. *Plant pathol. J.*, *23*, 22-25.
- Paulitz, T., & Belanger, R. (2001). Biological control in greenhouse systems. *Ann. Rev. Phytopathol.*, *39*, 103–133.
- Payasi, A., & Sanwal, G. (2010). Ripening of climacteric fruits and their control. *J. Food Biochem*, *34*, 679-710.
- Pereira, S., Korndorfer, H., Vidal, A., & Camargo, S. (2004). Silica sources for rice crop. *Sci. Agric.*, *61*, 522-528.
- Peralta, K. (2005). New Species of Wild Tomatoes (*Solanum Lycopersicon*: Solanaceae) from Northern Peru. *Systematic Botany*, *30*(2), 424-434.
- Pereira, D., Valentao, P., Pereira, J., & Andrade, P. (2009). Phenolics: From Chemistry to Biology. *Molecules Journal*, *14*, 2202-2211.
- Peterson, J., Dwyer, J., Bhagwat, S., Haytowitz, D., Holden, J., Eldridge, A.... & Aladesanmi, J. (2005). Major flavonoids in dry tea. *Journal of Food Composition and Analysis*, *18*(6), 487–501.

- Pinto, K., Do Nascimento, L., Gomes, E., da Silva, H., & Miranda, J. (2012). Efficiency of resistance elicitors in the management of grapevine Downy mildew (*Plasmopara viticola*): Epidemiological, biochemical and economic aspects. *European Journal of Plant Pathology*, *134*, 745-754.
- Prado, R., & Natale, W. (2005). Effect of application of calcium silicate on growth, nutritional status and dry matter production of passion fruit seedlings. *Revista Brasileira de Engenharia Agrícola e Ambiental*, *9*(2), 185-190.
- Prasad, K., Yang, B., Dong, X., Jiang, G., Zhang, H., Xie, H., & Jiang, Y. (2009). Flavonoid contents and antioxidant activities from *Cinnamomum* species. *Innov. Food Sci. Emerg. Technol.*, *10*, 627-632.
- Prasitsilp, M., Jenwithisuk, R., Kongsuwan, K., Damrongchai, N., & Watts, P. (2000). Cellular responses to chitosan in vitro: The importance of deacetylation. *J. Mater. Sci. Mater. Med.* *1*, 773-778.
- Pratibha, S., Saravanan, K., Ramesh, R., Vignesh, K P., Dinesh, S., Manika, S..., & Swati, D. (2012). Cloning and semi-quantitative expression of endochitinase (ech42) gene from *Trichoderma* spp. African, *Journal of Biotechnology*, *11*(66), 12930-12938.
- Prevost, K., Couture, G., Shipley, B., Brzezinski, R., & Beaulieu, C. (2006). Effect of chitosan and a biocontrol Streptomycete on field and potato tuber bacterial communities. *Biocontrol*, *51*, 533-546.
- Qian, Y., Goodell, B., & Felix, C. (2002). The effect of low molecular weight chelators on iron chelation and free radical generation as studied by ESR measurement. *Chemosphere*, *48*, 21-28.

- Ramesh, R., & Phadke, G. (2012). Rhizosphere and endophytic bacteria for the suppression of eggplant wilt caused by *Ralstonia solanacearum*, *Crop Protection*, *37*, 35–41.
- Renwick, A. (2008). *Toxicokinetics*. In: Hayes, A.W. ed. *Principles and Methods of Toxicology*, (5<sup>th</sup> ed.), Boca Raton: CRC Press.
- Roberts, D., Lohre, S., Meyer, S., Buyer, J., & Lewsis, J. (2005). Biocontrol agents applied individually and in combination or suppression of soil borne disease of cucumber. *Crop Prot.*, *24*, 141-155.
- Rodrigo, S., Vieira, M., & Beppu, M. (2006). Interaction of natural and cross-linked chitosan membranes with Hg (II) ions *Colloids and Surfaces Physicochem. Eng. Aspects*, *279*, 196–207.
- Rosi, N., & Mirkin, C. (2005). Nanostructures in biodiagnostics. *Chem Rev.*, *105*, 1547–1562.
- Safavi, A., & Abdollahi, H. (1999). Speciation of Fe (II) and Fe (III) with chromagenic mixed reagents by principal-component regression. *Microchem, J.*, *63*, 211–217.
- Saldajeno, M., & Hyakumachi, M. (2011). The plant growth promoting fungus *Fusarium equiseti* and the arbuscular mycorrhizal fungus *Glomus mosseae* stimulate plant growth and reduce severity of anthracnose and damping-off diseases in cucumber (*Cucumis sativus*) seedlings. *Annals of Applied Biology*, *159*, 28-40.
- Sambrook, J., Fritsch, E., & Maniatis, T. (1989). *Molecular cloning: a laboratory manual*. New York: Cold spring harbor laboratory press.

- Sato, S., Tabata, S., Hirakawa, H., Asamizu, E., Shirasawa, K., Isobe S..., & Shibata, D. (2012). The tomato genome sequence provides insights into fleshy fruit evolution. *Nature*, 485(7400), 635–641.
- Schmidt, B., Domonkos, M., Sumalan, R., & Biro, B. (2010). Suppression of arbuscular mycorrhiza's development by high concentration of phosphorus at *Tagetes patula* L. *Res. J. Agri. Sci.*, 42, 156-162.
- Se, K., & Niranjana, R. (2005). Enzymatic production of biological activities of chitosan oligosaccharides. *Carbohydr. Polym.*, 62, 357-368.
- Seminis-Kenya. (2007). Retrieved from: <http://www.freshplaza.com/news>
- Shahwan, T., Abu Sirriah, S., Nairat, M., Boyali, E., Eroglu, A., Scoh, T., & Hallam, K. (2011). Green synthesis of iron nanoparticles and their application as a Fenton-like catalyst for the degradation of aqueous cationic and anionic dyes. *J. Chem. Engin.*, 172, 258-266.
- Sharp, R. (2013). A Review of the Applications of Chitin and Its Derivatives in Agriculture to Modify Plant-Microbial Interactions and Improve Crop Yields. *J. Agronomy*, 3, 757-793.
- Shrifian-Esfahni, A., Salehi, M., Nasr-Esfahni, M., & Ekramian, E. (2015). Chitosan-modified superparamagnetic iron oxide nanoparticles: design, fabrication, characterization and antibacterial activity. *J. Chemik.*, 69(1), 19–32.
- Spadaro, D., & Gullun, M. (2005). Improving the efficacy of biocontrol agents against soil borne pathogens. *Crop. Prot.*, 24, 601-613.

- Spirk, S., Findenig, G., Doliska, A., Reichel, V., Swanson, N., & Kargl, R. (2013). Chitosan–silane sol–gel hybrid thin films with controllable layer thickness and morphology. *Carbohydr Polym.*, *93*, 285–90.
- Soad, A., Algam, E., Ahmed, A., Mahdi, B., & Guan, L. (2013). Effects of chemical inducers and *Paenibacillus* on tomato growth promotion and control of Bacterial wilt. *Asian Journal of Plant pathology*, *7*, 15-28.
- Soderberg, K, Olson, P., & Baath, E. (2002). Structure and activity of the bacterial community in the rhizosphere of different plant species and the effect of AMF colonization. *FEMS Microbiology Ecology*, *40*, 223-231.
- Soratto, R., Crusciol, C., Castro, G., & Claudi, C. (2012). Leaf application of silicic acid to white oat and wheat, *Agron. J.*, *36*(5), 1538–1544.
- Sood, S. (2003). Chemotactic response of plant growth promoting rhizobacteria towards roots of vesicular-arbuscular mycorrhizal tomato plants. *FEMS Microbiology Ecology*, *45*, 219-227.
- Sun, Y., Li, X., & Cao, X. (2007). A method for the preparation of stable dispersion of zero valent iron nanoparticles. *Colloids Surf.*, *308*, 60-66.
- Sun, H., Zhang, W., Lu, X., & Gao, P. (2008). Siderophore production from 27 filamentous fungal strains and a novel siderophore with potential biocontrol applications from *Aspergillus niger*. *J. Life Sci.*, *2*(1), 19-26.
- Sun, H., Lu, X., & Gao, P. (2010). The exploration of the antibacterial mechanism of Fe<sup>3+</sup> against bacteria. *Brazilian J. of Microl.*, *42*, 410-414.
- Sun, Y, Liu, Y., & Qu, W. (2009). Combining nanosurface chemistry and microfluidics for molecular analysis and cell biology. *Anal Chim Acta*, *650*, 98–105.

- Taraskiewicz, A., Fila, G., Grinholc, M., & Nakonieczna, J. (2013). Innovative strategies to overcome Biofilm resistance. *Biomed Research International*.
- Tim, M., Pingsheng, J., Ken, P., Robert, M., & Steve, O. (2008). Three Soilborne Tomato Diseases Caused by *Ralstonia* and *Fusarium* Species and their Field Diagnostics. Plant Pathology Department, Florida Cooperative Extension Service, Institute of Food and Agricultural Sciences, University of Florida. 1-6.
- Tsaih, M., & Chen, R. (2003). The effect of reaction time and temperature during heterogenous alkali deacetylation on degree of deacetylation and molecular weight of resulting chitosan. *J. Appl. Polym. Sci.*, 88, 2917-2923.
- USDA National Nutrient Database for Standard Reference. *Release 28*.
- Vahjen, W., Munch, J., & Tebbe, C. (1995). Carbon source utilization of soil extracted micro-organisms as a tool to detect the effect of soil supplemented with genetically engineered and non-engineered *Corynebacterium glutamiicum* and a recombinant peptide at the community level. *FEMS microbial. Ecol.*, 18, 317-328.
- Wan, W., Ngah, S., Ghani, A., & Kamari, A. (2005). Adsorption behaviour of Fe (II) and Fe (III) ions in aqueous solution on chitosan and cross-linked chitosan beads. *Bioresour. Technol.*, 96, 443–450.
- Wang, H., & Helliwell, K. (2001). Determination of Flavanols in Green Tea and Black Tea Leaves and Green Tea Infusions by High Performance Liquid Chromatography, *Food Reserves International*, 34, 223-227.

- Wang, S., Shen, L., Tong, Y., Chen, L., Phang, L., Lim, P., & Liu, T. (2005). Biopolymerchitosan/montmorillonite nanocomposites; preparation and characterization. *Polymer degradation and stability. J. chem.*, 90, 123-131.
- Wazed, A., Rajendran, S & Joshi, M. (2010). Modulation of size, shape and surface charge of chitosan nanoparticles with special reference to antimicrobial activity. *Applied Science Letters*, 3(1), 9- 18.
- Wazed, A., Joshi, M., & Rajendran, S. (2011). Synthesis and Characterization of Chitosan Nanoparticles with Enhanced Antimicrobial Activity. *International Journal of Nanoscience*, 4(5), 979-984.
- Wydra, K., & Semrau, J. (2006). Phenotypic and molecular characterization of the interaction of antagonistic bacteria with *Ralstonia solanacearum* causing tomato bacterial wilt. In: Wolfgang Zeller, Cornelia Ulrich (eds.). 1<sup>st</sup> International Symposium on Biological Control of Bacterial Plant diseases, Darmstadt, Germany 2005. 112-118.
- Xu, Y., & Du, Y. (2003). Effect of molecular structure of chitosan on protein delivery properties of chitosan nanoparticles. *Int. J. Pharm*, 250, 215-226.
- Yamada, Y., Katsura, K., Kawasaki, H., Widyastuti, Y., Saono, S, Seki, T..., & Komagata, K. (2000). *Asaiabogorensis* gen. nov., sp. nov., an unusual acetic acid bacterium in the  $\alpha$ -Proteobacteria. *International Journal of Systems Evolution Microbiology*, 50, 823-829.
- Yamada, T. (2007). Isolation and characterization of bacteriophages that infect the phytopathogen *R. solanacearum*. *Microbial*, 153, 2630-2639.

- Yamada, T. (2007). A jumbo phage infecting the phytopathogen *R. solanacearum* defines a new lineage of the Myoviride family. *Virology*, *398*, 135-147.
- Yang, X. (2010). *Effect of N Si fertilizer on the growth and yield of Chinese Cabbage*, MSc. thesis: Shan Dong Agricultural University.
- Yang, R., He, J., Xu, L., & Yu, J. (2009). *Polymer*, *50*, 5846–5850.
- Yang, Z., Zhuang, L., & Tan, G. (2002). Preparation and adsorption behavior for metal of chitosan cross-linked by dihydroxyazacrown ether. *J. Appl. Polym. Sci.*, *85*, 530–535.
- Yao, J., & Allen, C. (2006). Chemotaxis is required for virulence and competitive fitness in the bacterial wilt pathogen *Ralstonia solanacearum*. *J. Bacteriol.*, *188*, 3697-3708.
- Yuvakkumar, R., Elango, V., Rajendran, V., & Kannan, N. (2011). Preparation and characterization of zero valent iron nanoparticles. *Digest J. Nanomaterials and Biost.*, *6*(4), 1771-1776.
- Zhang, Z., Chen, D., & Chen, L. (2002). Preparation of two different serials of chitosan. *J. Dong Hua Univ. (Eng. Ed.)*, *19*, 36-39.
- Zhang, X., Guo, Q., & Cui, D. (2009), Recent Advances in Nanotechnology Applied to Biosensors, *Sensors*, 1033- 1053.
- Zeng, X., Liang, J., & Tan, Z. (2007). Effects of silicate on some photosynthetic characteristics of sugarcane leaves, *Journal of Huazhong Agricultural University*, *26*(3), 330–334.

Zouhour, L., Salah, S., Saloua, S., & Amor E. (2010). Extraction and characterization of chitin and chitosan from crustacean by-products-biological and physicochemical properties. *African J. of Biotech.*, 10(4), 640-647.

## APPENDICES

### Appendix 1: Pearson's Correlation Coefficient- Descriptive Statistics

---

	N	Mean	SD	Sum	Min	Max
Chitinases	18	1.6212105263158	0.40112128658263	30.803	1.06	2.61
	18	0.22962631578947	0.053181177143226	4.3629	0.1233	0.2667

---

2-tailed test of significance

## Appendix 2: Summary of ANOVA for Iron Nanoparticles Yield

Source of variation	d.f.	s.s.	m.s.	F v.r.	F pr.
Rep stratum	2	0.07401	0.03701	1.46	
Rep.*Units* stratumTreat	14	160.33089	11.45221	452.08	<.001
Residual	28	0.70931	0.02533		
Total	44	161.11421			

Pr > F, p-value associated with the F value of the test statistic

**Appendix 3: Summary of ANOVA for *R. Solanacearum* Optical Densities (OD) 600 nm**

Source of variation	d.f.	s.s.	m.s.	F v.r.	F pr.	
Rep stratum	2	0.018093	0.009046	1.09		
Rep.*Units* stratumTreat	6	2.454660	0.409110	49.27	<.001	
Residual	12	0.099645	0.008304			
<hr/>						
Total	20	2.572398				
s.e.	0.0359	cv%	2.9	l.s.d.	0.1621	Grand mean 1.219

Pr > F, p-value associated with the F value of the test statistic

**Appendix 4: Summary of ANOVA for *R. solanacearum* Inhibition by  
Bionanocomposites**

Source of variation	d.f.	s.s.	m.s.	F v.r.	F pr.
C1 stratum	2	0.933	0.467		0.07
C1.*Units* stratumInhibition					
	19	39974.583	2103.925	331.65	<.001
Residual	38	241.067	6.344		
Total	59	40216.583			

Pr > F, p-value associated with the F value of the test statistic

**Appendix 5: Summary of ANOVA for Bacterial Wilt incidence in Tomato**

Source of variation	d.f.	s.s.	m.s.	F v.r.	F pr.
Treatment	17	9954.11	585.54	7.99	<.001
Residual	54	3956.50	73.27		
Total	71	13910.61			

s.e. 8.56    cv% 23.4    l.s.d. 12.13    Grand mean 36.6

Pr > F, p-value associated with the F value of the test statistic

**Appendix 6: Summary of ANOVA for Hybrid Tomatoes Yield (Size in cm)**

Source of variation	d.f.	s.s.	m.s.	F v.r.	F pr.
Rep stratum	3	18.7930	6.2643	33.58	
Rep.*Units* stratum Treat	15	133.5586	8.9039	47.73	<.001
Residual	45	8.3945	0.1865		
Total	63	160.7461			

s.e. 0.6257 cv % 3.6 l.s.d. 1.342 Grand mean 8.93

Pr > F, p-value associated with the F value of the test statistic

**Appendix 7: Summary of ANOVA for Tomato Fruits Shelf Life (Days)**

Source of variation	d.f.	s.s.	m.s.	Fv.r.	F pr.		
Rep stratum	3	19.2976.432		1.14			
Rep.*Units* stratumTreat							
	15	2758.734		183.916	32.46 <.001		
Residual	45	254.953		5.666			
Total	63	3032.984					
s.e.	0.634	cv %	3.3	l.s.d.	3.390	Grand mean	18.98

Pr > F, p-value associated with the F value of the test statistic

**Appendix 8: Summary of ANOVA for Days to Flowering in Tomato**

<u>Source of variation</u>	<u>d.f.</u>	<u>s.s.</u>	<u>m.s.</u>	<u>F v.r.</u>	<u>F pr.</u>
C2 stratum	3	0.0417	0.0139	0.02	
C2.*Units* stratumC1	17	143.5694	8.4453	11.73	<.001
<u>Residual</u>	<u>51</u>	<u>36.7083</u>	<u>0.7198</u>		
Total	71	180.3194			

Pr > F, p-value associated with the F value of the test statistic

**Appendix 9: Summary of ANOVA for Days to Ripening of Tomato Fruits**

Source of variation	d.f.	s.s.	m.s.	F v.r.	F pr.
C2 stratum	3	1.500	0.500	0.12	
C2.*Units* stratumC1	17	755.444	44.438	10.35	<.001
<u>Residual</u>	<u>51</u>	<u>219.000</u>	<u>4.294</u>		
Total	71	975.944			

Pr > F, p-value associated with the F value of the test statistic

**Appendix 10: Chitosan Nanoparticles (90% DDA)**

No	2- theta(deg)	d (ang.)	Height(cps )	FWHM(deg )	Int. I(cps deg)	Int. W(deg)	Asym. factor
1	9.52(9)	9.29(9)	132(33)	0.84(9)	163(10)	1.2(4)	0.9(5)
2	19.16(7)	4.629(16)	261(47)	1.73(11)	831(16)	3.2(6)	0.31(8)
3	31.867(11)	2.8059(10)	558(68)	0.186(18)	167(6)	0.30(5)	0.74(19)
4	45.54(4)	1.9901(15)	227(43)	0.37(3)	98(6)	0.43(11)	1.1(4)
5	56.64(10)	1.624(3)	56(22)	0.41(7)	24(4)	0.4(2)	2.2(6)

### Appendix 11: Chitosan Immobilized Silica Nanocomposites (CISNC)

No.	2-theta(deg)	d (ang.)	Height(cps)	FWHM(deg)	Int. I(cps deg)	Int. W(deg)	Asym. factor
1	31.7(2)	2.82(2)	41(18)	4.8(6)	420(24)	10(5)	5(2)
2	45.47(8)	1.993(3)	80(26)	0.31(12)	43(4)	0.5(2)	2(3)

## Appendix 12: Iron oxide Nanoparticles

No.	2- theta(deg)	d (ang.)	Height(cps)	FWHM(deg)	Int. I(cps deg)	Int. W(deg)	Asym. factor
1	32.64(6)	2.742(5)	66(24)	0.41(5)	30(4)	0.4(2)	1.3(8)
2	46.26(10)	1.961(4)	47(20)	0.35(9)	20(3)	0.4(2)	1.3(16)

### Appendix 13: Nylon Nanofibres

No.	2- theta(deg)	d (ang.)	Height(cps)	FWHM(deg)	Int. I(cps deg)	Int. W(deg)	Asym. factor
1	32.64(6)	2.742(5)	66(24)	0.41(5)	30(4)	0.4(2)	1.3(8)
2	46.26(10)	1.961(4)	47(20)	0.35(9)	20(3)	0.4(2)	1.3(16)

No.	2- theta(deg)	d (ang.)	Height(cps)	FWHM(deg)	Int. I(cps deg)	Int. W(deg)	Asym. factor
1	28.420(16)	3.1379(17)	202(41)	0.18(3)	42(4)	0.21(6)	2.5(11)
2	31.622(11)	2.8271(10)	785(81)	0.128(14)	145(5)	0.18(3)	2.1(9)
3	45.340(15)	1.9985(6)	362(55)	0.13(2)	81(4)	0.22(4)	1.0(6)

#### Appendix 14: Nylon Iron Oxide Chitosan Immobilized Silica Nanocomposite

No.	2-theta(deg)	d (ang.)	Height(cps)	FWHM(deg)	Int. I(cps deg)	Int. W(deg)	Asym. factor
1	29.83(7)	2.992(7)	47(18)	0.49(16)	46(6)	1.0(5)	5(4)
2	39.12(4)	2.301(2)	225(39)	0.33(3)	97(5)	0.43(10)	4(3)
3	45.322(13)	1.9993(5)	147(31)	0.38(4)	73(4)	0.49(14)	4(3)
4	65.58(3)	1.4223(6)	134(30)	0.33(3)	53(4)	0.39(12)	3.0(11)
5	78.525(12)	1.21711(16)	144(31)	0.37(3)	60(4)	0.42(12)	0.5(2)
6	112.21(6)	0.9280(3)	56(19)	0.28(6)	19(3)	0.34(17)	0.5(6)
7	137.49(4)	0.82650(12)	51(18)	0.33(6)	24(3)	0.5(2)	0.5(3)

**Appendix 15: FeOCISNC-*R. solanacearum***

No	2- theta(deg)	d (ang.)	Height(cps )	FWHM(deg )	Int. I(cps deg)	Int. W(deg)	Asym. factor
1	32.27(4)	2.772(4)	123(29)	0.36(3)	47(4)	0.38(12)	2.6(14)
2	38.92(2)	2.3124(13)	165(33)	0.22(3)	49(4)	0.30(8)	0.4(3)
3	45.20(3)	2.0042(12)	334(47)	0.19(5)	97(6)	0.29(6)	0.7(6)
4	65.55(2)	1.4229(5)	351(48)	0.24(3)	110(5)	0.31(6)	1.2(5)
5	78.635(19)	1.2157(2)	269(42)	0.24(2)	72(4)	0.27(6)	0.7(2)
6	112.38(4)	0.9271(2)	92(25)	0.20(4)	27(3)	0.29(11)	2(3)
7	137.56(2)	0.82632(7)	99(26)	0.26(4)	40(4)	0.41(14)	0.53(19)